University of Strathclyde

Department of Pure and Applied Chemistry

Exploring the Chemistry of Soft scorpionate Ligands

Rajeev Rajasekharan Nair

Thesis submitted to the Department of Pure and Applied Chemistry, University of Strathclyde, in fulfilment of the requirement for degree of Doctor of philosophy

Dedicated to my Parents (M. Rajasekharan Nair and Sooraja P. Nair), brother (Rajesh) and to my soul (Chandrika).

Declaration of Copyright

This thesis is the result of the author's original research. It has been composed by the author and has not been previously submitted for examination which has led to the award of a degree.

Signed :

Date :

Acknowledgements

I am really thankful to my supervisors, Dr John Reglinski and Dr Mark D. Spicer for the help and guidance during my stay here at University of Strathclyde. I have been lucky enough to be taught by a series of good teachers. And I will put my supervisors Dr John Reglinski and Dr Mark D.Spicer among the top of this list. The way they teach and guide me during my PhD is really marvellous and it is something precious to admire always. Dr Reglinski is a very good teacher and for me he is the best in the world. The way he teaches and treats me during my PhD is highly remarkable. I hope these trainings will definitely help me to build my future career as a researcher, as a teacher and also as an individual human being. A thank you will not be enough but still... Sir, a very big thank you from the bottom of my heart.

Dr Spicer, the smartest person I have ever seen. Thank you very much to you for spending time with me and answering my silly questions. The problem solving skills that I tried to learn from him will really help me throughout my life. Not enough words to express my gratitude towards him. With all respects, a big thank you for you too Sir. I am really proud myself being trained by these two legends.

Thanks to The University of Strathclyde especially Mr Jim McGrath for the financial help towards the tuition fee. Special thanks to Mrs Isabel Scott for the help and assistance to overcome the issues with the registry during the studies.

Thanks to Dr Alan Kennedy for teaching me X-ray crystallography and solving all the puzzles that I produced and also for making me laugh always. A colourful squirrel from Kerala would be the right gift for him.

Thanks to Dr Dave Armstrong for all the DFT calculations and also for his valuable advices and support. Thanks to Dr John Parkinson for the NMR data interpretation. A special thanks to Dr Katherine Trotter for helping and teaching me the laboratory procedures and also teaching me how to manage the lab. She is my role model. Dr Trotter is a good teacher, a good researcher and a good friend. A very special and sincere salute to you with a cup of tea.

Dr Catriona Morrison needs a special acknowledgment for helping me to run and solve the X-ray crystal structure and also solve the puzzles in the data processing. Thank you very much Dr Morrison.

Thanks to Ibrahim Siraj for his assistance in the Lab and office. Without his help it would have been difficult to perform very well in the lab particularly during out of hours working. Thanks to Dr Dawn Wallace for her kind words and helps and also for all the guidelines for my thesis writing by already submitting a splendid work in the field.

Special acknowledgements to Dean Moore, Louise Diamond, Lisa Darby, Samuel Lutta and Annemarie Marckwordt and lots of others who worked on scorpionate ligands, for helping me in the projects with lots of data.

Thanks to Mrs Alaine Martin, the laboratory superintendent and all technicians Craig Irvine (NMR), Denise Gilmour (Elemental Analysis) Patricia Keating (Mass spectrometry) for their help, motivation and guiding to the right direction by answering my silly questions. Thanks to all present and past students in the lab R6-05 and R5-26.

William Farquhar my workplace manager (Morrisons, Partick) needs a special acknowledgement. Because of his kindness, I managed to work in the University at my will and thereby able to complete the work in the prescribed time.

Thanks to my cousin brothers Anad, Ajay and Ajith for their support and help to fulfil the studies. Thanks to all my friends especially Swagata Roy and Poornima Roy for the help and moral support during my studies. I am always thankful to you both for your kindness. Thanks to my other friends Lilly Thottam, Simon Moolayil, Philomina Vargese and Colin Whatley.

Thanks to my brother Rajesh for his moral support. Finally thanks to my parents. I am fortunate enough to be their son. Thank you very much for the help, moral support and continuous positive reinforcement throughout my life. For you both, I am dedicating this thesis along with Chandrika who is my soul.

Abstract

Alkylation of the soft scorpionate anions, Tm^R, Tbz and tzTtz have been successfully carried out. The resulting cationic species of Tm^{Me} were fully characterised. However, the formation of the cationic species is not always favourable and the alkylated products of Tbz and tzTtz were found to be unstable. The structures and degradation pathways of the three species were interrogated using *ab-initio* DFT calculations. This suggested that the B-N bond can lengthen when the scorpionate is alkylated and that this leads to thio-imidazole elimination.

This work was extended to the synthesis of cyclic ring system initially by linking two sulphurs in the anion using dihalo-alkane species. Ring formation can also be effected using mild oxidising agents and treatment of Tm^{Me} and Tm^{Ph} with NO^+ and I_2 leads to the synthesis of a series of unique polycyclic heterocycles. The importance of B-N bond elongation to complex stability is investigated further using the Tbz anion. As expected Tbz is unable to form complexes with the hard metals e.g. cobalt. Treatment with soft metals (mercury, antimony and bismuth) does produce complexes but these are not stable. These metal complexes rearrange to form a new class of polycyclic rings.

Studies using NO^+ are extended to its chemistry of soft scorpionate metal complexes. A study was conducted which sought to use ruthenium complexes as nitric oxide scavengers. This chemistry failed to materialise and NO^+ acts as a mild oxidising agent rather than a π acceptor with these species.

% Buried volume analysis is performed using a series of soft scorpionates (Tm^R R = Me, iPr, tBu, and Ph) to calculate the steric demand of the ligands at the central metal atom. The study reveals that there is a modest effect when the scorpionate is supporting a four coordinated metal (e.g. zinc). However, for six coordinated metals (e.g. manganese as its tricarbonyl) the scorpionate has minimal influence.

Glossary

Ad	: Adamantyl
Ada protein	: Adaptive response protein
An	: O-Anisyl
Anal.calc	: Analysis calculated
Bm/Bm^{Me}	: Dihydro*bis*(methimazolyl)borate
Bo	: Indazole
Calcd	: Calculated
Cbu	: Cyclobutyl
Cp	: Cyclopentadienyl
Cpe	: Cyclopentyl
CpG	: Cytosine phosphate guanine
Cpr	: Cyclopropyl
Cum	: Cumyl (4-isopropyl phenyl)
Cy	: Cyclohexyl
Cys	: Cysteine
DFT	: Density Functional Theory
DMF	: Dimethylformamide
DMSO	: Dimethyl sulfoxide
E coli	: Escherichia coli
GOF	: Goodness of fit
iPr	: Isopropyl
Me	: Methyl
Measd	: Measured
MeI	: Methyl iodide

Mins : Minutes

MtH : Methimazole

NaTm/NaTm^{Me} : Sodium Hydro*tris*(methimazolyl)borate

NHC : N-Heterocyclic carbene

NO : Nitric oxide

Ogt protein : O-Linked N-Acetylglucosamine Transferase protein

Ph : Phenyl

PzH : Pyrazole

Reflns : Reflections

tBu : Tertiary butyl

Tbz : Hydro*tris*(mercaptobenzothiazolyl)borate

Tbz-S : 6a,13-dihydro-5aH-benzo[4,5]thiazolo[2,3-]benzo[4,5]thiazolo[3,2e] [1,3,5,4]thiadiazabenzo[d]thiazole-2(3H)-thioneboronium

THF : Tetrahydrofuran

Tm/Tm^{Me} : Hydro*tris*(methimazolyl)borate/ Hydro*tris*(methylthioimidazolyl)borate

Tm^{iPr} : Hydro*tris*(isopropylthioimidazolyl)borate

Tm^{Ph} : Hydro*tris*(phenylthioimidazolyl)borate

Tm^{Ph}-S : 1,9-diphenyl-5,9,9a,10a-tetrahydro-1H-diimidazo[2,1-b:1',2'-e] [1,3,5,4]thiadiazo(1-phenyl-1H-imidazole-2(3H)-thione)boronium

Tm^{tButyl} : Hydro*tris*(tert-butylthioimidazolyl)borate

Tp* : Hydro*tris*(3,5-dimethylpyrazolyl)borate

Tp : Hydro*tris*pyrazolylborate

tzTtz : *Tetrakis*(thiazolyl)borate

V:V : Volume by volume

%V_{Bur} : Percentage volume buried

Structural formulae

$Bz^{allyl}Br$:

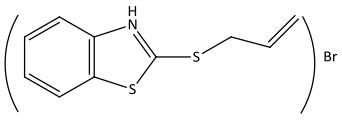

$Co(Bz)_2Br_2$:

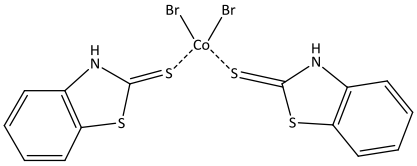

$Co(Bz\text{-}S)_2Br_2$:

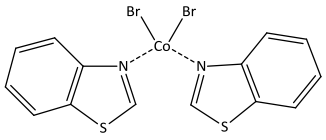

Crossbow :

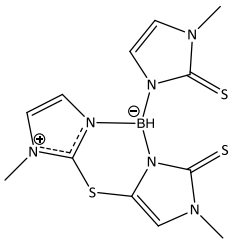

NaTbz :

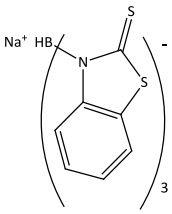

NatzTtz :

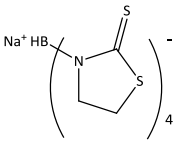

[Tbz-S]I :

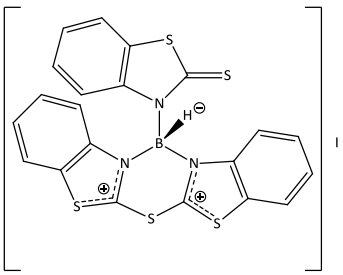

$(Tm^{Me}SS'^{decylene}Tm^{Me})I$:

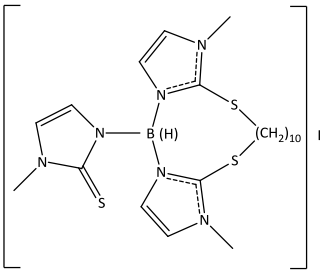

$(Tm^{Me}SS'^{ethylene}Tm^{Me})Br$:

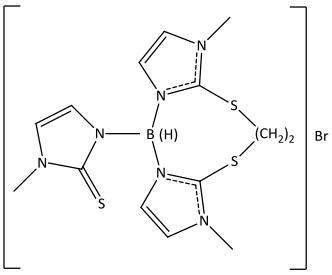

$(Tm^{Me}SS'^{butylene}Tm^{Me})Br$:

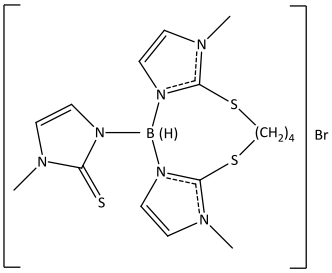

$(Tm^{Me}SS'^{hexylene}Tm^{Me})I$:

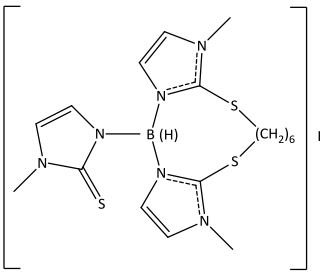

$(Tm^{Me}SS'^{pentylene}Tm^{Me})I$:

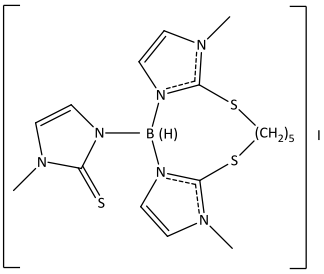

$(Tm^{Me}SS'^{propylene}Tm^{Me})I$:

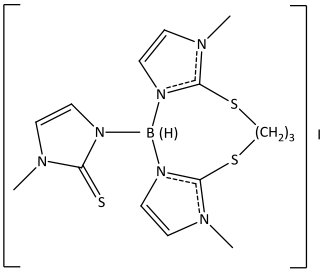

$(Tm^{Me}SS'^{octylene}Tm^{Me})I$:

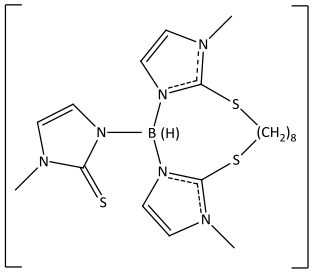

$(Tm^{Me}SS'^{xylylene}Tm^{Me})Br$:

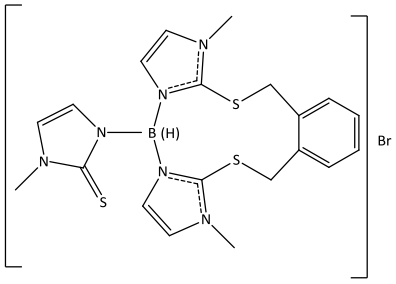

$(Tm^{Ph}SS'^{propylene}Tm^{Ph})I$:

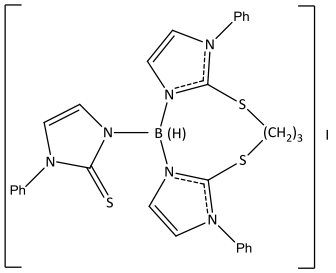

$(Tm^{Ph}SS'^{decylene}Tm^{Ph})I$:

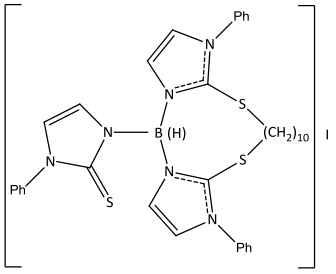

$[Tm^{Ph}\text{-}S]BF_4$:

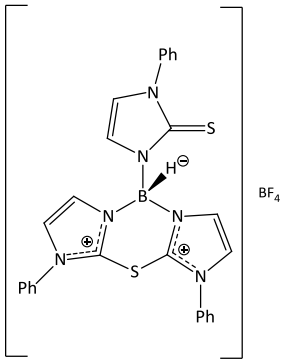

$[Tm^{Ph}\text{-}S]I_3$:

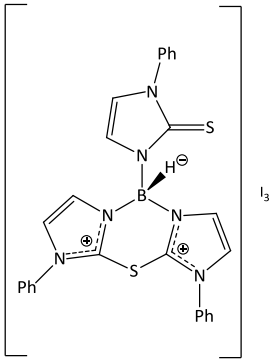

$[Tm^{Ph}\text{-}S]I$:

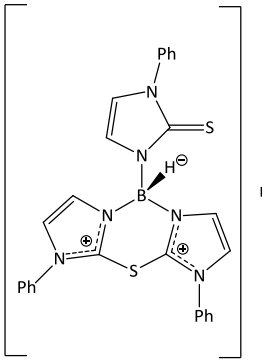

$TmS^{allyl}Br_2$:

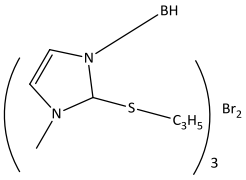

$TmS^{benzene}I_2$:

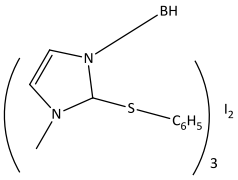

$TmS^{benzyl}Br_2$:

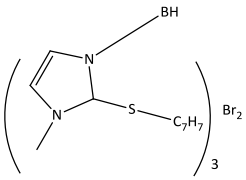

$TmS^{Me}I_2$:

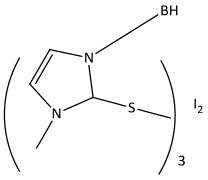

$TmS^{propyl}Br_2$:

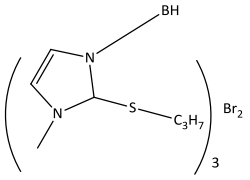

$Tz^{allyl}Br$:

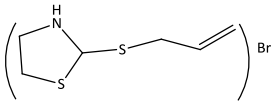

List of some scorpionates

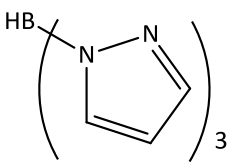

Tp

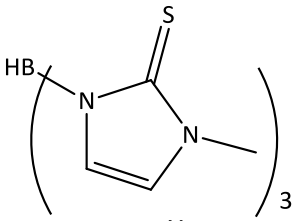

Tm^{Me}

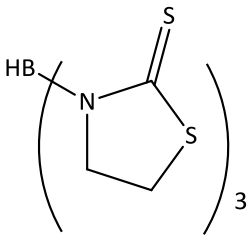

Ttz

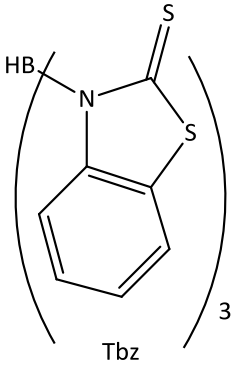

Tbz

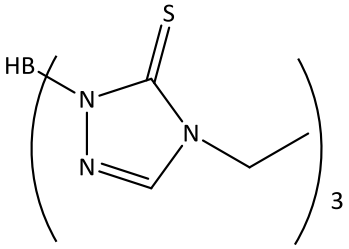

Tt

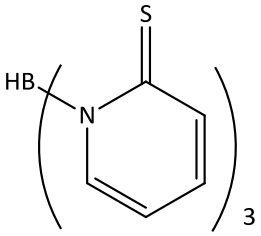

Tmp

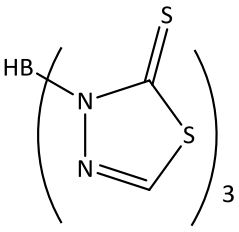

Janus

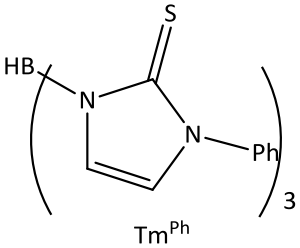

Tm^{Ph}

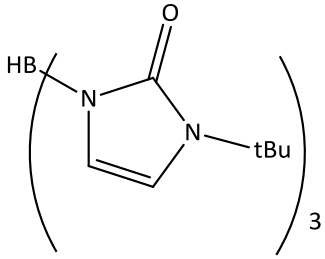

To

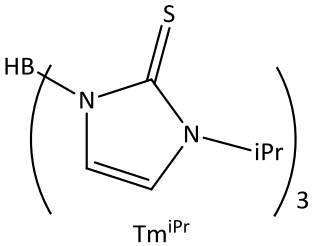

Tm^{iPr}

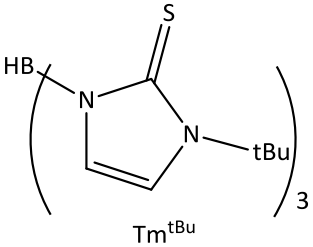

Tm^{tBu}

Contents

3.Oxidation of Soft Scorpionate anions

4. An Investigation on the stability of mercaptobenzothiazole based Soft Scorpionate (Tbz) complexes

5. An investigation on the stability of metal-hydride bond in soft scorpionate ruthenium complex

6.Buried volume analysis of soft scorpionate ligands

7. Final Conclusion

Appendix

Chapter 1

General Introduction

1.1 Background

Scorpionate ligands are a class of tripodal ligands that were first reported in 1966 by Swiatoslaw Trofimenko.[1] The structural conformation of these tridentate species resembles a scorpion where the ligand binds to the central metal atom via two donors in the same plane and a third one above the plane, similar to manner in which a scorpion holds its prey using its two arms to grip its prey and its tail as a stinger (figure 1.1). Trofimenko identified this remarkable invention as 'a new and fertile field of chemistry'.[1] The first scorpionate reported was pyrazole based i.e. poly(pyrazolyl)borate, which is simply abbreviated as Tp^R where R is the substituent on the pyrazole. Since the first reports in 1966, over 2800 publication on Tp^R ligands have been published to date including complexes with most of the metals in the periodic table.[2]

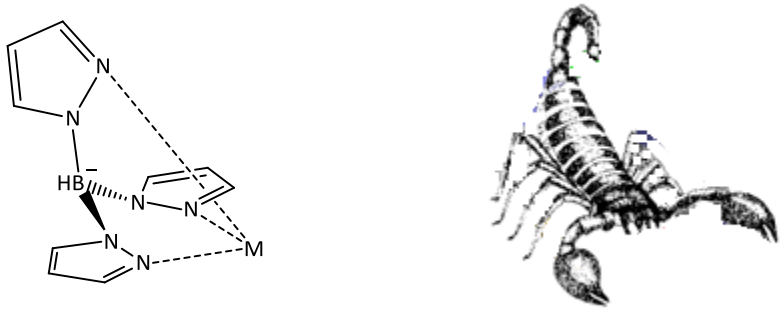

Figure 1.1: Illustration of first scorpionate hydro*tris*(pyrazolyl)borate (Tp). The metal is coordinated with two donor atom which lie in the same plane resembling the arms of the scorpion and the third donor atom above the plane resembling the tail.

Poly(pyrazolyl)borate complexes allow the formation of three six-membered rings using the boron and metal atom with general structure $RR'B(pz\text{-}H)_2M(L)_n$ (where R= H, alkyl or aryl; R'= H or pz-H (pz = pyrazole) depending on whether the ligand is a *bis* or *tris* pyrazolyl- species).[2] Scorpionates are mainly classified into homoscorpionates e.g. the hydro*tris*(pyrazolyl)borate anion or heteroscorpionates e.g. the dihydro*bis*(pyrazolyl)borate anion. (figure 1.2).[2,3]

Figure 1.2: Diagrammatic representation of a typical homoscorpionate (a: hydro*tris*(pyrazolyl)borate, Tp) and hetroscorpionate (b: dihydro*bis*(pyrazolyl)borate, Bp).

The nomenclature employed to define the scorpionates was developed by Curtis[2,4]. Briefly, the letters 'B' and 'T' represents *bis* and *tris* respectively indicating the number of reactant rings present. The heterocyclic arms of the scorpionate are identified by a small letter following the T or B. Pyrazole is abbreviated to p and methimazole to m, benzothiazole to bz, thiazoline to tz. Substituents present on the hetrocyclic rings are identified by a superscript (figure 1.3). For example, if an isopropyl group is present at the third position of Tp then it is written as Tp^{iPr}. If more than one substituent is present, both are written as superscript and separated by a comma. Convention demands that the substituent at position three comes first.[2,4]

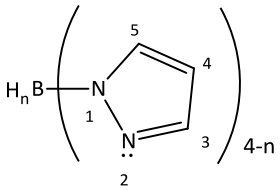

Figure 1.3: General numbering system for the pyrazole base scorpionates. 'n' is any whole number less than 4.

The third position on the ligand is probably the most important as the substituent placed at this position defines the steric bulk of the ligand. Simply replacing the hydrogen with a methyl group alters the structures of many metal complexes from a sandwich type structure to a piano stool type structure.[2-5] In the absence of bulky

substituents halo-bridged species are common.[2-5] When bulk substituents are present monomeric complexes with terminal halides predominate.[2-5] Studies have been carried out to measure the steric effects of the substituents on the pyrazole in Tp^R ligands by measuring the various cone angles and wedge angles (table 1.1).[2,3] These studies are important to studies which seek to control the available space at the metal centre.

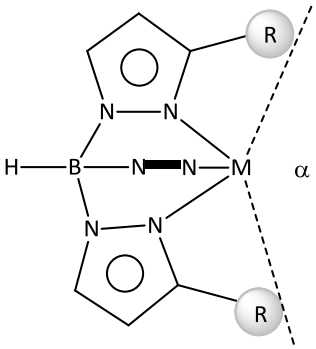

A

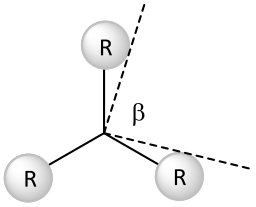

B

Complex	Cone angle (^{0})	Wedge angle (^{0})
Tp	183	70
Tp^{Br3}	234	60
$Tp^{4Bo,3Me}$	235	68
$Tp^{(CF3)2}$	237	49
Tp*	239	67
$Tp^{iPr,4Br}$	243	28
$Tp^{tBu,Me}$	243	31
Tp^{tBu}	251	29

Table 1.1: Cone angles and wedge angles of some selected thallium complexes of Tp scorpionates.[2,3] A pictorial representation of cone angle and wedge angle are shown above the table. Cone angle = (360-α) the side view (picture A) and wedge angle = β, view along the B-M axis (picture B).

Scorpionates ligands can be synthesised in many ways.[2,4] However, the most common method and also the first reported method is the solvent free melt

reaction[2,4] using an alkali metal borohydride and pyrazole or n-substituted pyrazole. The reaction is temperature controlled with the sequential addition of pyrazole units occurring within given ranges of temperature (scheme 1.1).

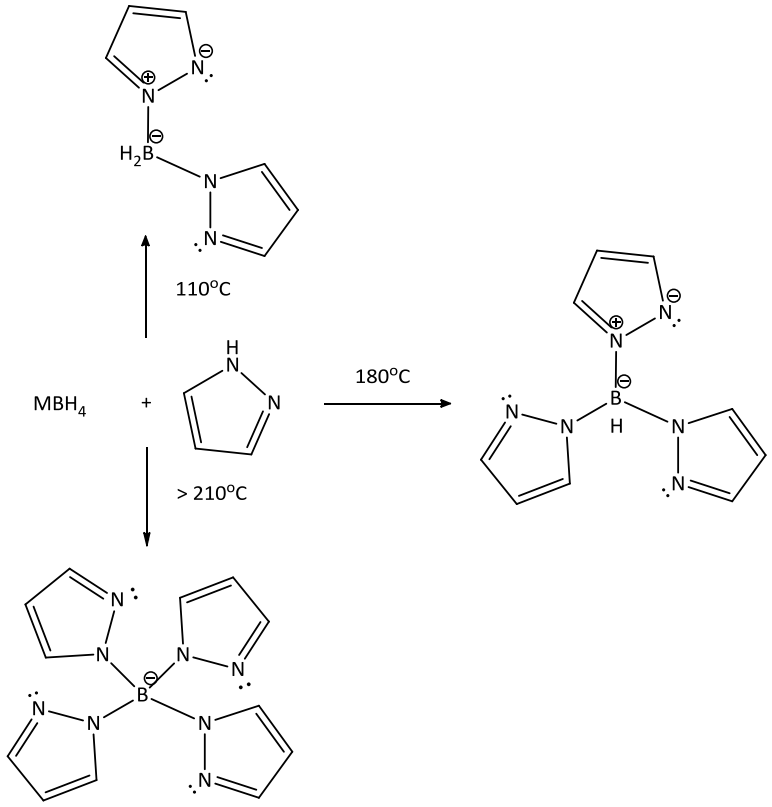

Scheme 1.1: Solvent free melt reaction of metal borohydride with pyrazole. Heating at 110°C leads to the formation of the dihydro*bis*(pyrazolyl)borate anion. At 180°C the adduct formed is the *tris*(pyrazolyl)borate anion. Temperatures over 210°C lead to the formation of the *tetrakis*(pyrazolyl)borate anion.

Over 200 different poly(pyrazolyl)borate anions have now been synthesised.[3] Curiously it took 30 years for the first reports of soft scorpionates to appear. Riordan *et al*. reported first on a series of anions based on highly flexible thioether moieties (figure 1.4).[6,7] In 1996 Reglinski and Spicer introduced the methimazole based scorpionates.[6,8] These were more effective analogues of the pyrazolylborates as their synthetic design was based simply on the replacement of pyrazole with methimazole. Soft scorpionates can also be prepared by heating the appropriate

thio-imidazole in presence of a metal borohydride in a suitable solvent (e.g. xylene or toluene). [9,10] Unlike the pyrazole base anions, it is not possible to synthesis *tetrakis*(thio-imidazolyl)borate anions using the solvent free reactions.[8] These are prepared by perfoming the melt reaction at 200^{o}C for an hour followed by an eleven hour reflux in toluene.[11]

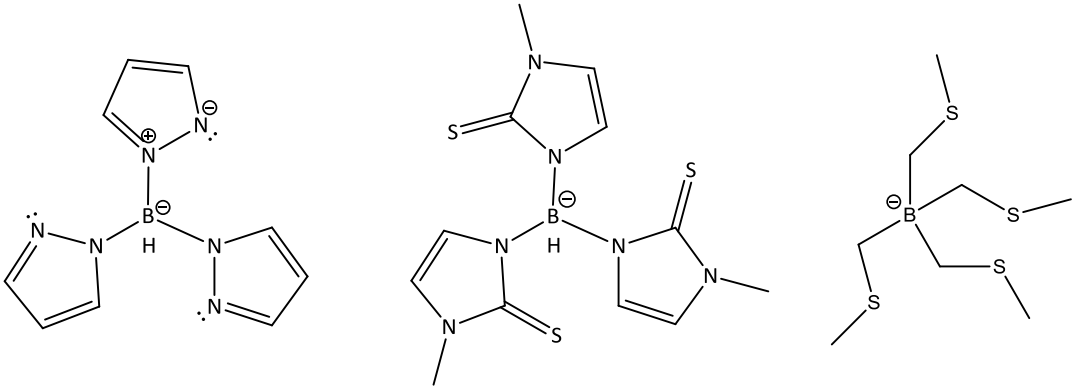

Figure 1.4: Pictorial representation of Tp (left) and Tm^{Me} (centre) and Riordan's tripodal thioether (right).

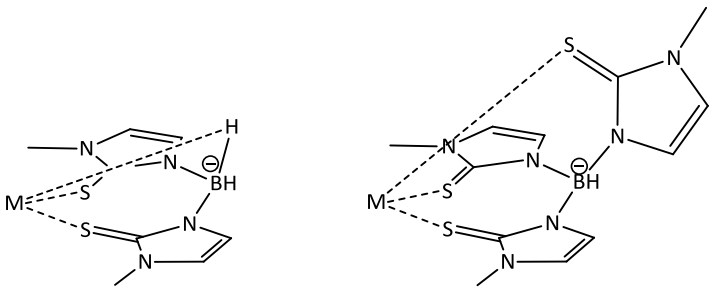

Figure 1.5: Pictorial representation of dihydro*bis*(methimazolyl)borate (Bm^{Me}) left and hydro*tris*(methimazolyl)borate (Tm^{Me}) right.

Unlike Tp^{R}, on complexation Tm^{R} forms an eight membered ring system with the metal.[5,6] This is a natural consequence of the position of the soft donor sulfur on the thio-imidazole ring. This feature gives the ligand more conformational flexibility.[5] Comparing the symmetries of the simple zinc complexes of Tm^{Me} and Tp, we find that whereas Tp has C_3 symmetry, Tm^{Me} has C_{3v} symmetry.[5] Initially studies sought to compare the soft scorpionate anions with the corresponding Tp^{R} anions

and cyclopentadienyl (Cp) anions. In the comparison of a series of six coordinate {$LM(CO)_3$} complexes of the three ligands (Tm^R, Tp^R and Cp), we observe that Tm^R is the strongest electron donor (table 1.2). This suggests that there is a significant contribution from the lone pairs on sulphur (π- basic character).[5,12-15] These effects can be seen in other simple measurements. For example, the magnitude of ligand field splitting, measured in a series of sandwich type iron(II) complexes, is found to follow the order Cp > Tp > Tm^{Me}.[5,12]

ν(CO)/cm^{-1}		
$CpW(CO)_3I$	$TpW(CO)_3I$	$Tm^{Me}W(CO)_3I$
2030	2021	2004
1944	1942	1916
1936	1904	1902

Table 1.2: Comparison of carbonyl stretching frequency for tungsten complexes of Cp, Tp and Tm^{Me} ligands.[14]

The mode of bonding in scorpionates is explained using the Greek letter 'kappa' (κ),[4] where κ^2 indicates bidentate and κ^3 indicating tridentate bonding. For Tp, there are almost always at least two pyrazole rings bonded to the central metal. However, in general Tp is predominantly observed in a κ^3 mode. From the outset it was noticed that Tm^R ligands have greater variety in its coordination modes. An inspection of the sodium complexes is of some value. Not only do we observe the formation of a series of well-defined complexes based on the bonding of the hard sodium cation to the soft sulfur, we find a wide range of coordination modes. Thus examples of sodium complexes where the ligand binds in the κ^3-S,S,S, κ^3-H,S,S, κ^2-H,S and κ^1-S have been reported.[5] There are also examples where the anion and the cation form discrete species and if we extend our analysis further to include related heterocycles (hydro*tris*(2-mercapto-1-phenylimidazolyl)borate, Tm^{Ph}) we find the formation of κ^4 species.[16] Unsurprisingly Bm^R, preferentially coordinates in the κ^3-H,S,S mode. The interaction between metal and the hydrogen in boron has been described as an 'agostic interaction'. However this is not a good description of the

bonding observed. The definition of agostic interaction is 'a distortion in the organometallic moiety which brings the appended -C-H bond into close proximity with the metal centre'.[17,18] It is better to consider this κ^3-H,S,S interaction as if it were a 3 centre 2 electron bond.

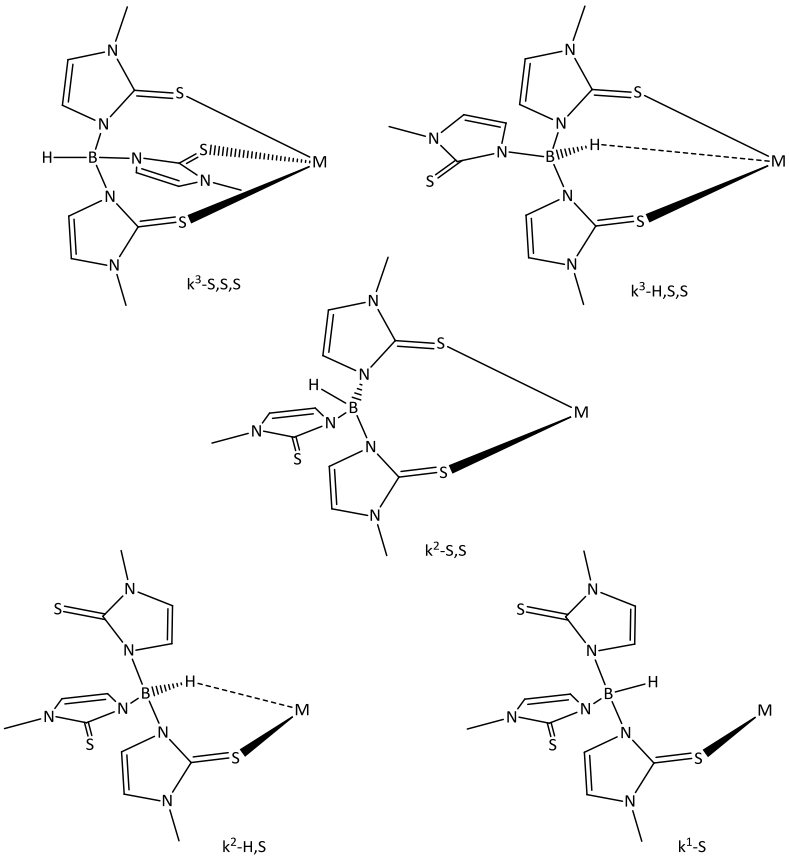

Figure 1.6: Pictorial representation of different coordination modes of Tm- anion.

In complexes where the hydride coordinates, the interaction of the metal with hydrogen results in the formation of κ^3-H,S,S coordination mode. The preference for this coordination mode over the expected κ^3-S,S,S mode is derived from electronic factors rather than the bulk of the rings as was initially thought. The M···H–B coordination is more common with electron-rich metal centres either with 6 or more d electrons or with a low formal oxidation state. Most probably, the high degree of orbital occupancy and high electron density at the metal ion, makes

coordination of the π-donating S atom unfavourable.[5] So the ligand prefers to bind with the hydride to form a κ^3-H,S,S coordination mode rather than the more common κ^3-S,S,S coordination mode because of the less electronically demanding 3-centre-2e interaction. The M···H–B interaction in certain cases can be very strong to the extent that it will resist exchange with Lewis bases such as water or chloride. [5] However, this interaction can be displaced with π-acceptors ligands such as isonitriles and phosphanes thus demonstrating that the nature of the bonding is important to the stability of these motifs.[5,19] This observation has great importance to the application of these anions to bioinorganic chemistry.[20]

The early reports on the soft scorpionates identified the potential for a series of anions involving a mix of methimazole and pyrazole. These have subsequently been prepared. As part of their studies on alcohol dehydrogenase mimics, Parkin and co-workers reported the synthesis of the *bis*(thioimidazolyl)(pyrazolyl)hydroborato anion (figure 1.7).[20] The routes to these anions are not straightforward and Parkin *et al.* prepared the compound by replacing the Zn···H-B interaction in a Bm^{Me} complex with a pyrazole ring. Varhenkamp synthesised the corresponding NS_2 donor system and its zinc complex for a similar purpose by reacting two equivalent of methimazole with one equivalent of potassium borohydride and 3-phenyl-5-methylpyrazole in boiling toluene.[5,21] Each of these groups have made claims about the prowess of these entities.

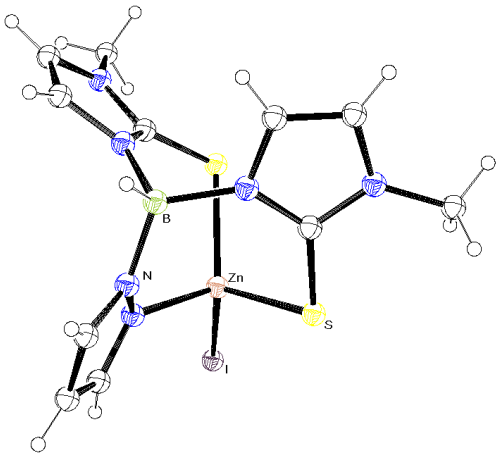

Figure 1.7: Pictorial representation of Zn complex of NS_2 donor scorpionate.[20]

The complex prepared by Vahrenkamp *et al*. (viz $pz^{Me,Ph}$)(Bm^{an}) (figure 1.8) is, to date, the best mimic of alcohol dehydrogenase.[21] However these anions are difficult to prepare and further reports on these anions are limited.

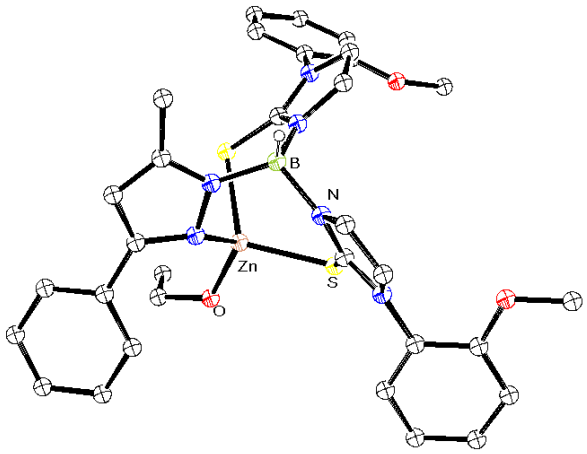

Figure 1.8: X-ray molecular structure of Zn($pz^{Me,Ph}$)(Bm^{an}), the structural model for alcohol dehydrogenase.[21]

Scorpionates have been used in a diverse range of chemistry e.g. C-H bond activation, metal extraction and catalysis.[2-4] As identified above one of the most common applications of the scorpionates is in enzyme modelling. Most of the work in this area is concerned with zinc centred enzymes.[22] However, other metallo-enzymes (table 1.3)[2,3,22] have been studied. Not only have soft scorpionates been used to model enzymes, they are under consideration as potential radiopharmaceuticals.[22]

Enzyme/protein	**Metal**	**Complex**
Active sites in bromoperoxidase	Vanadium	$[VO(O_2)(Tp)(pzH)]$
Alcohol dehydrogenase	Zinc	$Zn(Pz^{Me,Ph})Bm^{an}$, $[ZnTm^{Cum}OClO_3]$
Ada repair protein	Zinc	$[Zn(Tm^{Ph})SPh]$, $[Zn(Tm^{xylyl})SEt$
Sulfite oxidase	Molybdenum	$Mo^{VI}(Tm^{Me})(O)_2Cl$
PN cluster of nitrogenase	Tungsten	$[(Tp^*)_2W_2Fe_5S_9Na(SH)(MeCN)]^{3-}$
Superoxide dismutase	Manganese	$[Mn(Cl)(Tp^{iPr2})(Hpz^{iPr2})]$
Ni-Fe hydrogenase enzyme	Nickel	[Ni(*l*-cysteine)(Tp*)]
Pterin-dependent hydroxylase	Iron	$[Fe(Tp^{iPr2})(OOPtn)]$
Catechol dioxygenases	Iron	$[Fe(C_6H_4O_2)(Tp^*)(HPz^*)]$
α- Ketoglutarate-dependent dioxygenase	Iron	$[Fe^{II}(O_2CC(O)CH_3)(Tp^{Ph2})]$
Blue copper proteins	Copper	$[Cu(SC_6F_5)(Tp^{iPr2})]$, $[Cu(SCPh_3)(Tp^{iPr2})]$
Cu/Zn superoxide dismutase, dopamine monooxygenase, and peptidylglycine α- hydroxylating monooxygenase	Copper	Mononuclear Cu(II)-superoxo species
Mercury detoxification	Mercury	$[HgR(Tm^{tBu})]$

Table 1.3: Some selected metal enzymes and modelling metal scorpionates.[2,3,22]

Scorpionate ligands are well established now. Similar to the development of Tp, there has been a steady increase in the variety of soft scorpionates (figure 1.9). Reglinski and Spicer have reported soft scorpionates based on mercaptobenzothaizole (Tbz) and thiazoline (Ttz) by reacting sodium borohydride with the relevant amine-thione (figure 1.9)[23]

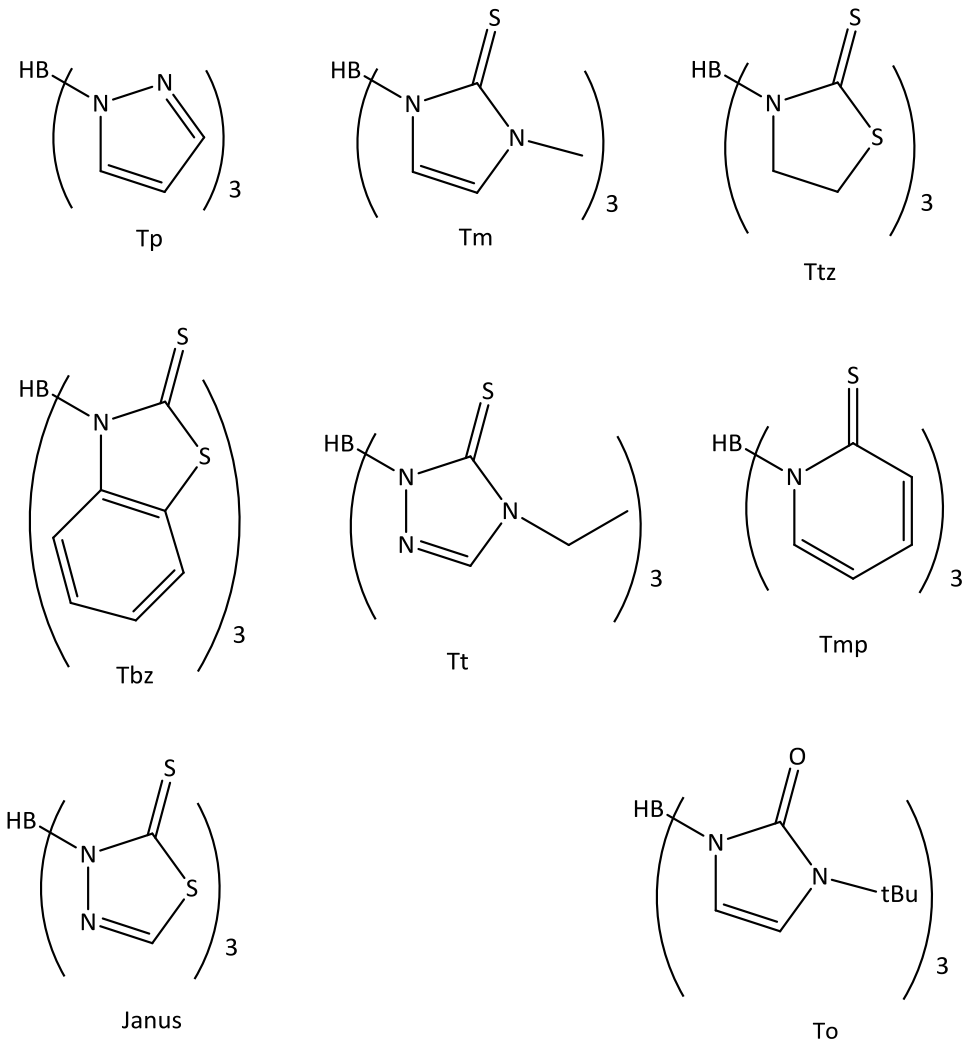

Figure 1.9: Pictorial representation of some of the scorpionate ligands reported.

Bailey *et al*. produced a hybrid N_3/S_3 scorpionate with the introduction of 5-thioxo-4,5-dihydro-3,4-dimethyl-1,2,4-triazole (abbreviated to thioxotriazole, Tt, figure 1.9).[24] This species contains both hard and soft donors within the one ligand. Thus the metal can coordinate with the ligand either through its hard donor nitrogen or through its soft donor sulphur depending on the nature of the metal ion (figure 1.10).

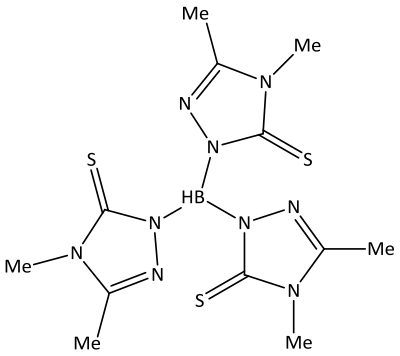

Figure 1.10: Pictorial representation of hybrid N_3/S_3 scorpionate, Tt reported by Bailey *et.al.* in 2001.[24]

In 2006 a hybrid scorpionate was reported by Silva et al., using mercaptothiadiazolyl. The expanding coordination modes for these species led to the introduction of the term Janus scorpionate[25] which provides two sets of donors i.e. hard donors (nitrogen) and soft donors (sulphurs). Thus, hard metal prefers to coordinate through nitrogen whereas soft metals prefer sulphur (Figure 1.11). Once the ability to replace the donor atoms themselves was appreciated reports of tripodal oxygen, phosphorus and selenium donor scorpionates appeared.[3,26,27]

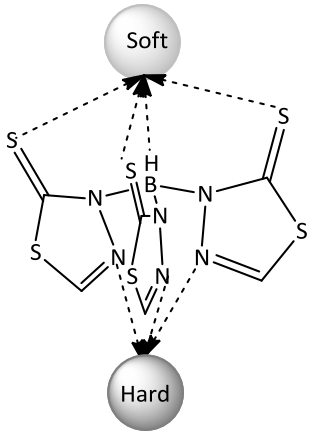

Figure 1.11: Pictorial representation of Janus scorpionate. Hard metal binds the ligands through hard donor nitrogen where as soft metals prefer to binds through soft donor sulphur.[25]

Replacing the hydrogen at the boron with an alkyl or aryl substituents (e.g. methyl, phenyl, cyclooctane-1,5-diyl), generates further new classes of ligand. Similarly

attempts have been made to replace the boron bridgehead atom and new families of ligands where carbon, aluminium, indium, silicon and gallium replace the boron have been reported (figure 1.12).[2]

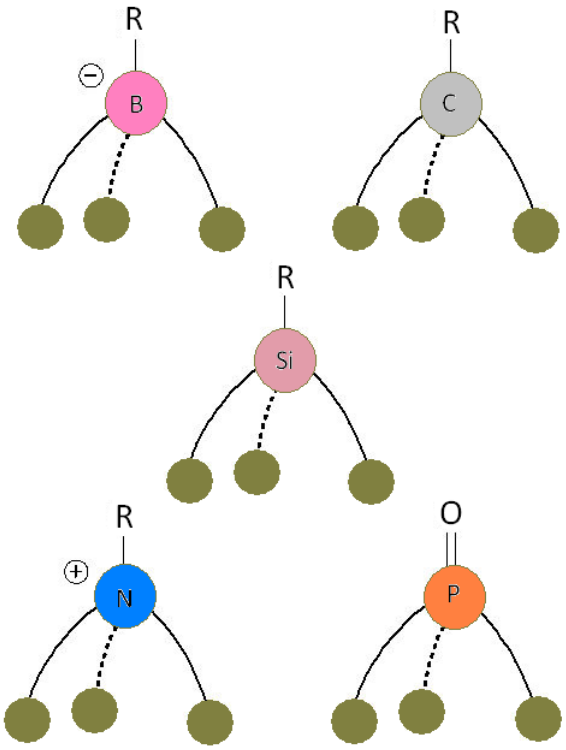

Figure 1.12: Pictorial representation of different tripodal ligands. Donor atoms are indicated in dark green colour. R= H, alkyl or aryl substituent. The picture is adapted from reference 28 and redrawn.

Interestingly, not all these scorpionates produce metal complexes and many studies focus on the decomposition of the species.[5,29] It is becoming evident that soft scorpionates are not as stable as their Tp analogues and they can be prone to oxidative degradation or rearrangement.[5] For example, the product formed from the reaction of $Cu(II)Cl_2$ with $NaTm^{Me}$ namely, $[Cu(I)Cl(mtH)(\mu\text{-}mtH)]_2$ (where mtH = methimazole (scheme 1.2) is a good example of oxidative degradation.[5]

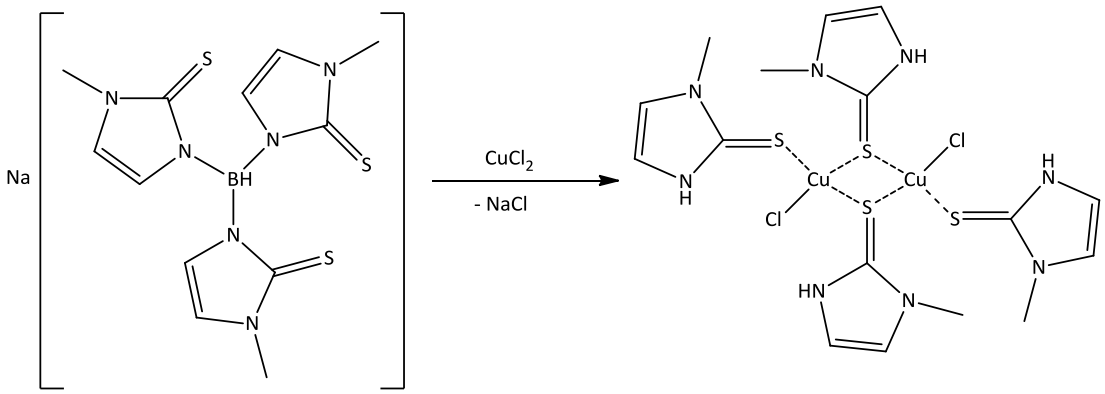

Scheme 1.2: Reaction of $NaTm^{Me}$ with $CuCl_2$.

Similar reactions have been observed in reactions of soft scorpionates with iron(III) and platinum(II) salts.[5] There are a number of notable examples where complexes of soft scorpionates have not been reported or are rare. These reactions are typically prone to degradation.

The chemistry of the soft scorpionates has produced some interesting serendipitous chemistry. Hill *et al*. identified the presence of the retrodative M-B bond.[30] This is a motif which is rare in inorganic chemistry in general but is now common for the soft scorpionates. Such complexes are commonly known as boratranes. To date the mechanism by which these species form is not agreed. It has been suggested that oxidative addition leads the metal to activate the B-H bond and thereby the metal has an interaction with the hydrogen in the boron (M·····H-B). The metal hydride now reacts with hydrogen acceptors by the reductive elimination which leads to the formation of a metal boron dative bond.[5]

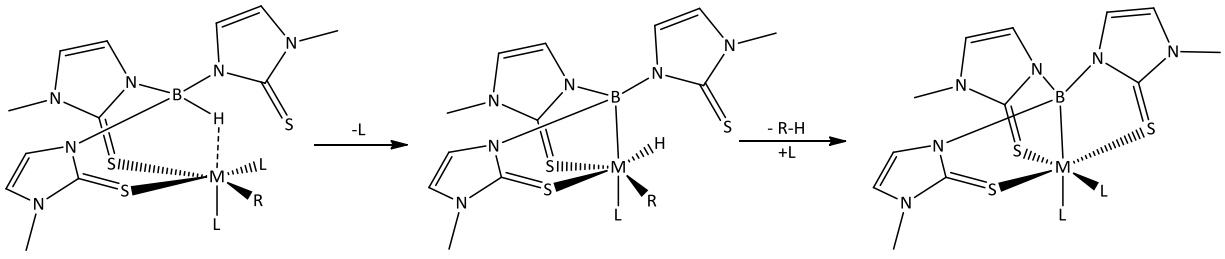

Chart 1.1: Schematic representation of possible boratrane formation mechanism.

A ring closed compound has been isolated from the mixtures of $NaBm^{Me}$ or $NaTm^{Me}$ during prolonged Soxhlet extraction with dichloromethane (scheme 1.3).[31] This reaction will be explored further in this work (Chapter 3).

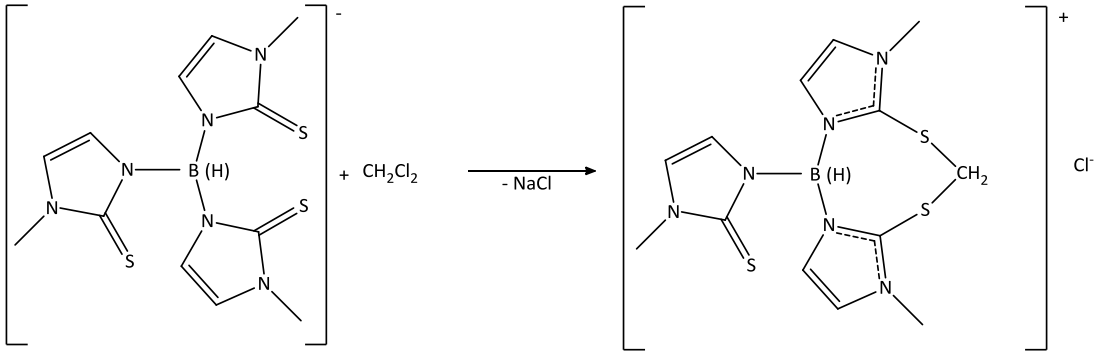

Scheme 1.3: Reaction of $NaTm^{Me}$ with dichloromethane to form ring closure in soft scorpionates.

The reactions of $[TmMo(CO)_3]^-$ with NO^+, produces a number of intriguing species (figure 1.13) including a novel heterocycle and a DMF-borane adduct.[15] Bailey *et al*. has recently reported the rational synthesis of the DMF borane.[32] Work presented in this thesis will explore the formation of heterocycles further. However, an inspection of many of these reactions suggests that the hydride in Tm^R is much more reactive than the corresponding hydride in Tp^R.[5,15]

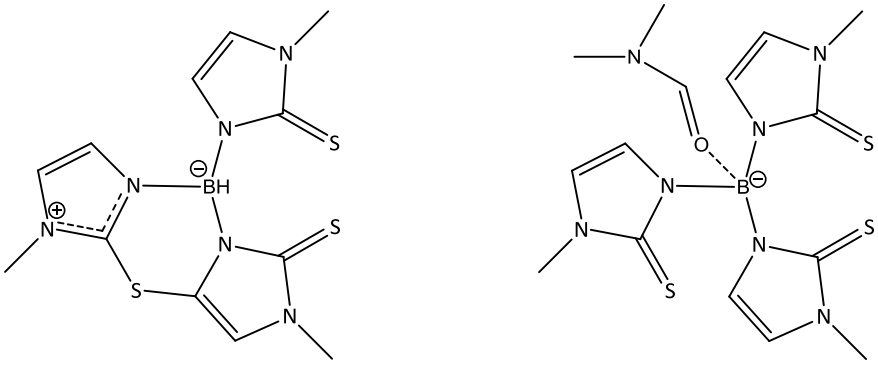

Figure 1.13: The products isolated from the reaction of Tm^{Me} with NO^+. Left is the so-called "crossbow complex" which is described in more detail in chapter 3 and, right, the DMF-$B(mt)_3$ adduct.

The chemistry of soft scorpionates is still a growing field and many groups worldwide are studying their behaviour and influence.[2,3] Representative compounds and metal complexes of the soft scorpionates from all regions of the periodic table apart from the lanthanoids have now been reported. The stability of the soft scorpionates with lower main group elements leads to the observation that the chemistry of soft analogues of Tp are now more expansive than the parent pyrazolyl based species.[5] As Trofimenko said in his first report, the branch is fertile and has remarkable scope and this thesis 'Exploring the chemistry of soft scorpionate ligands' focuses on the further recent development of the methimazole based hetero and homo soft scopionates.

1.2 Aim of the study

The aim of this work was to explore the chemistry of soft scorpionate ligands further. Thus far the chemistry has been based on the ligand being complexed to metals. Species such as phosphine-gold and $Mn(CO)_5$ fragments are isolobal with the alkyl groups.[33-38] This suggest that the chemistry with Me^+ (and other electrophiles) requires to be explored further.[33-38] Thus we have investigated the reactivity of soft scorpionates with alkylating agents.

The mode of coordination differs in soft scoprpionate complexes. This leads to a wide variety of applications including the biomimetic studies of sulphur donor soft scorpionate complexes. Studies on the κ^3-H,S,S technetium complexes suggest that these molecules which contain this motif might be selective for π-acid ligands. This suggests that there may be new, selective applications for soft scorpionate complexes. Nitric oxide remains an important bio-molecule and its interaction with soft scorpionates complexes may be of some interest to the design of nitric oxide scavengers.

A remaining issue of importance are the steric effects on soft scorpionate ligands. Tp was developed using bulky substituents and much of the variety in the chemistry reported is derived from the steric influence of Tp^R ligands.[2] The importance of steric effects in Tm^R is not properly understood and an analytical inspection of the volumes these ligands occupy would be timely.

1.3 References:

1. Trofimenko, S. *J. Am. Chem. Soc*. **1966**, *88*, 1842-1843.
2. Trofimenko, S. *Scorpionates The coordination chemistry of polypyrazolylborate ligands, Imperial College Press.* **1999.**
3. Pettinari, C. *Scorpionates II: Chelating borate ligands, Imperial College Press*. **2008**.
4. Trofimenko, S. *J. Chem Ed.* **2005**, *82*, 1715-1720.
5. Spicer, M. D.; Reglinski, J. *Eur. J. Inorg. Chem*. **2009**, 1553-1574.
6. Reglinski, J.; Garner, M.; Cassidy, I. A.; Slavin, P. A.; Spicer, M. D.; Armstrong, D. R. *J. Chem. Soc. Dalton Trans*. **1999**, 2119-2126.
7. Ge, P.; Haggerty, B. S.; Rheingold, A. L.; Riordan, C. G. *J. Am. Chem. Soc.* **1994**, *116*, 8406-8407.
8. Garner, M.; Reglinski, J.; Cassidy, I.; Spicer, M. D.; Kennedy, A. R. *Chem Commun*. **1996**, 1975-1976.
9. Bailey, P. J.; Dawson, A.; McCormack, C.; Moggach, S. A.; Oswald, I. D. H.; Parson, S.; Rankin, D. W. H.; Turner, A. *Inorg. Chem*. **2005**, *44*, 8884-8898.
10. Hill, A. F.; Owen, G. R.; White, A. J. P.; Williams, D. *Angew. Chem. Int. Ed*. **1999**, *38*, 2759-2761.
11. Kunz, K.; Bolte, M.; Wagner, M.; Lerner, H. *Z. Anorg. Allg. Chem*. **2009**, 1580-1584.
12. Smith, J. M. *Comments on Inorg. Chem*. **2008**, *29*, 189-233.
13. St.-J. Foreman, M. R.; Hill, A. F.; White, A. J. P.; Williams, D. J. *Organometallics* **2003**, *22*, 3831-3840.
14. Garner, M.; Lehmann, M.; Reglinski, J.; Spicer, M. D. *Organometallics* **2001,** *20*, 5233-5236.

15. Schwalbe, M.; Andrikopoulos, P. C.; Armstrong, D. R.; Reglinski, J.; Spicer, M. D. *Eur. J. Inorg. Chem*. **2007**, 1351-1360.

16. Bridgewater, B. M.; Parkin, G. *Inorg. Chem. Commun*. **2000**, *3*, 534-536.

17. Brookhart, M.; Green M. L. H. *J. Organomet. Chem*. **1983**, *250*, 395-408.

18. Scherer, W.; McGrady, G. S. *Angew. Chem., Int. Ed. Engl*. **2004**, *43*, 1782-1806.

19. Abernethy, R. J.; St.-J. Foreman, M. R.; Hill, A. F.; Tshabang, N. Willis, A. C.; Young, R. D. *Organometallics* **2008**, *27*, 4455-4463.

20. Kimblin, C.; Hascall, T.; Parkin, G. *Inorg. Chem*. **1997**, *36*, 5680-5681.

21. Seebacher, J.; Shu, M.; Vahrenkamp, H. *Chem. Commun.* **2001**, 1026-1027.

22. Reglinski, J.; Spicer, M. *Curr. Bioact. Compd.* **2009**, *5*, 264-276.

23. Ojo, J. F.; Slavin, P. A.; Reglinski, J.; Garner M.; Spicer, M. D.; Kennedy, A. R.; Teat, S. J. *Inorg. Chim. Acta* **2001**, *313*, 15-20.

24. Bailey, P. J.; Lanfranchi, M.; Marchio, L.; Parsons, S. *Inorg. Chem*. **2001**, *40*, 5030-5035.

25. Silva, R. M.; Gwengo, C.; Lindeman, S. V.; Smith, M. D.; Gardinier, J. R. *Inorg. Chem*. **2006**, *45*, 10998-11007.

26. Al-Harbi, A.; Sattler, W.; Sattler, A.; Parkin, G. *Chem. Commun*. **2011**, *47*, 3123-3125.

27. Minoura, M.; Landry. V. K.; Melnick, J. G.; Pang, K.; Marchio, L.; Parkin, G. *Chem. Commun.* **2006**, 3990-3992.

28. Gennari, M. PhD Thesis **2007**, University of Parma, Scorpionate ligands and surroundings; Coordination properties –solution studies.

29. Wallace, D. PhD Thesis **2008**, University of Strathclyde, An insight into the chemistry and applications of soft scorpionates.

30. Hill, A. F.; Owen, G. R.; White, A. J. P.; Williams, D. J. *Angew. Chem. Int. Ed.* **1999**, 38, 2759-2761.

31. Crossley, I. R.; Hill, A. F.; Humphrey, E. R.; Smith, M. K.; Tshabang, N.; Willis, A. C. *Chem. Commun*. **2004**, 1878-1879.

32. Bailey, P. J.; Bell, N. L.; Nichol, G. S.; Parsons, S.; White, F. *Inorg. Chem.* **2012**, *51*, 3677-3689.

33. Mohamed, A. A.; Rabinovich, D.; Fackler, J. P. *Acta Crystallogr., Sect. E,* **2002**, *58*, m726-m727.

34. Patel, D. V.; Mihalcik, D. J.; Kreisel, K. A.; Yap, G. P. A.; Zakharov, L. N.; Kassel, W. S.; Rheingold, A. L.; Rabinovich, D. *Dalton Trans.* **2005**, 2410-2416.

35. Dodds, C. A.; Garner, M.; Reglinski, J.; Spicer, M. D. *Inorg. Chem.* **2006,** *45,* 2733-2741.

36. Bailey, P. J.; Lorono-Gonzales, D. J.; McCormack, C.; Parsons, S.; Price, M. *Inorg. Chim. Acta* **2003**, *354*, 61-67.

37. Graham, L. A.; Fout, A. R.; Kuehne, K. R.; White, J. L.; Mookherji, B.; Marks, F. M.; Yap, G. P. A.; Zakharov, L. N.; Rheingold, A. L.; Rabinovich, D. *Dalton Trans.* **2005**, 171-180.

38. Bailey, P. J.; Budd, L.; Cavaco, F. A.; Parsons, S.; Rudolphi, F.; Sanchez-Perucha, A.; White, F. J. *Chem. Eur. J*. **2010**, *16*, 2819-2829.

Chapter 2

Alkylation of soft scorpionates

2.1 Introduction

2.1.1 DNA methylation and the Ada repair protein

DNA methylation controls gene expression and is thus an important process in all organisms. Consequently, organisms contain a wide range of methylating agents. These include S-adenosylmethionine, N-methyl-N-nitro-N-nitroso-guanidine, N-methyl-N-nitrosourea and methyl methanesulfonate. Typically methylation occurs at the cytosine residues (figure 2.1) on CpG dinucleotides. These dinucleotides are unevenly distributed in mammalian DNA and have a higher density in special regions commonly called CpG islands.[1] CpG islands are genomic regions in the DNA that contains cytosine and guanine residue bonded through a phosphodiester bond. It has been estimated that there are approximately 30,000-40,000 CpG islands within the nucleic acid strands and within these islands the density of CpG dinucleotides can be 10-20 times higher than found in "normal DNA" .[2]

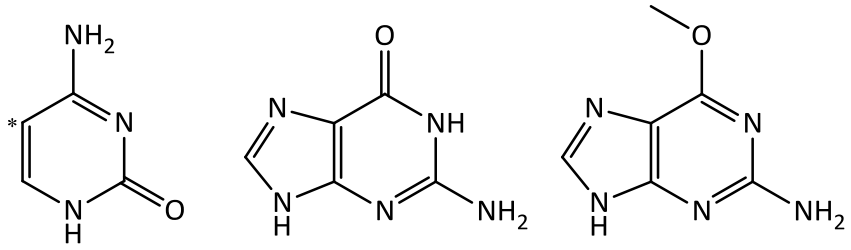

Figure 2.1: (a) Cytosine, (b) Guanine and (c) O^6-Methylguanine. * denotes the position at which methylation occurs on cytosine.

Random alkylation of DNA can also occur (figure 2.2). However, this is potentially damaging to the host organism. Alkylation can lead to cross linking of DNA strands preventing their separation and thus protein synthesis. Alkylating agents can induce irreparable radical mediated DNA fragmentation. The undesired methylation at the O^6 position on guanine residues (figure 2.1) leads to the formation of O^6-methylguanine which in turn leads to the mis-pairing of the DNA strands. Under these circumstances guanine pairs more favourably with thymine rather than guanine's natural partner cytosine. This modification has been implicated in the

onset of certain diseases such as cancer.[3] The first two processes make the DNA unavailable for transcription whereas the latter introduces mutations.

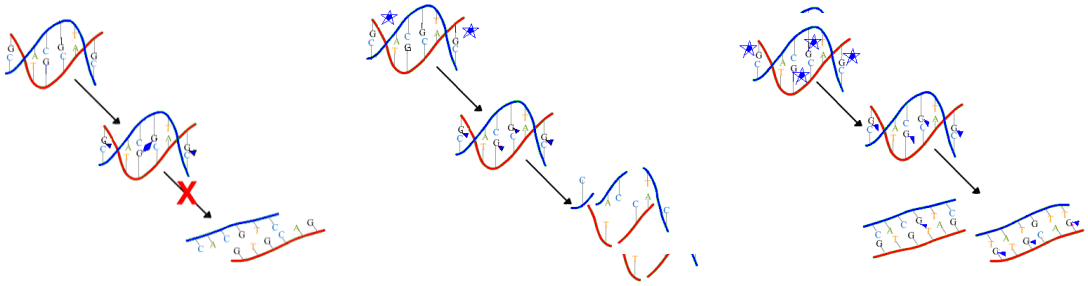

Figure 2.2: Alkylation damage of DNA. Left. The formation of cross bridges prevent DNA fragmentation. Middle. DNA has been fragmented as a result of repair. Right. the mis-pairing of DNA. The stars indicating alkylating agents. Small carbon compounds are represented as blue triangles. The picture has been adapted and redrawn from http://www.cancerquest.org/genotoxic-chemotherapy-drugs.

For DNA viability and gene regulation it is important that, where possible, these alkylation processes can be reversed. In E-coli, there are two types of methyltransferase employed for this purpose namely the 39-kDa Ada protein (figure 2.3) and the 19-kDa Ogt protein.[3] It is the Ada protein which is of interest here.

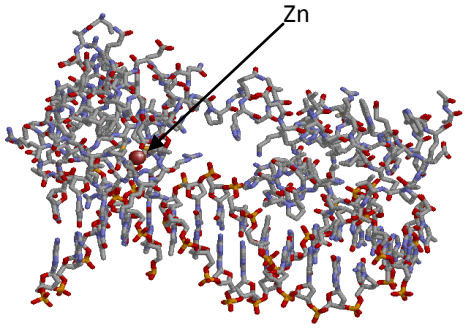

Figure 2.3: Ada bound DNA complex.[4] The zinc atom is shown in space fill mode. The figure has been redrawn from the coordinates downloaded from the PDB database (1U8B).

As discussed above (figure 2.2) alkylation damage at DNA occurs at many points. The Ada repair protein is able to remove unwanted methyl groups from both O^6-methyl guanine and those attached to the phosphodiester chains. However, the

methyl groups on the methylphosphodiester are transferred by the N-terminal domain of the Ada protein and the methyl groups on O^6-methylguanine by the C-terminal domain of Ada.[3]

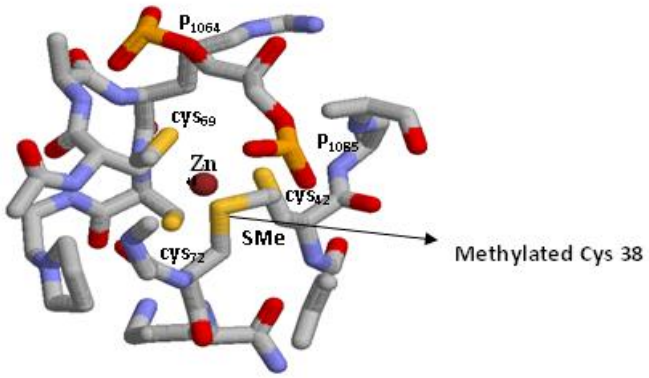

Figure 2.4: The active site on the N terminal of domain of the Ada protein.[4] Zinc is coordinated to four cysteine residues namely Cys42, Cys69, Cys72 and Cys38. During demethylation of DNA the methyl group from methylphosphodiester is transferred to Cys38 of the Ada protein and the methyl group from O^6-methylguanine transfers to Cys321. This irreversible transformation inactivates Ada. However, it activates other proteins in the repair system. The figure has been redrawn from the coordinates downloaded from the PDB database (1U8B).

Ada is a zinc protein. In the resting state the metal is co-ordinated to four cysteine residues Cys69, Cys42, Cys72 and Cys38.[5] In the native enzyme all four cysteine residues are found in the S-configuration.[6] Alkylation involving the methyl phosphodiester leads to the migration of a methyl group to Cys38. The migration is controlled by the absence of hydrogen bonding and by the use of the zinc at the enzymes active site. The latter makes the thiolate at Cys38 more nucleophilic.[7] Thus the zinc plays a catalytic rather than a conformational role in the overall process.[8] After alkylation the zinc remains coordinated to the thioether generated (figure 2.4).[6]

In contrast to the above, alkylation from O^6-methyl guanine and O^4-methylthymine involves the active site on the C-terminal domain of the Ada protein i.e. Cys321. Unlike the site on the N-terminal domain, this site is buried under the protein surface. Alkylation of Cys321 is also mediated by the zinc atom, but in this instance it is accompanied by a conformational change in the protein. Consistent with the

alkylation of Cys38, methylation at Cys321 inactive the proteins. However in this case it increases the trans-activating capacity of Ada protein.[6]

There are very few ligands that can generate ZnS_3 and ZnS_4 complexes which can mimic the active site of the Ada repair protein. Significantly the methimazolyl based soft scorpionates are preeminent in this regard.[9,10]

2.1.2 Biomimetic applications of the Scorpionates

Scorpionates have been used in a diverse range of chemistry e.g. C-H bond activation, metal extraction and catalysis. One of their earliest applications was in enzyme modelling.[9,11] Kitajima *et al*. was instrumental in showing functional and structural zinc centred enzyme modelling.[10,12] More recently Parkin and Vahrenkamp have demonstrated the importance of the soft scorpionates of zinc as models of zinc containing enzymes e.g. carbonic anhydrase, liver alcohol dehydrogenase, S-aminolevulinate dehydratase.[13,14] Attempts have also been made to model Ada using Tm^R. Bridgewater *et al*. investigated the reactivity of $[Tm^{Ph}]$ZnSPh as a potential model of Ada. In this instance the methyl is transferred to a coordinated thiolate which in turn leads to the formation of the thioether, PhSMe, and $[Tm^{Ph}]$ZnI (Scheme 2.1).[15] Although they have successfully transferred the methyl group the zinc thioether bond severs. Thus the model does not properly represent the process taking place. A related reaction has been reported by Ibrahim *et al.* using Tm^{xyly}Zn-SR and methyl iodide or trimethyl phosphate. Again the alkyl group migrates to the thiolate and not the scorpionate thione.[16]

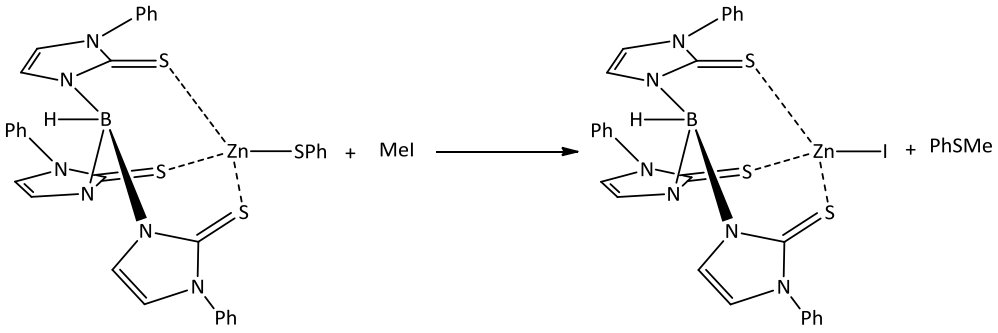

Scheme 2.1: The reaction of [Tm^{Ph}]ZnSPh with methyl iodide.[15]

Reactions employing methyl iodide can be considered as models of alkyl transfer to Cys321 from the O^6-methylguanine to C-terminal domain of Ada. In contrast the use of trimethylphosphate as the methyl source generates a process which models the transfer of a methyl group from the methylphosphodiester using the N-terminal domain of the Ada protein.[16] However, in neither of the models described does the scorpionate sulphur act as an alkyl group acceptor. A precedent for this reaction exists. Crossley *et al.* have reported the reaction of Tm^{Me} with dichloromethane which produces a novel polycyclic ring compound where two methimazole rings are connected via a $–CH_2-$ group (figure 2.5).[17] Crossley's study indicates that Tm^{Me} will react with alkyl halides. Indeed reactions such as that described above serve as models of the behaviour of the Ada apo-enzyme. It is thus of some interest to further investigate the reactions of the Tm^{Me} anion with alkylating agents in the absence of zinc.[17]

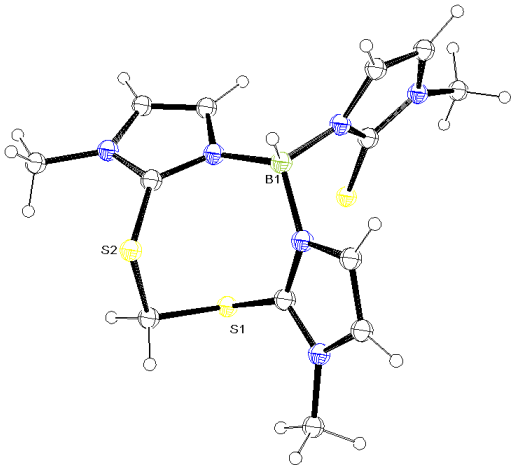

Figure 2.5: The X-ray molecular structure of (*bis*(1-methylimidazol-2-yl-thio)methane-N,N')-(1-methyl-2-thioimidazol-3-yl) borane chloride monohydrate.[17] Counter ions and solvent molecules are omitted for clarity.

The aim of this study is to explore the reactions of soft scorpionate anions with alkylating agents.

2.2 Experimental section

All chemicals used were commercially available and used without any purification. $NaTm^{Me}$ was prepared using literature method.[18] NMR spectra were recorded using a Bruker AV500 or Bruker DPX400. All the spectra obtained were referenced to the residual solvent peaks. IR spectra were recorded as KBr discs using a Nicolet Avatar 360 FT-IR spectrometer. Mass spectra were recorded using a Thermo Finnigan LCQDuo by electrospray ion trap and a Thermo scientific LTQ orbitrap for accurate mass. Crystals obtained were coated in mineral oil and mounted on glass fibres or a glass loop. Data were collected at 123K on Oxford diffraction diffractometer using graphite monochromated Mo-Kα radiation. The heavy atom positions were determined by Patterson methods and the remaining atoms located in the difference electron density maps. Data were solved using Shelx 97 [19] and SIR 92 [20] using the graphical interface, Wingx.[21] All non-hydrogen atoms are anisotropic. The hydrogen atoms are placed as a mixture of independent and constrained refinement in the calculated positions around the parent atoms. Density Functional Theory Calculations were performed by Dr. D. R. Armstrong (University of Strathclyde) using the Gaussian computational package G03. In this series of calculations the B3LYP density functionals and the 6-311G(d,p) basis set were used. After each geometry optimisation, a frequency analysis was performed. The energy values quoted include the zero point energy contribution.

2.2.1 Preparation of $TmS^{Me}I_2$

Methyl iodide (0.30 g, 2.11 mmol) and $NaTm^{Me}$ (0.19 g, 0.50 mmol) were stirred in chloroform (20 ml) for 24 hours. The white powder formed was filtered off using a Buchner funnel and extracted with DMF. The soluble part was filtered through celite. The crystals were obtained by the vapour diffusion of this clear solution with diethyl ether. Yield 0.091 g (26%). Anal. calcd. for $C_{15}H_{25}N_6BS_3I_2$: C, 27.70; H, 3.88; N, 12.92%. Found C, 26.99; H, 3.59; N, 12.85%. ESI-MS $[TmS^{methyl}]^{2+}$: 198 (100%). Accurate mass predicted 198.06925, found 198.06970. ^{1}H-NMR (500 MHz, DMSO): δ = 8.07 (d, 3H, ^3J(H,H) = 2.1 Hz; CH), 7.30 (d, 3H, ^3J(H,H) = 2.1 Hz; =CH), 4.02 (s, 9H, -

CH_3), 3.40 (s, 9H, -CH_3). ^{13}C- NMR (125 MHz,DMSO): δ = 143.1, 127.0, 125.1, 36.4, 17.97 ppm. FT-IR (KBr, cm^{-1}): 2450 (B-H), 754.7 (C-S).

2.2.2 Preparation of $TmS^{allyl}Br_2$

Allyl bromide (0.183 g, 1.53 mmol) and $NaTm^{Me}$ (0.188 g, 0.50 mmol) were refluxed in chloroform (20 ml) overnight. The white powder formed (NaBr) was removed by gravity filtration and the resulting clear solution taken to dryness under vacuum. The resultant white residue was re-dissolved in the minimum amount of DMF and filtered through celite. The crystals were obtained by the vapour diffusion of this clear solution with diethyl ether. Yield 0.198 g (64%). Anal. calcd. for $C_{21}H_{31}N_6BBr_2S_3$: C, 39.78; H, 4.89; N, 13.26%. Found C, 39.69; H, 4.82; N, 13.07%. ESI-MS $[TmS^{allyl}]^{2+}$: 236.5 (100%). Accurate mass predicted 237.09272, found 237.09238. ^{1}H-NMR (500 MHz, $CDCl_3$): δ = 7.93 (d, 1H, ^3J(H,H) = 1.95 Hz; CH), 7.75 (d, 1H, ^3J(H,H) = 1.95 Hz; CH), 5.84 (sex, 1H, -CH), 5.13 (m, 2H, =CH_2), 4.12 (s, 3H, CH_3), 3.67 (d, 2H, ^3J(H,H) = 7.2 Hz; -CH_2). ^{13}C- NMR (125 MHz,CDCl): δ = 140.5, 131.7, 127.9, 126.3, 120.7, 39.1, 37.2 ppm. FT-IR (KBr, cm^{-1}): 2492 (B-H), 760 (C-S).

2.2.3 Preparation of $TmS^{benzyl}Br_2$

Benzyl bromide (0.256 g, 1.50 mmol) and $NaTm^{Me}$ (0.187 g, 0.50 mmol) were refluxed overnight in chloroform (20 ml). The white precipitate formed (NaBr) was removed by gravity filtration and the resulting clear solution taken to dryness in a vacuum. The white residue formed was re-dissolved in methanol and filtered through celite. Crystals were obtained by the vapour diffusion of this solution with diethyl ether. Yield 0.285 g (78%). Anal. calcd. for $C_{33}H_{37}N_6BBr_2S_3$: C, 50.54; H, 4.72; N, 10.72%. Found: C, 49.74; H, 4.85; N, 10.22%. ESI-MS $[TmS^{benzyl}]^{2+}$: 311.5 (100). Accurate mass predicted 198.06925, found 198.06970. ^{1}H-NMR (500MHz, $CDCl_3$): δ = 7.93 (s, 1H, -CH), 7.65 (d, 1H, -CH), 7.36 (Mix, 1 or 2H, -CH Aro), 7.05 (d, ^3J(H,H) = 6.3 Hz, 1H, -CH Aro) 4.2 (s, 2H, -CH_2) 3.55 (s, 3H, -CH_3). ^{13}C-NMR (125 MHz, $CDCl_3$): δ = 139.9, 135.6, 129.35, 128.8, 128.6, 128.05, 126.8, 40.7, 36.5 ppm. FT-IR (KBr, cm^{-1}): 2361(B-H), 755 (C-S).

2.2.4 Attempted preparation of $TmS^{Propyl}Br_2$

2- Bromopropane (0.1832 g, 1.49 mmol) and $NaTm^{Me}$ (0.1862 g, 0.497 mmol) were heated to reflux in chloroform (10 ml) overnight. The white precipitate formed (NaBr) was removed by gravity filtration and the resulting clear solution was taken to dryness in a vacuum. The white residue was re-dissolved in methanol and filtered through celite. Crystals are obtained by the vapour diffusion with diethyl ether. Yield 0.064 g (36%). Anal. calcd. for ($C_{12}H_{17}N_6BS_3.3H_2O$): C, 35.46; H, 5.71; N, 20.69%. Found: C, 36.21; H, 4.63; N, 20.66%. ESI-MS $[Tm]^-$: 351 (100). Mass predicted 351.

2.2.5 Attempted preparation of $TmS^{benzene}Br_2$

Iodobenzene (0.306 g, 1.50 mmol) and $NaTm^{Me}$ (0.188 g, 0.50 mmol) were refluxed in chloroform (20 ml) overnight. The white precipitate formed (NaBr) was removed by gravity filtration and the resulting solution taken to dryness in a vacuum. The white residue formed was dissolved in the minimum amount of methanol and filtered through celite. Crystals were obtained by the vapour diffusion of this solution with diethyl ether. Yield 0.013 g (7%). (Anal. calcd. for ($C_{12}H_{17}N_6BS_3.3H_2O$): C, 35.46; H, 5.71; N, 20.69%. Found: C, 33.18; H, 4.84; N, 19.24%. ESI-MS $[Tm]^-$: 351 (100). Mass predicted 351.

2.2.6 Preparation of sodium hydro*tris*(mercaptobenzothiazolyl)borate ligand (NaTbz)

2-mercaptobenzothiazole (13 g, 78 mmol) and sodium borohydride (1.01 g, 26 mmol) were placed in a dry 100 ml round bottom flask fitted with an air jacket and heated in an oil bath with continuous stirring (see experimental setup 1, page number 87). The mixture was heated to 160 ^oC releasing hydrogen gas as the mixture melts. The temperature was raised slowly to 180-185^oC being maintained at this temperature for a further 30 mins. The temperature was slowly raised to 190^oC and held there for an hour. The hydrogen gas evolved was measured throughout to ensure that almost three molar equivalent of gas was released. The mixture was

allowed to cool to room temperature to give a hard yellow mass. A 1:1 v:v mixture of chloroform and THF (20 ml total volume) was added and the mixture stirred vigorously overnight to remove any un-reacted mercaptobenzothiazole. The yellow suspension formed is filtered under vacuum and powder washed a further three times with 10 ml aliquots of 1:1 $CHCl_3$/THF. The yellow residue thus obtained was washed with diethyl ether (20 ml) and air dried. The material obtained was sufficiently pure for further use. However, pure crystalline NaTbz ($Na(C_{21}H_{13}B_1N_3S_6).1.5\ H_2O$) could be obtained by extracting NaTbz into chloroform. The extract was filtered through celite and recrystallised by vapour diffusion with diethyl ether. Yield 2.091 g (15%). Anal. calcd. for $Na[B(C_{21}H_{16}N_3S_6)].3H_2O$: C, 44.11; H, 3.48; N, 6.68%. Found: C, 44.23; H, 3.87; N, 6.73%. ESI-MS $[Tbz]^-$: 512 (5%), 166 (100%). Accurate mass predicted 511.96778; found: 511.96835. ^{1}H-NMR (500 MHz, $(CD_3)_2CO$): δ = 7.05 (br, 2H), 7.35 (br, 2H). ^{13}C-NMR (125 MHz, $(CD_3)_2CO$): δ = 195, 146.9, 130.8, 126.6, 124.4, 120.1, 115.6 ppm. FT-IR (KBr, cm^{-1}): 750 (C=S) -BH stretch cannot be seen in the spectrum.

2.2.7 Preparation of $Bz^{allyl}Br$

NaTbz (0.28 g, 0.5 mmol) and allyl bromide (0.20 g, 1.67 mmol) were refluxed in chloroform (20 ml) overnight. The mixture was taken to dryness to give a yellow oil. The oil was extracted with methanol and the resulting solution filtered through celite. Crystals were obtained by the vapour diffusion of this solution with diethyl ether. ESI-MS $[Tbz^{allyl}]^-$: 208 (100), Mass predicted: 208. ^{1}H-NMR (500MHz, DMSO): δ = 8.02 (d, ^3J(H,H) = 8 Hz, -CH), 7.86 (d, ^3J(H,H) = 8 Hz, -CH), 7.47 (m, -CH), 7.37 (t, ^3J(H,H) = 8 Hz, -CH), 6.1 (m, -CH allyl), 5.45 (d, ^3J(H,H) = 17 Hz, -**H**CH), 5.35 (d, ^3J(H,H) = 10 Hz, -HC**H**), 4.1 (d, ^3J(H,H) = 7 Hz, $-CH_2$) ppm.

2.2.8 Preparation of sodium *tetrakis*(thiazolyl)borate ligand (NatzTtz)

Sodium borohydride (0.5 g, 13 mmol) was mixed with thiazoline (6.584 g, 56 mmol) in a dry 100 ml round bottom flask fitted with an air jacket and heated in oil bath with constant stirring. The mixture was slowly heated to 160^{o}C resulting in the evolution of hydrogen gas. The temperature was maintained at 160-165^{o}C for an

hour or until gas evolution ceased. The mixture was allowed to cool to room temperature to give a hard off-white mass. Toluene (20 ml) was added to the flask and the mixture stirred vigorously overnight. The resulting suspension was filtered by Buchner filtration and re-suspended in hot toluene and stirred for another 15 minutes. The precipitate was collected in a crucible and washed with hot toluene (3 x 20 ml) to remove un-reacted thiazoline and then air dried. The resulting powder can be re-crystallised from methanol/diethyl ether by vapour diffusion. Yield 2.013 g (28%). Anal. calcd. for $Na[B(C_{12}H_{16}N_4S_8.2H_2O)]$: C, 26.56; H, 3.71; N, 10.32%. Found: C, 26.04; H, 3.71; N, 10.23%. ESI-MS $[tzTtz]^-$: 482.93(100). Accurate mass predicted 482.9242; found 482.9239. ^{1}H-NMR (500 MHz, DMSO): δ = 4.97 (m, 4H, -**H**CH), 4.45 (m, 4H, -HC**H**), 3.25 (m, 4H, -**H**CH), 3.16 (m, 4H, -HC**H**). ^{13}C-NMR (125 MHz, DMSO): δ = 199.46, 61.73, 31.26 ppm. FT-IR (KBr, cm^{-1}): 722.08 cm^{-1} (C=S).

2.2.9 Preparation of $Tz^{allyl}Br$

Sodium *tetrakis* thiazolyl borate (NatzTtz: 0.2510 g, 0.5 mmol) and allyl bromide (0.2565 g, 2 mmol) were mixed in chloroform (20 ml) and stirred overnight. A white precipitate (NaBr) formed which was removed by gravity filtration and the resulting clear solution taken to dryness in vacuum. The white residue obtained was re-suspended in the minimum amount of DMF. The resulting solution was filtered through celite and crystallised by vapour diffusion with diethyl ether. Yield 77%. Anal. calcd. for $(C_6H_{10}NS_2)Br$: C, 30.01; H, 4.2; N, 5.84%. Found: C, 29.67; H, 4.08; N, 5.90%. ESI-MS $[Tz^{allyl}]^+$: 160 (100). Accurate mass predicted, 160.0249; found: 160.0247. ^{1}H-NMR (500 MHz, $CDCl_3$): δ = 7.6 (br, 1H, -NH), 5.85 (m, 1H, -CH), 5.5 (d, ^3J(H,H) = 17 Hz, 1H, -**H**CH), 5.32 (d, ^3J(H,H) = 10 Hz, 1H, -HC**H**), 4.45 (t, ^3J(H,H) = 8.5 Hz, 2H, $-CH_2$), 4.12 (d, ^3J(H,H) = 7 Hz, 2H, -CH), 3.81 (t, ^3J(H,H) = 8.5 Hz, 2H, $-CH_2$). ^{13}C-NMR (125 MHz, $CDCl_3$): δ = 191.26, 129.09, 122.65, 54.84, 39.1, 33.64 ppm.

	$TmS^{Me}I_2$	$TmS^{allyl}Br_2$	$TmS^{Benzyl}Br_2$	$NaTbz(OH_2)_2$	$Bz^{allyl}Br$	$tzTtz(OH_2)$	$Tz^{allyl}Br$
Empirical formula	$C_{15}H_{25}B_1I_2N_6S_3$	$C_{21}H_{31}B_1Br_2N_6S_3$	$C_{33}H_{37}B_1Br_2N_6S_3$	$C_{21}H_{17}N_3NaO_2S_6$	$C_{10}H_{10}N_3S_6Br_1$	$C_{12}H_{18}N_3Na_1O_1S_6$	$C_6H_{10}N_1S_2Br_1$
FW	650.20	633.99	784.50	533.5	288.2	506.61	239.93
Crystal system	Trigonal	Monoclinic	Orthorhombic	Monoclinic	Triclinic	Cubic	Monoclinic
Space group	P3	$P2_1/c$	$P2_12_12_1$	$P2_1/c$	P-1	F -4 3c	C 2/c
a/Å	17.2093(5)	16.4292(5)	10.2283(5)	15.9795(2)	8.0480(50)	29.5550(5)	31.3780(50)
b/ Å	17.2093(5)	11.8480(2)	16.7477(10)	10.49680(10)	8.3620(50)	29.5550(5)	4.5870(50)
c/ Å	7.0659(2)	16.2564(4)	42.015(3)	19.8988(2)	8.9860(50)	29.5550(5)	14.4010(50)
α/°	90	90	90	90	77.702(5)	90	90
β/°	90	117.458(2)	90	112.4030(10)	84.268(5)	90	113.834(5)
γ/°	120	90	90	90	69.016(5)	90	90
Z	3	4	8	6	2	68	4
V/A^3	1812.28(9)	2807.9(1)	7191.1(7)	3085.79(6)	551.49(14)	25816.23(8)	1895.98(51)
μ_{calc}/mm^{-1}	2.875	3.13	2.459	0.704	4.063	0.860	4.708
No. Reflns Measd	23659	27091	28336	87297	10163	13102	12557
No. Unique reflns	5526	8089	13991	10828	2524	2362	2494
No Observed reflns	3989	4750	6170	8893	2395	1618	1842
No. Parameters	250	289	813	379	131	127	95
R^a (1>2σ(I))	0.0499	0.0440	0.0672	0.0429	0.024	0.040	0.037
R_w^b (all reflns)	0.0984	0.1001	0.1610	0.1419	0.064	0.129	0.088
GOF	0.010	0.905	0.844	1.08	1.096	0.981	0.997

2.3 Results and Discussion

The ability to generate metal-sulphur bonds using Tm^R ligands has led to biomimetic studies of sulfite oxidase, alcohol dehydrogenase and hydrogenase.[9,10] Specifcally Bridgewater *et al*. and Ibrahim *et al*. have previously investigated the use of Tm^R in modelling studies of reaction mechanism of Ada. [15, 16] Their results show that it is possible for a methyl group to migrate from alkylating agents to a coordinated thiolate. However, in these reactions the alkylation occurs at a coordinated thiol and not the thione. Significantly the study of Crossley *et al.* on the formation of (*bis*(1-methylimidazol-2-yl-thio)methane-N,N')-(1-methyl-2-thioimidazol-3-yl)borane from Tm^{Me} and dicholoromethane (scheme 1.3, page 16) indicates that the anion itself is not inert towards alkylation.[17] This led to our interest in the ability of these anions to react with alkylating agents.

2.3.1 Reaction of sodium hydro*tris*(methimazolyl)borate with alkyl halides.

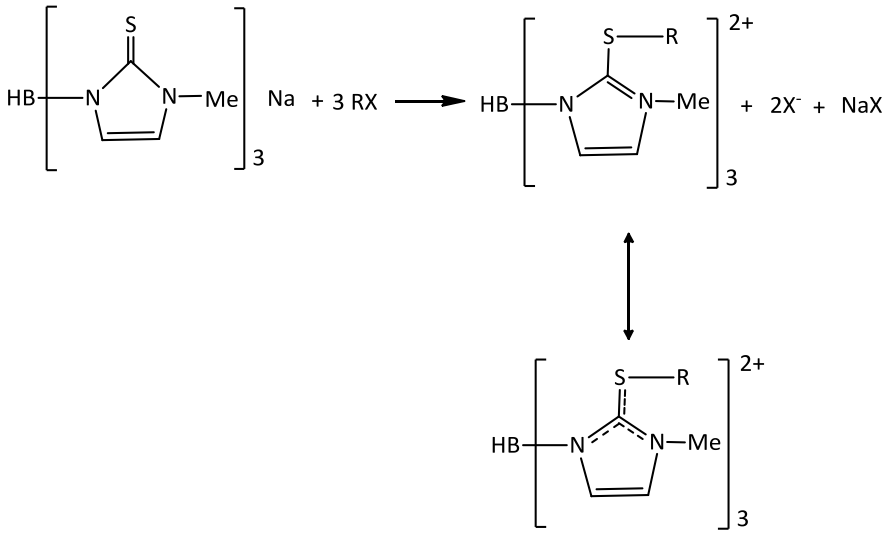

Scheme 2.2: Summarised reaction procedure for the alkylation of soft scorpionates.

The treatment of $NaTm^{Me}$ with a selected range of alkyl halides (RX, where R = Me, C_3H_5, $PhCH_2$, X= Br, I, equation 1) affords the corresponding sulphur alkylated product (TmS^R, figure 2.6). Crystallographic analysis confirms the transfer of alkyl groups onto the thione (figure 2.6). It also shows that, in the solid state, the newly

formed thio-ether groups remain above the plane defined by the three nitrogen donors (N1) bonded to the B-H group in a similar manner to that observed in Tm^{Me} itself. Despite the elongation of the C-S bond, the internal C-NMe distances do not alter markedly, indicating that the positive charge which accompanies alkylation is distributed within the heterocyclic ring and not simply by the formation of a quaternary nitrogen at N2 (figure 2.9) as is described in scheme 2.2 (table 2.1). These alterations are also evident in the ^{13}C and ^{1}H NMR spectra where the >C=S and methine resonances shift markedly (table 2.1, figure 2.7). The shift in ν(BH) to higher frequency (table 2.1) in response to these alterations is somewhat smaller than might be expected and probably reflects the manner in which the three alkylated sulfurs shield the B-H moiety (figure 2.8) and/or how the positive charge is distributed within the heterocyclic rings.

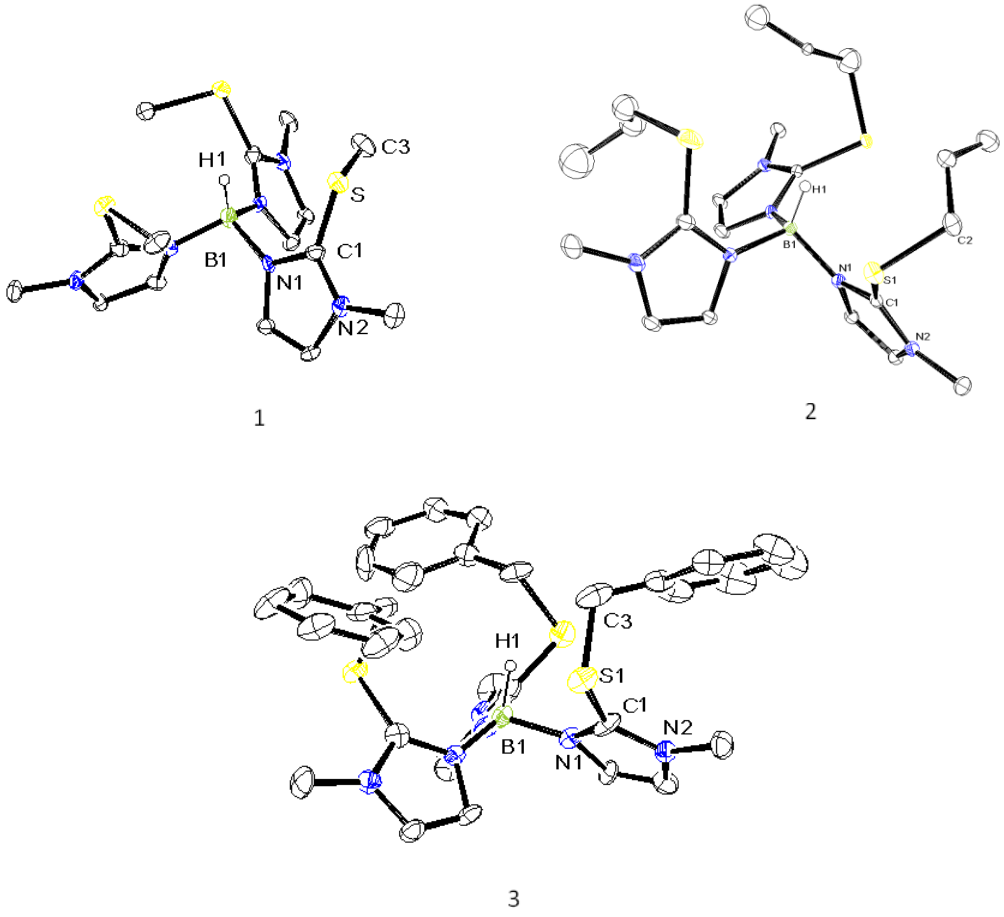

Figure 2.6: X-ray molecular structures of TmS^{Me} (1), TmS^{allyl} (2) and TmS^{benzyl} (3). Thermal ellipsoids are shown at 30% probability. Hydrogen atoms and counter ions are omitted for clarity.

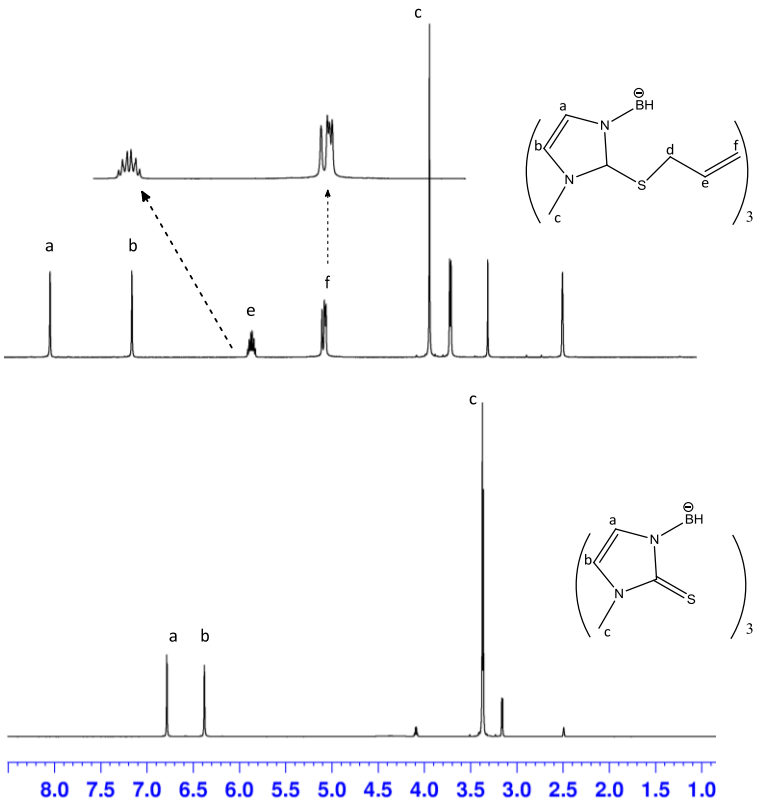

Figure 2.7: A comparison of ^{1}H NMR of $NaTm^{Me}$ (bottom) with its allyl adduct, $[TmS^{allyl}]^{2+}$ (top). The shift in the methimazolyl resonances can be clearly seen. All peaks are calibrated to the solvent peak (DMSO).

	$[Tm^{Me}]^-$	$[TmS^{Me}]^{2+}$	$[TmS^{allyl}]^{2+}$	$[TmS^{Benzyl}]^{2+}$
C-S	1.706(9) 1.699(8) 1.695(8)	1.729(8) 1.749(8) 1.752(8)	1.746(4) 1.735(3) 1.744(3)	1.7538(1) 1.7132(1) 1.7245(1)
SC-NMe	1.37(1) 1.36(1) 1.35(1)	1.36(10) 1.343(9) 1.356(10)	1.353(4) 1.344(4) 1.340(3)	1.3442(1) 1.3288(1) 1.4024(1)
B-N	1.55(1) 1.54(1) 1.55(1)	1571(8) 1.544(8) 1.545(9)	1.563(3) 1.554(4) 1.553(4)	1.5328(1) 1.5674(1) 1.5574(1)
BN-CS	1.351(9) 1.353(9) 1.368(9)	1.35(1) 1.35(1) 1.35(1)	1.336(5) 1.345(5) 1.348(4)	1.3527(1) 1.3678(1) 1.2948(1)
13CNMR >C-S	163.4	143.1	140.5	139.9
υ (B-H) cm^{-1}	2478	2450	2492	2483

Table 2.1: Selected bond lengths (Å) for the TmS^R complexes.

2.3.2 Reaction of sodium hydro*tris*(methimazolyl)borate with iodobenzene and 2-bromopropane.

Similar reactions were carried out with iodobenzene and 2-bromopropane. These however, did not generate the expected alkylated products. Mass spectral analysis continued to give a peak at 351 in negative ion mode with an isotope pattern consistent with Tm. This is supported by X-ray crystallographic analysis. Curiously a counter cation is absent indicating that we had isolated the free acid of the soft scorpionate H[Tm]. The inability of 2-bromopropane and iodopropane to form the

desired adducts probably stems from the poor nucleophilicity of the carbon centres in these species.

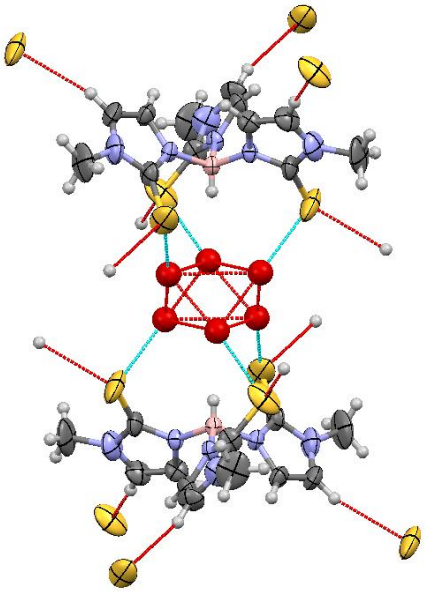

Figure 2.8: The X-ray structure of "$[H_3O][Tm^{Me}]$". The red spheres represent the oxygen atoms of H_3O^+ ions, each having a site occupation factor of 1/3. The structure failed to refine to a satisfactory solution (R ~ 10%).

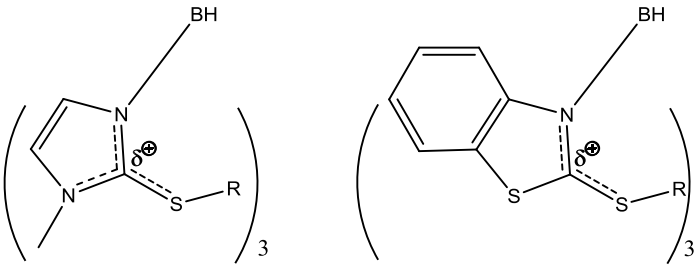

Figure 2.9: (Left) Delocalisation of positive charge within TmS^R R= $-CH_3$, C_3H_5 and $PhCH_2$. (Right) Pictorial representation of the possible charge delocalisation within $TbzS^R$ (where R is CH_3, C_3H_5 and $PhCH_2$).

The efforts discussed above indicate that the alkylation reaction is not universal. Our ability to generate alkylated adducts could depend heavily on the delocalisation of the positive charge in the ring. Thus the role of NMe in the ring is of some interest. This concept can be tested by replacing the nitrogen heteroatom with

sulphur, thus extending the study to include an alternative soft scorpionate, hydro*tris*(mercaptobenzothiozolyl)borate (Tbz).

2.3.3 Preparation of sodium hydro*tris*(mercaptobenzothiazolyl)borate (NaTbz).

Sodium hydro*tris*(mercaptobenzothiazolyl)borate was reported in 2000 by Ojo *et al.*[22] This species was revisited here to interrogate the S-alkylation reactions further. During this study an improved reaction procedure was identified and the vapour diffusion of the product, obtained using chloroform/diethyl ether, produced X-ray quality crystals.

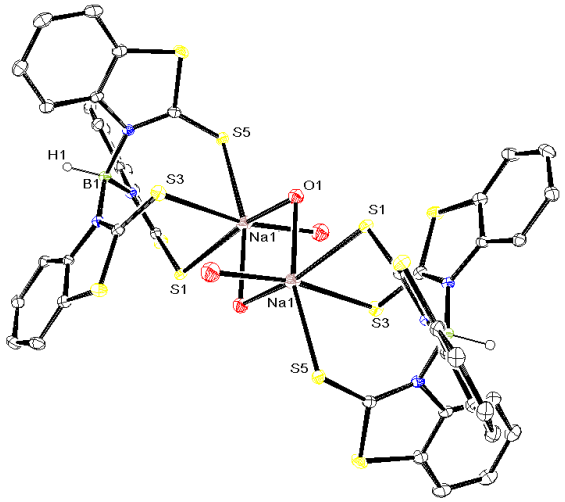

Figure 2.10: X-ray molecular structure of {NaTbz(OH_2)}μ-(OH_2)$_2$. Each sodium in NaTbz is coordinated to three water molecules two of which bridge between the two sodium atoms. Hydrogen atoms are omitted for clarity. Selected bond distances C8-S4, 1.737 Å; C8-S3, 1.676 Å Thermal Ellipsoids are shown at 30% probability.

The structure shows that we have two NaTbz moieties coupled via bridging water molecules. The coordination sphere of the sodium is completed with an additional water molecule. In contrast to Tm^{Me}, Tbz coordinates in a κ^3-S,S,S mode. This most likely arises due to the steric problems of the interleaving aryl rings. NMR spectroscopic analysis of NaTbz reveals the complex to be highly dynamic. At room

temperature the compound displays two broad resonances. By lowering the temperature, the spectrum coalesces and then separates into a number of resonances. These resonances are currently assigned to the two low energy forms of NaTbz identified by DFT analysis (figure 2.11). Variable temperature NMR of NaTbz clearly indicating the presence of more than one conformation in the solution with a low energy barrier (~ 10 kcal mol^{-1}) between these two forms. We have been unable to retrieve the thermodynamic data from this study at this time and the further analysis of this system is unavailable.

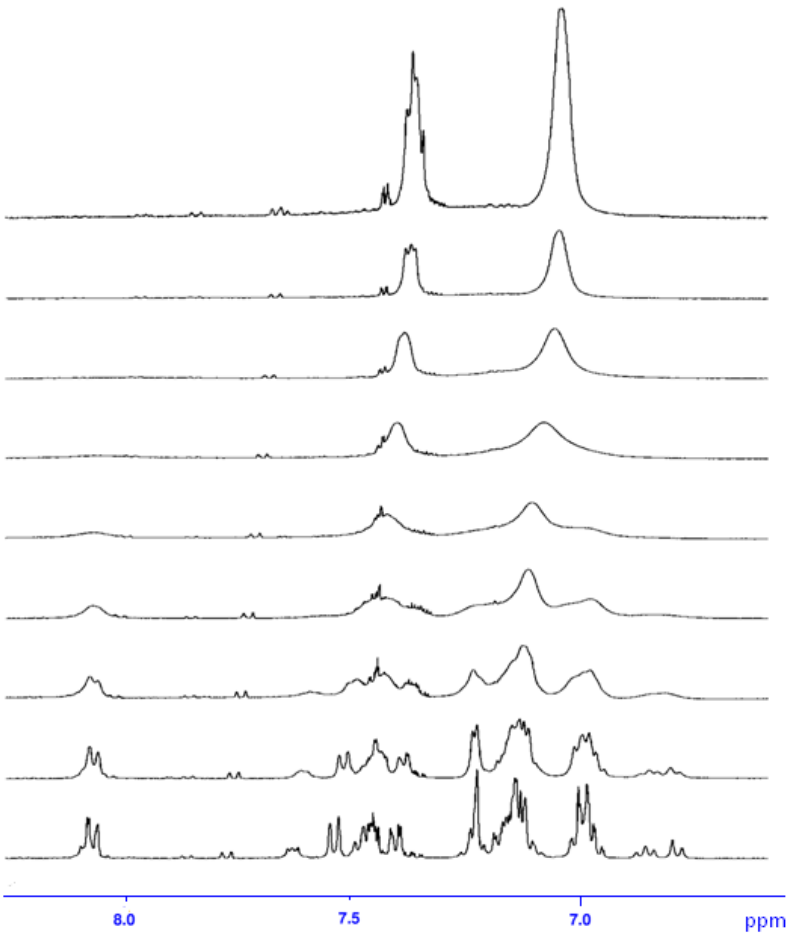

Figure 2.11: Variable temperature (220 K – 300 K) ^{1}H NMR of NaTBz. Only selected spectra are shown. The top spectrum was recorded at 300K and the bottom at 220 K with an interval of 10 K.

2.3.4 Reaction of sodium hydro*tris*(mercaptobenzothiazolyl)borate with allyl bromide.

Treating Tbz with allyl bromide (c.f. Tm^{Me}) led to catastrophic decomposition of the scorpionate ligand and the formation of allylated mercaptobenzothiazole (figure 2.12). Interestingly the two different soft scorpionates (Tm^{Me} and Tbz) subjected to alkylation give two different products. Alkylation can occur by one of the two possible mechanism (scheme 2.3). An alkyl cation can react with the –BH moiety in the Tbz anion to form a hydrocarbon. Consequently, the ligand decomposes to form the free mercaptobenzothiazole anion which reacts with allyl bromide to form the observed product. Alternatively the allyl group couples with the Tbz anion to form the desired product. However, the positive charge generated in the heterocyclic ring changes the character of the B-N bond from covalent to dative. Thus the B-N bond elongates and severs leading to decomposition and thus the final product.

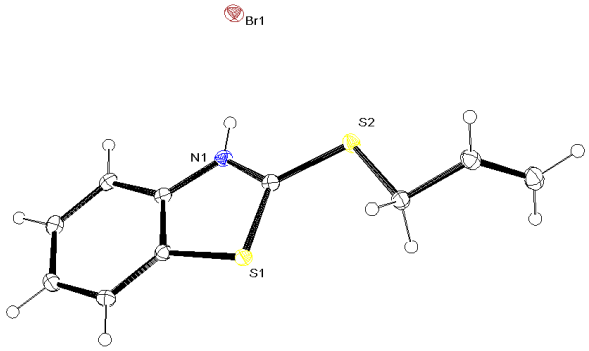

Figure 2.12: X-ray molecular structure of S-allyl-mercaptobenzothiazole hydrobromide. Thermal ellipsoids are showing at 30% probability.

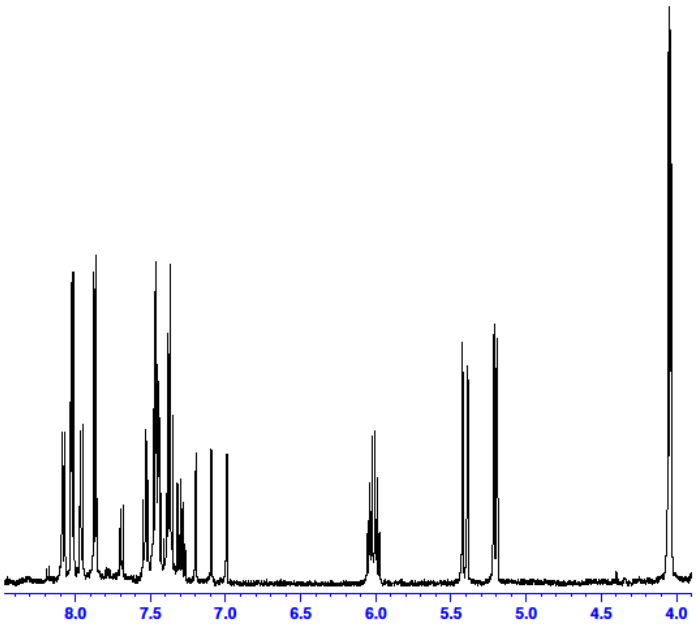

Figure 2.13: NMR spectrum of S-allyl mercaptobenzothiazole hydrobromide which is obtained by the reaction between NaTbz and allyl bromide. All peaks are calibrated to the solvent peak (DMSO).

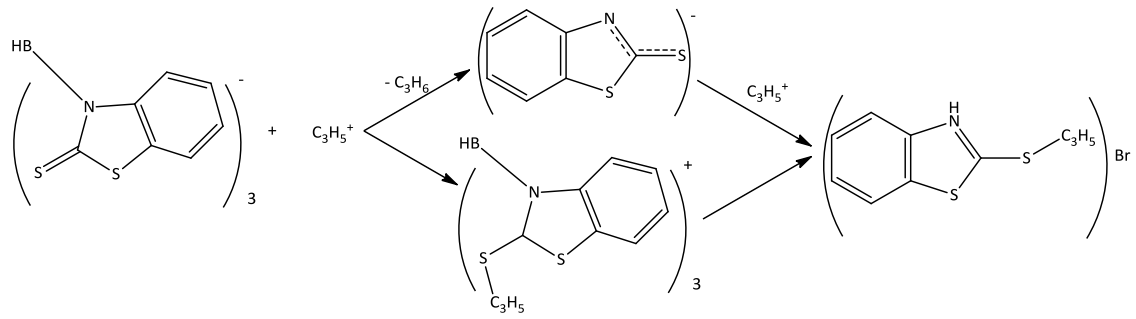

Scheme 2.3: Two different possible reaction pathways of decomposition of Tbz anion with methyl addition.

To understand the reaction mechanism further it would be of value to nullify one of the reaction pathways. To do this we selected a third thiazoline based soft scorpionate, tzTtz (figure 2.14). This species ligand does not contain a -BH unit and as such formation of hydrocarbon is not possible.

2.3.5 Preparation of sodium *tetrakis*(thiazolyl)borate ligand.

Thiazoline-based soft scorpionates have been known for some time. Ojo *et al.* reported the synthesis of the hydro*tris*(thiazolyl)borate anion (Ttz) in 2000.[22] Soares *et al.* reported the synthesis of the *tetrakis*(thaizolyl)borate anion (tzTtz) in 2004.[23] These two ions demonstrate great similarity in their spectroscopy. For this reason we re-collected the X-ray data to confirm the species used in this part of the study was tzTtz. Thus tzTtz was prepared (figure 2.14) using a slightly modified route to that of Soares and re-characterised. The crystal structure shows that, as expected, the boron is bonded to thiazoline units through the nitrogen and that unlike Tm^R and Tbz, tzTtz lacks a B-H unit.

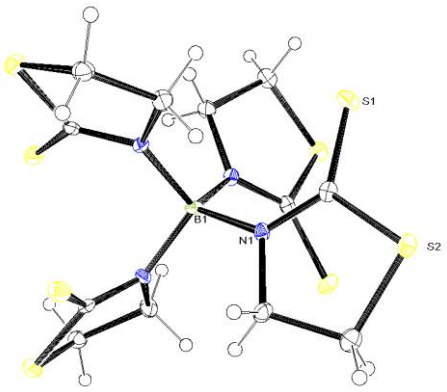

Figure 2.14: The single crystal X-ray molecular structure of sodium salt of *tetrakis*(thiazolyl)borate. The product is iso-structural with the previously reported potassium salt by Soares *et al.*[23] The sodium atom and solvated water molecules are omitted for clarity. The thermal ellipsoids are shown at 30% probability. tzTtz has S_4 symmetry.

Treating tzTtz with allyl bromide did not lead to the formation of the cationic alkylated scorpionate but to allylated thiazoline (figure 2.15). Thus it would seem that the decomposition mechanism operates by S-alkylation (scheme 2.3). In an attempt to further understand the behaviour of Tm^{Me}, Tbz and tzTtz and the overall

reaction mechanism with the alkylating agents (scheme 2.3) we subjected these species and their reactions with alkyl halide to analysis by DFT methods.

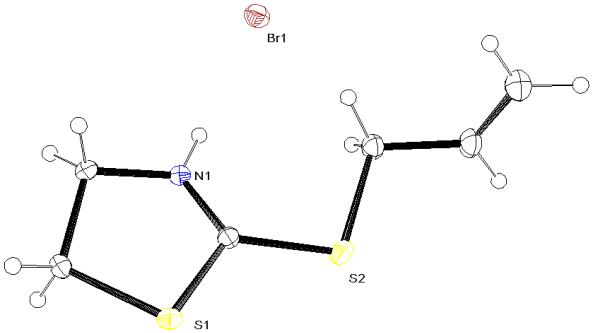

Figure 2.15: Single X-ray molecular structure of allylated thiazoline. Thermal ellipsoids are shown at 30% probability.

2.3.6 DFT calculations on sodium salt of Tm and Tbz class scorpionates.

The four conformations of the Tm^{Me} anion were analysed sequentially using DFT methods to identify the most favoured form (figure 2.16).

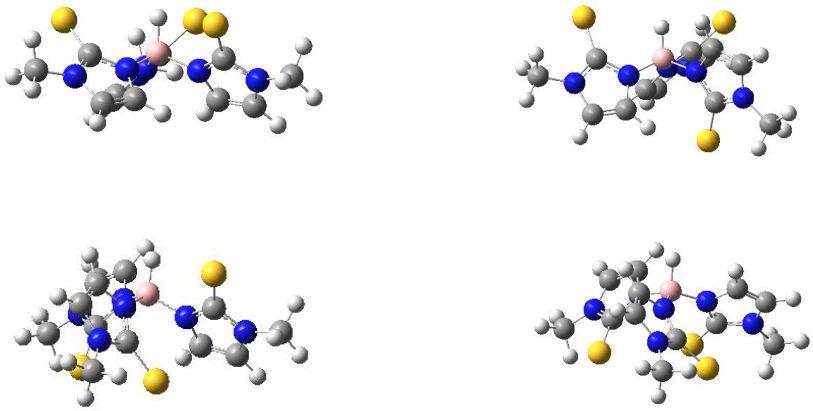

Figure 2.16: DFT calculations of Tm anion with its relative energy. Top left, three S atom pointing towards –BH (total energy= -2015.022656 au; relative energy= 2.90 kcal mol^{-1}). Top right, Two S atom pointing towards –BH and one S atom pointing away from -BH (total energy = -2015.027270 au; relative energy = 0.00 kcal mol^{-1}). Bottom left, two S atoms pointing away from –BH and one is pointing towards -BH (total energy = -2015.027270 au; relative energy= 0.00 kcal mol^{-1}). Bottom right, all S atoms are pointing away from –BH (total energy= -2015.004252 au; relative energy= 14.44 kcal mol^{-1}).

DFT analysis identified the form (2:1) where two thiones lies parallel with the B-H unit and one anti-parallel as the most stable form. However, the difference in energy between the 2:1 form and that where all three thiones lie parallel with the B-H unit (viz 3:0) is only 2.90 kcal mol^{-1}. There are a number of crystallographic reports which contain uncoordinated Tm^{Me} anions.[18, 24-27] These are all observed to adopt the 3:0 form indicating that local effects play an important role in the conformation adopted. The form regularly observed once coordinated where all three thione lie below the BN_3 plane (0:3) is the highest in energy (14.44 kcal mol^{-1}) indicating that metal complexation requires the anion to reorganise. The final form (1:2) where only one thione lies parallel to the B-H axis does not achieve a stable solution. In each case it reorganises during optimisation to give the 2:1 form.

All three conformations were subjected to methyl addition by placing methyl groups in different positions including above and below B-H unit in the C_3 axis, adjacent to the sulphur and also predisposed towards the thione sulphur (summarised in figure 2.17).

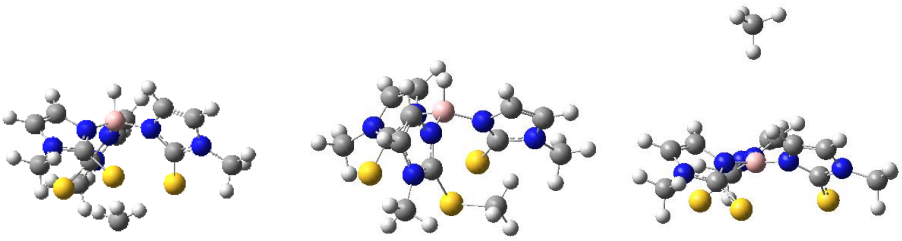

Figure 2.17: DFT calculation of alkylation of Tm anion: (left) $–CH_3$ initially lying along the C_3 axis (total energy= -2054.729710 au; relative energy= 64.86 kcal mol^{-1}), (central) $–CH_3$ attacks on sulphur in the ring (total energy= -2054.803661 au; relative energy= 18.46 kcal mol^{-1}), (right) $–CH_3$ attacks on –BH bond (total energy= -2054.833072 au; relative energy= 0.00 kcal mol^{-1}).

From the calculations, two possible pathways are observed. One is S- alkylation and the other is hydrocarbon formation which is observed by the reaction of alkyl group with the B-H moiety. The data obtained are summarised in the table 2.2 below

(table 2.2). The most favourable product obtained using the most stable conformation is the S- alkylated product which is seen experimentally. Formation of hydrocarbon is most favourable with the conformations **3:0** and **0:3**. In the solution state all three conformations are present so that all three pathways are possible. But experimentally there was no evidence of the production of hydrocarbon. So it is believed that there was a kinetic energy barrier to hydrocarbon production and the thermodynamically more favourable pathway i.e. S- alkylation is observed.

Ligand Conformation	$[Tm^{Me}]^-$	S-alkylation	B-H alkylaton
3:0	-2015.022656 a.u. 2.90 kcal mol^{-1}	-2054.810335 a.u. 14.27 kcal mol^{-1}	-2054.831214 a.u. 1.17 kcal mol^{-1}
2:1	-2015.027270 a.u. 0.00 kcal mol^{-1}	-2054.818395 a.u. 9.21 kcal mol^{-1}	-2054.810926 a.u. 13.90 kcal mol^{-1}
0:3	-2015.004252 a.u. 14.44 kcal mol^{-1}	-2054.803669 a.u. 18.45 kcal mol^{-1}	-2054.833072 a.u. 0.00 kcal mol^{-1}

Table 2.2: DFT calculation of alkylation of Tm^{Me} anion. The three stable conformations are used to find the most favourable reaction pathway.

(i) Hydro*tris*(mercaptobenzothiazolyl)borate anion(Tbz^- anion)

Subjecting Tbz to DFT analysis indicates that there are two forms of the free anion with roughly comparable stability. Although the **1:2** form is observed to be the most stable, the **2:1** form is only marginally higher in energy (0.18 kcal mol^{-1}).

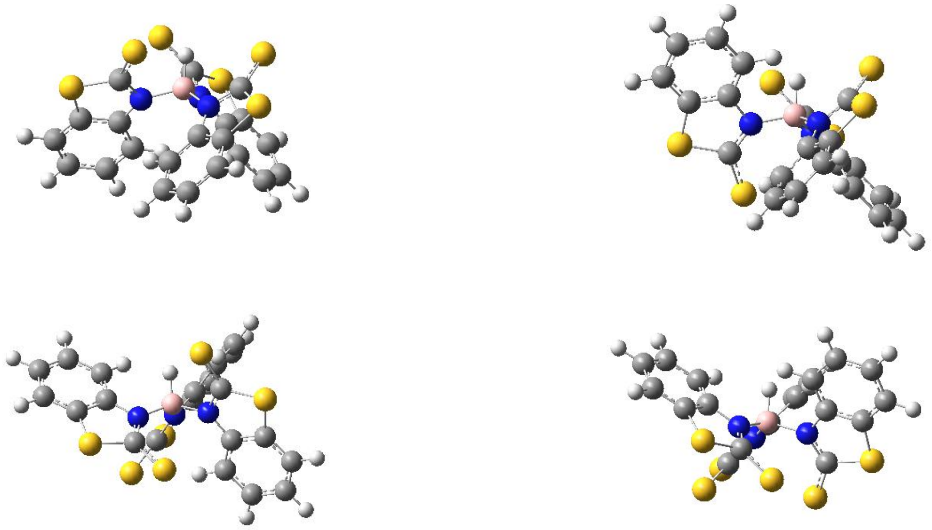

Figure 2.18: DFT calculations of Tbz anion with its relative energy. Top left, three S atoms pointing towards –BH (total energy= -3386.611672 au; relative energy= 3.27 kcal mol^{-1}). Top right, Two S atoms pointing towards –BH and one S atom pointing away from -BH (total energy = -3386.616601 au; relative energy = 0.18 kcal mol^{-1}). Bottom left, two S atoms pointing away from –BH and one is pointing towards -BH (total energy = -3386.616883 au; relative energy= 0.00 kcal mol^{-1}). Bottom right, all S atoms are pointing away from –BH (total energy= -3386.610726; relative energy= 3.86 kcal mol^{-1}).

In solution the Tbz anion freely rotates, changing its conformation from **1:2** to **2:1.** This explains the observed NMR spectra (Figure 2.11) for Tbz which gives two broad signals at room temperature. In turn the NMR spectra support the view that the energy barrier between these two forms is small. On cooling the rotation of the ligand slows down and the expected resonances for the most stable forms (**1:2** & **2:1** form) of the ligand can be independently observed. NMR analysis of these spectra (figure 2.11) suggests that the energy barrier in Tbz is low (~ 10 kcal/mol) and that in solution there is likely to be free conversion between the two forms of each of the anions. Although the energy difference between the two most stable forms of Tm^{Me} and Tbz anion is less than 3 kcal mol^{-1}, it is as yet unclear what the activation barrier to rotation of the methimazolyl units is.

(ii) *Tetrakis*(thiazolyl)borate anion (tzTtz$^-$ anion)

In contrast to Tm^{Me} and Tbz, tzTtz is of higher symmetry (S_4) and only has one conformation. Its structure was optimised using DFT methods for use in the studies below.

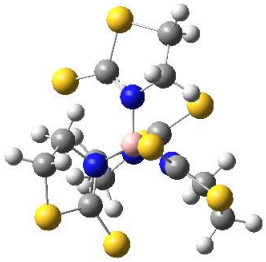

Figure 2.19: DFT calculation of tzTtz anion. Since there is no BH unit, this molecule possesses S_4 symmetry and has only one possible stable conformation.

2.3.7 Alkylation of Tbz and tzTtz salts.

In contrast to Tm^{Me}, DFT analysis indicates that S-alkylation of the Tbz is preferred over a reaction at the B-H bond by 16.36 kcal mol^{-1}. Once again the DFT calculations would seem to be at odds with the experimental results as there is little evidence to support the formation of a stable alkylated Tbz species. A similar observation is found for the alkylation of tzTtz.

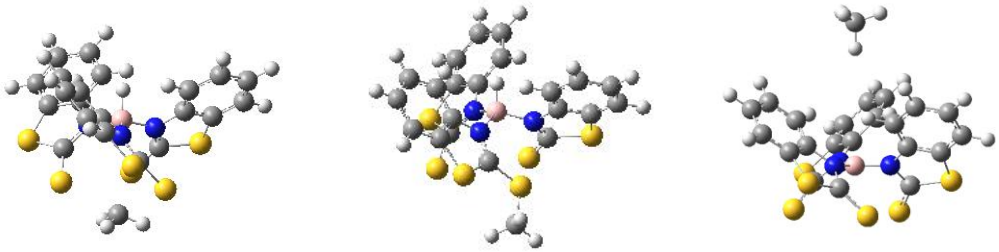

Figure 2.20: DFT calculation of alkylation of Tbz anion: (left) –CH_3 initially takes the position of sodium (total energy= -3426.304210 au; relative energy= 64.14 kcal mol^{-1}), (central) –CH_3 attacks on sulphur in the ring (total energy= -3426.380356 au; relative energy= 16.36 kcal mol^{-1}), (right) –CH_3 attacks on –BH bond (total energy= -3426.406423 au; relative energy= 0.00 kcal mol^{-1}).

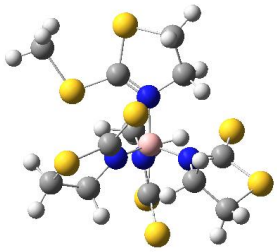

Figure 2.21: DFT calculation of the possible product by the reaction of tzTtz ligand with methyl iodide (total energy = -3936.361316; relative energy= 0.00 kcal mol^{-1}).

Two points remain. The preference for S-alkylation over hydrocarbon formation in the chemistry of Tm^{Me} and the instability of the alkylated products of Tbz and tzTtz.

2.3.8 The alkylation reaction and the transition state

The first generation model (Tm^{Me} + Me^{+}) used above cannot provide information on a transition state and the calculations require to be refined using $NaTm^{Me}$ and MeI. Experimental analysis shows that the sodium can be bonded with Tm^{Me} in either κ^3-S,S,S form or through κ^3-H,S,S form. Models of these species were optimised. Once this had been achieved water molecules were introduced sequentially to identify the most stable hydrated species. DFT analysis suggests that in solution the κ^3-S,S,S species has a preference for the trihydrate (-2406.675405 a.u.) whereas the κ^3-H,S,S bonding mode prefers a dihydrate (-2330.230398 a.u.). Addition of third water molecule to the κ^3-H,S,S species leads to the undesired hydrolysis of one of the Na-S bonds. Once these two species had been optimised methyl iodide was introduced to both species. This allows for a comparison of the respective energies of reaction and transition state energies. The results obtained are summarised in table 2.3.

	S-Alkylation	-BH alkylation	Transition state	
			S-alkylation	-BH alkylation
[Na (κ^3-S,S,S-Tm^{Me})$(OH_2)_3$	-9366.109030 a.u.	-9325.640735 a.u.	16.35 kcal mol^{-1}	25.06 kcal mol^{-1}
[Na (κ^3-H,S,S-Tm^{Me})$(OH_2)_2$	-9289.631741 a.u.	N/A	12.56 kcal mol^{-1}	N/A

Table 2.3: Energy and transition state energy of alkylation of most stable forms of coordinated Tm^{Me} with methyl iodide. Alkylation values for [Na (κ^3-H,S,S-Tm^{Me})$(OH_2)_3$ at BH are not available as access to the B-H is unfavoured due to sterric effects. The other forms od sodiated Tm^{Me} were modelled, i.e. κ^2-S,S; κ^2-H,S; κ^1-S; κ^1-H. These however were of higher energy.

DFT calculations suggests that the S-alkylation product is favoured in the κ^3-S,S,S species over the –BH alkylation by ~8.71 kcal mol^{-1}. On the other hand the species κ^3-H,S,S form has only one pathway available namely S- alkylation. Alkylation at the –BH group is effectively blocked by the steric effects. Of central importance however is the calculated transition state for the κ^3-S,S,S- bonding mode. The calculations predict that there is a substantial difference in the transition states making S-alklyation more favourable (by 8.7 kcal mol^{-1}). This explains the absence of hydrocarbon formation in the reactions.

2.3.9 Metrical parameters

Closer inspection of the metrical parameters (table 2.4, 2.5) for the three alkylated model compounds assembled in the DFT calculations offer an explanation why the alkylated products are unstable. We can inspect the Mulliken charges on the various atoms within the three heterocycles (table 2.4). The replacement of the NMe by sulfur effectively exchanges an atom with a negative charge with one which has a positive charge. This and the subsequent alkylation of the thione makes the carbon (>C=S) more negative for TBz and tzTtz. This is a major re-distribution of charge within the heterocycle.

	Tm^{Me}	TmS^{Me}	Tbz	$TbzS^{Me}$	tzTtz	$tzTtzS^{Me}$
B	+0.49	+0.46	+0.49	+0.42	+0.84	+0.80
N(B)	-0.38 -0.35 -0.35	-0.30 -0.37 -0.36	-0.45 -0.42 -0.42	-0.39 -0.46 -0.43	-0.39	-0.43
C(=S)	+0.20 +0.18 +0.22	+0.18 +0.20 +0.16	-0.14 -0.14 -0.09	-0.04 -0.16 -0.17	-0.10	-0.13
S	-0.43 -0.40 -0.43	+0.11 -0.39 -0.39	-0.21 -0.25 -0.24	+0.35 -0.20 -0.23	-0.30	+0.30
N_{Me}/S	-0.34 -0.34 -0.35	-0.32 -0.34 -0.34	+0.26 +0.25 +0.26	+0.35 +0.29 +0.31	+0.14	+0.38

Table 2.4: Calculated charges of some selected atoms in pre and post methylated Tm, Tbz and tzTtz ligands.

	Tm observed	Tm calculated	TmS^{Me} observed	TmS^{Me} Calculated	Tbz observed	Tbz calculated	Alkylated Tbz calculated*	tzTtz observed	tzTtz calculated	Alkylated tzTtz Calculated*
C=S	1.706(9)Å 1.699(8) Å 1.695(8) Å	1.707 Å	1.749(8) Å 1.729(8) Å 1.752(9) Å	1.759 Å	1.674(2) Å 1.6758(19) Å 1.684(2) Å	1.666 Å	1.738 Å	1.682(5) Å	1.680 Å	1.746 Å
B-N	1.55(1) Å 1.54(1)Å 1.55(1)Å	1.577 Å	1.571(8) Å 1.544(8) Å 1.545(9) Å	1.596 Å	1.552(2) Å 1.556(2) Å 1.559(2) Å	1.566 Å	1.593 Å	1.572(4) Å	1.586 Å	1.657 Å
$C\text{-}N^{B}$	1.35(1) Å 1.37(1) Å 1.351(9) Å	1.369 Å	1.336(10)Å 1.341(9) Å 1.354(10) Å	1.342 Å	1.351(2) Å 1.357(2) Å 1.342(2) Å	1.364 Å	1.324 Å	1.327(7) Å	1.344 Å	1.305 Å
$C\text{-}N^{Me}$	1.37(1) Å 1.36(1) Å 1.35(1) Å	1.374 Å	1.360(10)Å 1.343(9) Å 1.356 (10)Å	1.359 Å	1.746(2) Å 1.7434(19) Å 1.7383(18) Å **(C-S)**	1.785 Å **(C-S)**	1.743 Å **(C-S)**	1.757(5) Å **(C-S)**	1.790 Å **(C-S)**	1.760 Å **(C-S)**

Table 2.5: A comparison of Tm, Tbz and tzTtz class ligands pre and post alkylated states. Observed and calculated bond lengths of some selected atoms.
*The observed values of alkylated Tbz and alkylated tzTtz are not available because of ligand decomposition
.

An inspection of bond lengths for the compound (table 2.5) pre and post alkylation confirms that the bond order of the C-S bond falls with the values typically shifting from 1.707 to 1.759 Å. The bond distance between C-N and C-N^{Me} also decreases. There is a concomitant increase the B-N bond length from 1.577 Å to 1.596 Å. A description of the bonds suggest that within the heterocyclic ring there is a shift to increasing double bond character for the C-N bond and a shift from a B-N covalent bond to a dative interaction. For species such as TmS^{R} where the B-N distance is modest the alkylated adduct is stable and isolable. In contrast in species such as Tbz and tzTtz the B-N bond is longer and under greater steric strain. Consequently it is unsurprising that alkylation leads to decomposition.

In conclusion, the three anions, Tm^{Me}, Tbz and tzTtz can all accept alkyl groups at the thione sulphur moiety. The resulting modest extension of the B-N bond then controls the eventual product obtained. In the case of the Tm anion the change of B-N bond character from covalent to dative and the degree of extension does not compromise product stability, whereas the alkylated Tbz^{-} and tzTtz anions quickly degrade. This observation has implications for the chemistry of the soft scorpionates in general.

2.4 References

1. Prokhortchouk, E.; Defossez, P. *Biochim. Biophys. Acta* **2008**, *1783*, 2167-2173.
2. Ohgane, J.; Hattori, N; Oda, M.; Tanaka, S.; Shiota, K. *Biochem. Biophys. Res. Commun.* **2002,** *290*, 701-706.
3. Sekiguchi, M.; Nakabeppu, Y.; Sakumi, K.; Tuzuki, T. *J. Cancer. Res. Clin. Oncol*. **1996**, *122*, 199-206.
4. He, C.; Hus, J.; Sun, L. J.; Zhou, P.; Norman, D. P. G.; Dötsch, V.; Wei, H.; Gross, J. D.; Lane, W. S.; Wagner, G.; Verdine, G. L. *Mol. Cell* **2005**, *20*, 117-129.
5. Myres, L. C.; Cushing, T. D.; Wagner, G.; Verdine, G. L. *Chem. Biol.* **1994,** *1,* 91-97.
6. Lin, Y.; Dötsch, V.; Winter, T.; Pearsio, K.; Myres, L. C.; Penner-Hahn, J. E.; Verdine, G. L.; Wagner, G. *Biochemistry* **2001**, *40*, 4261-4271.
7. Penner-Hahn, J. *Curr. Opin. Chem. Biol.* **2007**, *11*, 166-171.
8. Huang, C.; Casey, P. J.; Fierke C. A. *J. Biol. Chem.* **1997,** *272*, 20-23.
9. Reglinski, J.; Spicer. M. D. *Curr. Bioact. Compd.* **2009,** *5*, 264-276.
10. Parkin,G. *Chem. Rev*. **2004**, *104*, 699-767.
11. Trofimenko, S. *Scorpionates: The coordination chemistry of Polypyrazolyl borate ligands*. 1999: Imperial College Press. 282.
12. Kitajima, N.; Tolman, W. B.; *Prog. Inorg. Chem*. **1995**, *43*, 419-531.
13. Looney, A.; Han, R.; McNeill, K.; Parkin, G. *J. Am. Chem. Soc*. **1993**, *115*, 4690-4697.
14. Vahrenkamp, H. *Acc. Chem. Res.* **1998,** *32*, 589-596.
15. Bridgewater, B. M.; Fillebeen, T.; Friesner, R. A.; Parkin, G. *J. Chem. Soc. Dalton Trans.* **2000**, 4494-4496.
16. Ibrahim, M. M.; Shaban, S.Y.; *Inorg. Chim. Acta* **2009**. *362,* 1471-1477.
17. Crossley, I. R.; Hill, A. F.; Humphery, E. R.; Smith, M. K.; Tshabang, N.; Willis, A. C. *Chem. Commun.* **2004**, 1878-1879.

18. Reglinski, J.; Garner, M.; Cassidy, I. D.; Slavin, P. A.; Spicer, M. D.; Armstrong, D. R. *J. Chem. Soc. Dalton. Trans.* **1999,** 2119-2126.

19. Sheldrick, G. M. *Acta Cryst.* **2008**, *A64*, 112-122.

20. Altomare, A.; Cascarano, G.; Giacovazzo, C.; Gualardi, A. *J. Appl. Cryst.* **1993**, *26*, 343-350.

21. Farrugia,L. J. *J. Appl. Crystallogr.* **1999**, *32*, 837.

22. Ojo, J. F.; Slavin, P. A.; Reglinski, J.; Garner, M.; Spicer, M. D.; Kennedy, A. R.; Teat, S. J. *Inorg. Chim. Acta* **2000,** *313*, 15-20.

23. Soares, L.F.; Menezes, D. C.; Silva, R. M.; Doriguetto, A. C.; Ellena, J.; Mascarenhas, Y. P.; Castellano, E. E. *Polyhedron* **2004**, *23*, 205-209.

24. Dodds, C. A.; Jagoda, M.; Reglinski, J.; Spicer, M. D. *Polyhedron* **2004,** *23*, 445-450

25. Dodds, C. A.; Reglinski, J.; Spicer, M. D. *Chem. Eur. J.* **2006**, *12*, 933-941

26. Cetin, A.; Ziegler, C. J. *Dalton Trans.* **2006**, 1006-1008

27. Biernat, A.; Schwalbe, M.; Wallace, D.; Reglinski, J.; Spicer, M. D. *Dalton Trans.* **2007**, 2242-2244.

Chapter 3

Oxidation of soft scorpionate anions

3.1. Introduction

Stable compounds of the hydro*tris*(methimazolyl)borate anion (Tm^R, figure 3.1) have been isolated for the majority of the elements within the periodic table.[1] Within this large catalogue of compounds are species which utilise phosphine-gold and $Mn(CO)_5$ fragments.[1-7] These fragments are isolobal with the alkyl groups. This suggested that it should be possible to extend the chemistry of Tm^{Me} and generate a series of cationic *tris*-alkyl adducts of the soft scorpionates (TmS^R, where R = methyl, allyl, benzyl, figure 3.1, chapter 2).[8,9]

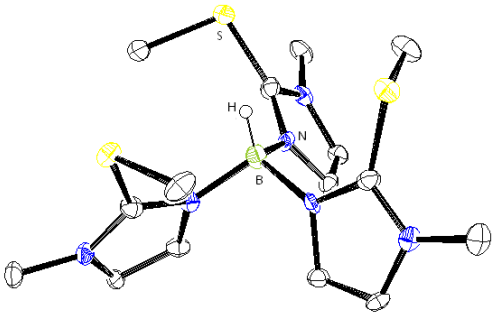

Figure 3.1: Molecular structure of methylated Tm cation; $[TmS^{Me}]^{2+}$. Counter anions and hydrogen atoms apart from the borohydride are omitted for clarity. Thermal ellipsoids are shown at 30% probability.

An analysis of these species using crystallographic and DFT methods (chapter 2) indicated that there is a preference for conformations where the thiones (Tm^R) and thioethers (TmS^R) respectively lie parallel to the B-H moiety.[9] This observation suggested that Tm^{Me} will be predisposed to the formation of polycyclic rings when treated with dihaloalkanes (equation 3.1). Indeed on the prolonged reaction of Tm^{Me} with dichloromethane Hill *et al*. isolated *bis*(1-methylimidazol-2-yl-thio)methane-N,N')-(1-methyl-2-thioimidazol-3-yl)borane i.e. a species in which the two thiones are connected by a methylene unit (Figure 3.2).[8]

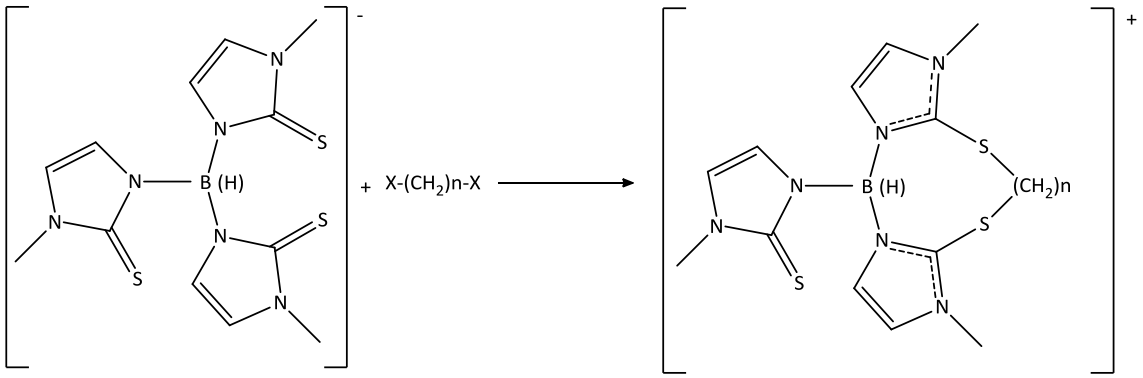

Equation 3.1: Formation of polycyclic rings by the reaction of $NaTm^{Me}$ with dihaloalkanes.

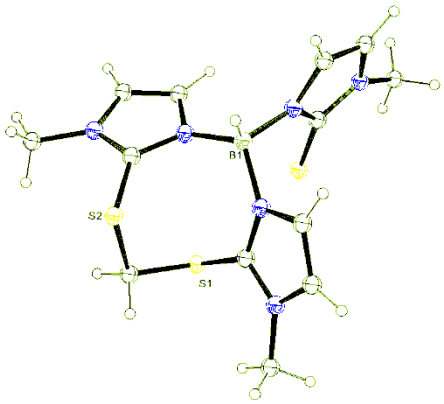

Figure 3.2: The X-ray crystal structure of (*bis*(1-methylimidazol-2-yl-thio)methane-N,N')-(1-methyl-2-thioimidazol-3-yl) borane chloride monohydrate. Counter ions and solvent molecules are omitted for clarity. Thermal ellipsoids are shown at a probability of 30%.

The aim of this work is to further investigate the ability of the soft scorpionate anions to form polycyclic rings.

3.2. Experimental section

All chemicals used were commercially available and used without any purification. $NaTm^{Me}$ was prepared as previously described.[11] NMR spectra were recorded using a Bruker AV500. All the spectra obtained were referenced to the residual solvent peaks. IR spectra were recorded as KBr discs using a Nicolet Avatar 360 FT-IR spectrometer. Mass spectra were recorded using a Thermo Finnigan LCQDuo by electrospray ion trap. Crystals obtained were coated in mineral oil and mounted on glass fibres or a glass loop. Data were collected at 123K on Oxford diffraction diffractometer using graphite monochromated Mo-Kα radiation. The heavy atom positions were determined by Patterson methods and the remaining atoms located in the difference electron density maps. Data were solved using Shelx 97[12] and SIR 92[13] using the graphical interface, Wingx.[14] All non-hydrogen atoms are anisotropic. The hydrogen atoms are placed as a mixture of independent and constrained refinement in the calculated positions around the parent atoms.

3.2.1. The reactions of $NaTm^{Me}$ with dihaloalkanes

A suspension of $NaTm^{Me}$ (0.187 g, 0.50 mmol) in chloroform (20 ml) was refluxed overnight with 1 mol equivalent of the relevant dihaloalkane. The mixture obtained was filtered to remove the sodium halide and then taken to dryness. The resulting mass was purified as described below.

3.2.1.a. Attempted preparation of ($Tm^{Me}SS'^{ethylene}Tm^{Me}$)Br: recrystallised from methanol: n-hexane by vapour diffusion. Anal. Calcd. for $C_{15}H_{23}N_6BS_3.3H_2O$: C, 35.46; H, 5.71; N, 20.69%. Found: C, 37.99; H, 5.18; N, 19.51%. ESI-MS $[Tm]^-$: 351 (100). Mass predicted 351. FT-IR (KBr, cm^{-1}): 2448 (νB-H), 753.34, (νC-S).

3.2.1.b. Preparation of ($Tm^{Me}SS'^{propylene}Tm^{Me}$)I: recrystallised from methanol: n-hexane by vapour diffusion. Yield 0.076 g (29%). Anal. Calcd. for $C_{15}H_{22}N_6BS_3I$: C, 34.64; H, 4.23; N,16.16%. Found: C, 34.01; H, 3.99; N, 15.41%. ESI-MS $[TmS,S^{prop}]^+$: Accurate mass predicted 393.11556, found 393.11526. ^{1}H-NMR (500 MHz, $CDCl_3$): δ = 7.62 (s, 2H, -CH), 7.37 (s, 2H, -CH), 6.8 (s, 1H, -CH), 6.75 (s,1H, -CH), 4.08 (s, 6H, -CH_3), 3.57 (s, 3H, -CH_3), 3.42 (m, 2H, HCH) 3.37 (m, 2H, HCH) 2.38 (s, 1H, HCH), 1.94 (s, 1H, -HCH). ^{13}C-NMR (125 MHz, $CDCl_3$): δ = 164.8, 142.1, 126.1, 121.0, 19.9, 35.9, 34.4, 34. 2, 30.6 ppm. FT-IR (KBr, cm^{-1}): 2505 (νB-H), 740, (νC-S).

3.2.1.c. Preparation of ($Tm^{Me}SS'^{butylene}Tm^{Me}$)Br: recrystallised from methanol: diethyl-ether by vapour diffusion. Yield 0.085 g (35%). Anal. Calcd. for $C_{16}H_{24}N_6BS_3I.H_2O$: C, 38.02; H, 5.19, N, 16.64%. Found: C, 38.29; H, 4.97; N, 17.05%. ESI-MS $[TmS,S^{but}]^+$: Accurate mass predicted, 407.13121, found 407.13147. ^{1}H-NMR (500 MHz, $CDCl_3$): δ = 8.02 (d, 2H, -CH), 7.59 (d, 2H, -CH), 6.76 (d, 1H, -CH), 6.65 (d, 1H, -CH), 4.1 (s, 6H, -CH_3), 3.52 (s, 3H, -CH_3), 3.15 (m, 2H, HCH), 2.99 (m, 2H, HCH), 2.15 (m, 2H, -HCH), 1.43 (m, 2H, -HCH). ^{13}C-NMR (125 MHz, $CDCl_3$): δ = 164.5, 142.5, 127.4, 125.2, 120.8, 119.1, 36.5, 35.8, 34.7, 27.1 ppm. FT-IR (KBr, cm^{-1}): 2565 (νB-H), 745(νC-S)

3.2.1.d. Preparation of ($Tm^{Me}SS'^{pentylene}Tm^{Me}$)I: recrystallised from methanol: diethyl-ether. Yield 0.068 g (25%). Anal. Calcd. for $C_{17}H_{26}N_6BS_3I.2H_2O$: C, 34.93; H, 5.18, N, 14.25%. Found: C, 35.39; H, 4.92; N, 14.25%. ESI-MS $[TmS,S'^{pentyl}]^+$: Accurate mass predicted, 421.14686, found 421.14719. ^{1}H-NMR (500 MHz, $CDCl_3$): δ = 7.87 (d, 2H, -CH), 7.62 (d, 2H, -CH), 6.70 (d, 1H, -CH), 6.35 (d, 1H, -CH), 4.11 (s, 6H, -CH_3), 3.54 (s, 3H, -CH_3), 3.17 (m, 2H, **H**CH), 3.07 (m, 2H, HCH), 2.31 (m, 1H, HCH) 1.88 (m, 2H, HCH), 1.72 (m, 1H, HCH), 1.55 (m, 2H, HCH). ^{13}C-NMR (125 MHz, $CDCl_3$): δ= 165.0, 142.0, 127.0, 125.0, 120.3, 119, 36.9, 37.1, 35.0, 29.8, 25.6 ppm. FT-IR (KBr, cm^{-1}): 2540 (νB-H), 745 (νC-S).

3.2.1.e. Preparation of ($Tm^{Me}SS'^{hexylene}Tm^{Me}$)I: recrystallised from methanol: diethyl-ether. Yield 0.083 g (30%). Anal. Calcd. for $C_{18}H_{28}N_6BS_3I.3H_2O$: C, 35.06; H, 5.56, N, 13.64%. Found: C, 35.47; H, 4.82; N, 13.01%. ESI-MS $[TmS,S^{hexyl}]^+$: Accurate mass predicted, 435.16251, found 435.16272. ^{1}H-NMR (500 MHz, $CDCl_3$): δ =7.61 (d, 2H, -CH), 7.59 (d, 2H, -CH), 6.72 (d, 1H, -CH), 6.42 (d, 1H, -CH), 4.04 (s, 6H, $-CH_3$), 3.5 (s, 3H, $-CH_3$), 3.40 (m, 2H, **H**CH), 2.95 (m, 2H, HC**H**), 1.81 (m, 2H, HC**H**), 1.69 (m, 2H, -**H**CH), 1.55 (m, 2H, -HC**H**), 1.33 (m, 2H, -HC**H**). ^{13}C-NMR (125 MHz, $CDCl_3$): δ = 164.8, 142.1, 127.1, 125.0, 120.8, 119.0, 36.9, 35.5, 34. 4, 27.2, 23.9 ppm. FT-IR (KBr, cm^{-1}): 2515 (νB-H), 740 (νC-S).

3.2.1.f. Preparation of ($Tm^{Me}SS'^{octylene}Tm^{Me}$)I: recrystallised from methanol: diethyl-ether. Yield 0.094 g (32%). Anal. Calcd. for $C_{20}H_{32}N_6BS_3I$: C, 40.69; H, 5.46, N, 14.23%. Found: C, 40.27; H, 5.39; N,13.90%. ESI-MS $[TmS,S'^{octyl}]^+$: Accurate mass predicted, 463.19381, found 463.19424. ^{1}H-NMR (500 MHz, $CDCl_3$): δ = 7.65 (d, 2H, -CH), 7.53 (d, 2H, -CH), 6.73 (d, 1H, -CH), 6.51 (d, 1H, -CH), 4.03 (s, 6H, $-CH_3$), 3.56 (s, 3H, $-CH_3$), 3.40 (m 2H, -**H**CH), 2.84 (m, 2H, -**H**CH), 1.18 (m, 2H, -HC**H**), 1.60 (m, 4H, -HC**H**), 1.46 (br, 4H, -**H**CH), 1.25 (m, 2H, -HC**H**). ^{13}C-NMR (125 MHz, $CDCl_3$): δ = 164.6, 141.7, 126.9, 125.3, 120.6, 119.2, 36.7, 35.2, 34.6, 27.4, 25.7, 25.0 ppm. FT-IR (KBr, cm^{-1}): 2535 (νB-H), 745 (νC-S).

3.2.1.g. Preparation of ($Tm^{Me}SS'^{decylene}Tm^{Me}$)I: recrystallised from methanol: diethyl-ether. Yield 0.085 g (27%). Anal. Calcd. for $C_{22}H_{36}N_6BS_3I.H_2O$: C, 41.50; H, 6.02; N, 13.21%. Found: C, 41.68; H, 5.75; N, 12.64%. ESI-MS $[TmS,S'^{decyl}]^+$: Accurate mass predicted, 491.22565, found 491.22511. ^{1}H-NMR (500 MHz, $CDCl_3$): δ = 7.62 (d, 2H, -CH), 7.46 (d, 2H, -CH), 6.75 (d, 1H, -CH), 6.49 (d, 1H, -CH), 4.2 (s, 6H, $-CH_3$), 3.55 (s, 3H, $-CH_3$), 3.21 (m, 2H, **H**CH), 2.96 (m, 2H, **H**CH), 1.75-1.56 (m, 5H, HC**H**), 1.52-1.41 (m, 5H, **H**CH), 1.41-1.23 (m, 6H, HC**H**). ^{13}C-NMR (125 MHz, $CDCl_3$): δ = 164.8, 142.2, 126.3, 125.4, 120.2, 119.3, 36.7, 36.1, 34.7, 28.6, 26.3, 26.0, 15.3 ppm. FT-IR (KBr, cm^{-1}): 2520 (νB-H), 755 (ν C-S).

3.2.1.h. Preparation of ($Tm^{Me}SS'^{xylylene}Tm^{Me}$)Br: recrystallised from methanol: diethyl-ether. Anal. Calcd. for $C_{20}H_{24}N_6BS_3Br$: C, 44.86; H, 4.52; N, 15.70%. Found: C, 42.17; H, 5.08; N, 14.29%. ESI-MS $[TmS^{xylyl}]^+$: 455 (100%). Accurate mass predicted, 4455.1312, found 455.1313. ^{1}H-NMR (400 MHz, $CDCl_3$): δ = 7.89 (d, 2H, -CH), 7.80 (d, 2H, -CH), 7.28 (s, 1H, Ar CH), 7.21 (m, 2H, Ar CH), 7.10 (m, 1H, Ar CH), 6.61 (d, 1H, -CH), 6.24 (d, 1H, -CH), 4.67 (d, 1H, **H**CH), 4.34 (d, 1H, HC**H**), 3.87 (s, 3H, $-CH_3$) 3.58 (s, 6H, $-CH_3$). ^{13}C-NMR (100 MHz, $CDCl_3$): δ = 164.7, 140.03, 135.84, 134.88, 130.87, 128.74, 128.24, 126.03, 125.58, 36.53, 35.54, 34.95, 33.97 ppm. FT-IR (KBr, cm^{-1}): 2523 (νB-H), 746.55 (ν C-S).

3.2.2. Preparation of ($Tm^{Ph}SS'^{propylene}Tm^{Ph}$)I:

$NaTm^{Ph}$ (0.14 g, 0.25 mmol) in chloroform (20 ml) was refluxed for 2 hours with 1,3-diiodopropane (0.07 ml, 0.24 mmol). The white precipitate formed was filtered off and the solution is taken into dryness. The product was re-crystallised by the slow vapour diffusion of a solution of the compound in methanol with diethyl ether. Anal. Calcd. for $C_{30}H_{28}N_6BS_3I.3H_2O$: C, 47.36; H, 4.51; N, 11.05%. Found: C, 47.06; H,4.07; N, 10.66. ESI-MS $[Tm^{Ph}SS'^{propyl}]^+$: Accurate mass predicted, 579.1625, found, 579.1621. ^{1}H-NMR (400 MHz, DMSO): δ = 8.14 (d, 2H, -CH), 7.77 (d, 2H, -CH), 7.69-7.64 (br m, 14H, Ar), 7.49 (t, 2H, -CH (Ar)), 7.46 (d, 1H, -CH), 7.42 (t, 1H, Ar), 7.16 (d, 1H, -CH), 2.66 (m, 2H, HCH), 2.31 (m, 2H, HCH). 1.79 (m, 1H, HCH), 1.39 (m, 1H, HCH). ^{13}C-NMR (100 MHz, DMSO): δ = 164.6, 143.1, 142.7, 138.1, 135.3, 130.7, 129.9, 128.7, 127.6, 126.2, 125.5, 122.8, 119.7, 64.9, 33.5, 29.9 ppm. FT-IR (KBr, cm^{-1}): 2465 (B-H), 760 (C=S), 740 (C-S).

3.2.3. Preparation of ($Tm^{Ph}SS'^{decylene}Tm^{Ph}$)I:

0.12 g NaTmPh (0.21 mmol) in 20 ml chloroform was refluxed 2hours with 1 equivalent 1,10-diiododecane (0.083 g, 0.21 mmol). The white precipitate formed is filtered off and the solution was taken to dryness. The substance could be further purified by re-crystallising by the slow vapour diffusion of the compound in methanol with diethyl

ether. Anal. calcd. for $C_{37}H_{42}N_6BS_3I$: C, 55.21; H, 5.26; N,10.45%. Found: C, 50.67; H,5.35; N, 9.86. ESI-MS $[Tm^{Ph}SS'^{decyl}]^+$: 677 (100). Accurate mass predicted, 677.2721, found, 677.2715. ^{1}H-NMR (400 MHz, DMSO): δ = 8.42 (d, 2H, -CH), 8.03 (d, 2H, -CH), 7.91 (d, 2H, -CH(Ar)), 7.46-7.88 (mixture of doublets and triplets), 7.49 (t, 1H, -CH(Ar)), 7.29 (t, 1H, -CH), 7.08 (t, 1H, -CH), 3.11-3.03 (broad multiplet, -**H**CH), 2.69 (br, -HC**H**), 1.42 (br, -**H**CH), 1.23-1.02 (broad multiplet, -HC**H**). ^{13}C-NMR (100 MHz, DMSO): δ= 161.49, 142.43, 141.62, 137.81, 130.74, 129.88, 127.61, 127.57, 126.63, 125.65, 125.51, 124.98, 122.55, 119.46, 115.38, 64.89, 34.89, 28.68, 27.62 ppm. FT-IR (KBr,cm^{-1}): 2469.5 (B-H), 753.34 (C=S), 737.98 (C-S).

3.2.4. Preparation of $[Tm^{Ph}\text{-}S]BF_4$:

0.14 g NaTmPh (0.25 mmol) was added to $NOBF_4$ (0.0292 g, 0.25 mmol) in dry THF. Liberation of NO gas was noticed. The reaction mixture was stirred overnight. The solution was filtered and taken to dryness. The yellow oily substance obtained was purified by re-crystallisation by the vapour diffusion of the product in minimum amount of methanol with diethyl ether. ESI-MS $[Tm^{Ph}\text{-}S]^+$: 505 (100). Accurate mass predicted, 505.1435, found, 505.1443. FT-IR (KBr,cm^{-1}): 2453.49 (B-H), 768.71 (C=S).

3.2.5. Preparation of $[Tm^{Ph}\text{-}S]I_3$:

0.14 g NaTmPh (0.25 mmol) in 20 ml dry DCM was stirred under nitrogen atmosphere with 1 equivalent phosphorous iodide (0.1029 g, 0.25 mmol). The dark red coloured solution was filtered and reduced the volume into 2 ml. Dark red X-ray quality crystals of the product were formed when this solution was diffused with diethyl ether. Yield 0.164 g (57%). Anal. calcd. for $C_{27}H_{22}N_6BS_2I_5$, C, 28.43; H, 1.95; N,7.37%. Found: C, 29.69; H,1.28; N, 6.65%. ESI-MS $[Tm^{Ph}\text{-}S]^+$: 505 (100). Accurate mass predicted, 505.1435, found, 505.1432. ^{1}H-NMR (400 MHz, DMSO): δ = 8.34 (d, 2H, -CH), 8.11 (d, 2H, -CH), 7.74 (br, 1H, -CH), 7.69-7.63 (broad multiplets, 11H), 7.60-7.39 (broad multiplets, 10H). ^{13}C-NMR (100 MHz, DMSO, 3072 Scans, 2secs relaxation): δ = 135.47,

133.08, 131.42, 130.63, 129.09, 128.95, 128.53, 126.41, 126.16, 125.95, 125.87, 125.53, 124.67, 64.88 pm. FT-IR (KBr,cm^{-1}): 2468.85(B-H), 763.58(C=S), 737.98 (C-S).

3.2.6. Preparation of [Tm^{Ph}-S]I:

$NaTm^{Ph}$ (0.13 g, 0.24 mmol) was dissolved in THF (40 ml) to which iodine (0.030 g, 0.12 mmol) was added. The reaction vessel was kept in the dark and stirred for six days. The solvent was removed and the residue washed with diethyl ether to remove excess iodine. The residue was recrystallised from dichloromethane by vapour diffusion with diethyl ether. Yield: 36% Anal. Calcd. for $C_{27}H_{22}N_6BS_2I_3.H_2O$: C, 35.85; H, 2.68; N, 9.30%. Found: C, 36.11; H, 3.27; N, 8.78%. ESI-MS $[M]^+$: Accurate mass predicted, 505.1350, Found. *m/z* 505.1435. ^{1}H-NMR (500 MHz, DMSO) δ = 8.30 (d, 2H -CH), 8.11 (d, 2H, -CH), 8.00-7.4 (Ar, 15H), 7.47 (d, 1H, -CH), 7.31 (d, 1H, -CH). ^{13}C-NMR (500 MHz, $CDCl_3$): δ = 137.88, 135.45, 133.21, 131.32, 130.60, 129.92, 128.66, 127.62, 126.16, 126.10, 125.87, 125.49, 122.55, 120.88, 119.42 ppm. The ^{1}H, ^{13}C, ^{13}C-135DEPT and the ^{1}H-^{13}C correlated NMR spectra are reproduced in results and discussion for inspection. FT-IR (KBr, cm^{-1}): 1610 (ν arom), 765 (νC-S).

	$Tm^{Me}SS'(CH_2)_3$	$Tm^{Me}SS'(CH_2)_4$	$Tm^{Me}SS'(CH_2)_5$	$Tm^{Me}SS'(CH_2)_8$	Polycyclic cation
Empirical formula	$C_{15}H_{22}B_1I_1N_6S_3$	$C_{16}H_{24}B_1Br_1N_6S_3$	$C_{17}H_{26}B_1I_1N_6S_3$	$C_{20}H_{32}B_1I_1N_6S_3$	$C_{27}H_{22}BI_5N_6S_2$
FW	520.01	487.03	548.04	590.09	1139.66
Crystal system	Monoclinic	Monoclinic	Monoclinic	Monoclinic	Tetragonal
Space group	C2/c	P 1 21/n 1	P 1 21/c 1	C 1 2/c 1	I -4
a/Å	12.0(4)	13.7955(9)	14.1166(10)	35.6670(30)	26.773396)
b/ Å	17.080(10)	11.1555(7)	13.8444(9)	13.8826(18)	26.7733(6)
c/ Å	20.15(10)	15.4311(12)	11.5688(6)	11.2541(10)	10.1745(3)
$\alpha/^o$	90.0	90.0	90.0	90.0	90.0
$\beta/^o$	102.2(2)	100.007(7)	91.106(5)	95.421(9)	90.0
$\gamma/^o$	90.0	90.0	90.0	90.0	90.0
Z	4	4	4	10	8
V/A^3	4036.67(50)	2338.65(29)	2260.54	5547.55(49)	7293.18(3)
μ_{calc}/mm^{-1}	1.910	3.748	1.710	1.415	4.405
No. Reflns Measd	16696	15244	24298	8074	10343
No. Unique reflns	5068	5875	5878	4421	7408
No Observed reflns	3755	3283	2724	2990	6773
No. Parameters	239	349	327	307	375
R^a (1>2σ(I))	0.052	0.050	0.067	0.146	0.043
R_w^b (all reflns)	0.129	0.112	0.100	0416	0.107
GOF	0.983	0.942	0.904	1.628	1.038

3.3. Results and Discussion.

The serendipitous formation of a polycyclic compound from the reaction of Tm^{Me} and dichloromethane was reported previously by Hill *et al*.[8] However, studies discussed in chapter 2 suggested that this and further members of this class of compound could be produced rationally and in good yield using suitable di-bromo or di-iodo alkanes. Extending this family of compounds would allow us to investigate the conformational changes which occur as the length of the bridge increases. Furthermore the size of the rings produced would provide further information on the influence of the B-H…S=C interactions which hold the anion in its **0:3** and **1:2** conformations (chapter 2).

Treating Tm^{Me} with a range of terminal dihalides ($X-(CH_2)_n-X$ where X= Br, I: n = 1, 3, 4, 5, 6, 8 and 10) leads to the formation of a series of discrete tricyclic species (equation 3.1). A selection of these were crystallised and subjected to X-ray crystallographic analysis (figure 3.3). Except for the increase in the central ring formed between two sulfur atoms the species all adopt a similar conformation where the thioethers remain above the BN_3 plane (table 3.1). Little strain is transferred into the BN3 fragment with the B-N distances (1.553 - 1.610 Å) and the <N-B-N angles (108.7 -109.7^o) occurring within a very small range. The influence of the increasing ring size is observed in the imaginary S-N-N-S torsion angle which defines how the two modified methimazolyl rings lie in relation to one another. These change in a non-uniform manner with largest and smallest rings returning the larger values (table 3.1). The species which did not crystallise were characterised by high resolution mass spec and ^{1}H NMR. Mass spectrometry demonstrates that all these species are discrete cations. The ^{1}H NMR spectrum, by virtue of the downfield shift in the methine resonances, confirms the modification of two of the three methimazole rings.

Compounds	B-N	C-S	$C\text{-}N_{(Me)}$	$\angle N_{(B)}\text{-}C\text{-}S$	∠N-C-N	∠H-B-N
$Tm^{Me}S\text{-}S'^{propyl}Tm^{Me}$	1.6099(5) 1.5546(4) *1.5203(3)	1.7223(4) 1.7305(3) *1.7111(5)	1.3524(3) 1.4779(4) *1.4412(4)	125.7(3) 127.6(3) *126.8(3)	110.1(4) 109.9(4) *105.6(4)	109.4(4) 109.4(4) *109.3(4)
$Tm^{Me}S\text{-}S'^{butyl}Tm^{Me}$	1.5719(1) 1.5767(1) *1.5366(1)	1.7390(1) 1.7377(1) *1.6930(1)	1.3427(1) 1.3416(1) *1.3609(1)	128.7(3) 123.5(3) *127.0(3)	108.8(3) 108.6(3) *106.8(3)	111.7(16) 110.8(16) *109.3(15)
$Tm^{Me}S\text{-}S'^{pentyl}Tm^{Me}$	1.5731(1) 1.5623(1) *1.5278(1)	1.7423(1) 1.7377(1) *1.6875(1)	1.3368(1) 1.3462(1) *1.3678(1)	126.3(5) 126.8(5) *128.1(5)	108.6(5) 108.3(5) *107.0(6)	111.0(3) 106.0(3) *110.0(3)
$Tm^{Me}S\text{-}S'^{octyl}Tm^{Me}$	1.5534(2) 1.5639(1) *1.6027(1)	1.7319(1) 1.7519(1) *1.6766(1)	1.3660(2) 1.3742(1) *1.3927(1)	126.5(13) 130.8(15) *129.8(11)	107.3(15) 108.8(14) *101.7(16)	112.2(1) 112.2(1) *112.2(1)

Table 3.1: Selected bond lengths (Å) and bond angles (∠) of polycyclic compounds formed between Tm^{Me} and a range of dihaloalkanes. * indicating the the bond lengths and bond angles of methimazole ring which do not take part in the ring formation.

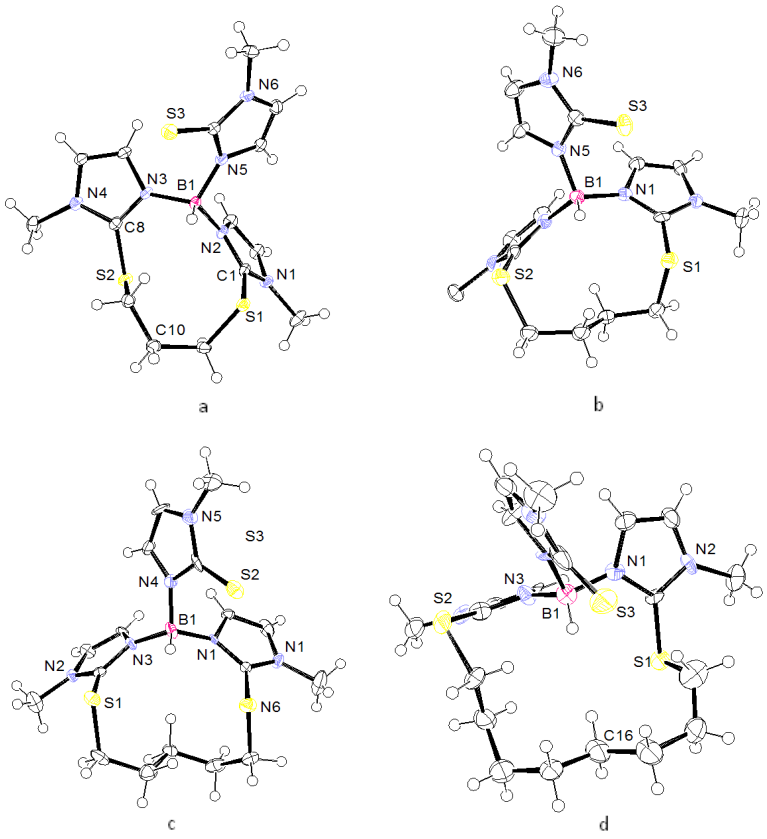

Figure 3.3: Molecular structures of (a) *bis*(1-methylimidazol-2-yl-thio) propane-N,N')-(1-methyl-2-thioimidazol-3-yl)borane; $[TmS^{propyl}]^{+}$, (b) *bis*(1-methylimidazol-2-yl-thio)butane-N,N')-(1-methyl-2-thioimidazol-3-yl)borane; $Tm^{Me}SS'^{butyl}Tm^{Me}$, (c) *bis*(1-methylimidazol-2-yl-thio)pentane-N,N')-(1-methyl-2-thioimidazol-3-yl)borane; $Tm^{Me}SS'^{pentyl}Tm^{Me}$, (d) *bis*(1-methylimidazol-2-yl-thio)octane-N,N')-(1-methyl-2-thioimidazol-3-yl)borane; $Tm^{Me}SS'^{octyl}Tm^{Me}$ catons. Counter ions are omitted for clarity. Thermal ellipsoids are shown at a probability of 30%. The N•S•S•N torsion angle for the series of heterocyclic rings are: Me 65.7°, Pr 58.8°, Bu 29.3°, Pen 11.9°, Oct 98.5°.

The ability to generate these ring species especially those with fifteen (figure 3.3) and seventeen membered rings suggests that the cyclisation process is pre-organised. Our *ab-initio* analysis of Tm^{Me} clearly suggests that there is a preference for motifs where the thione sulfurs lie adjacent to the B-H unit.[9] This conformation makes intramolecular cyclisation preferrable over intermolecular coupling. A comparison of some selected bond lengths and bond angles of these complexes are given in table 3.1 (above).

Notable by its absence from this series of compounds is an adduct of the 1,2-dihaloethanes. These do not form ring compounds and instead generate species identified as the soft scorpionate free acid H[Tm^{Me}]. Consistent with our studies on iodobenzene and 2-bromopropane a metathesis reaction occurs but the carbocation generated does not add to the sulfur.[9] Instead it is believed that an elimination reaction occurs which leads to the formation of vinyl bromide (Scheme 3.2).

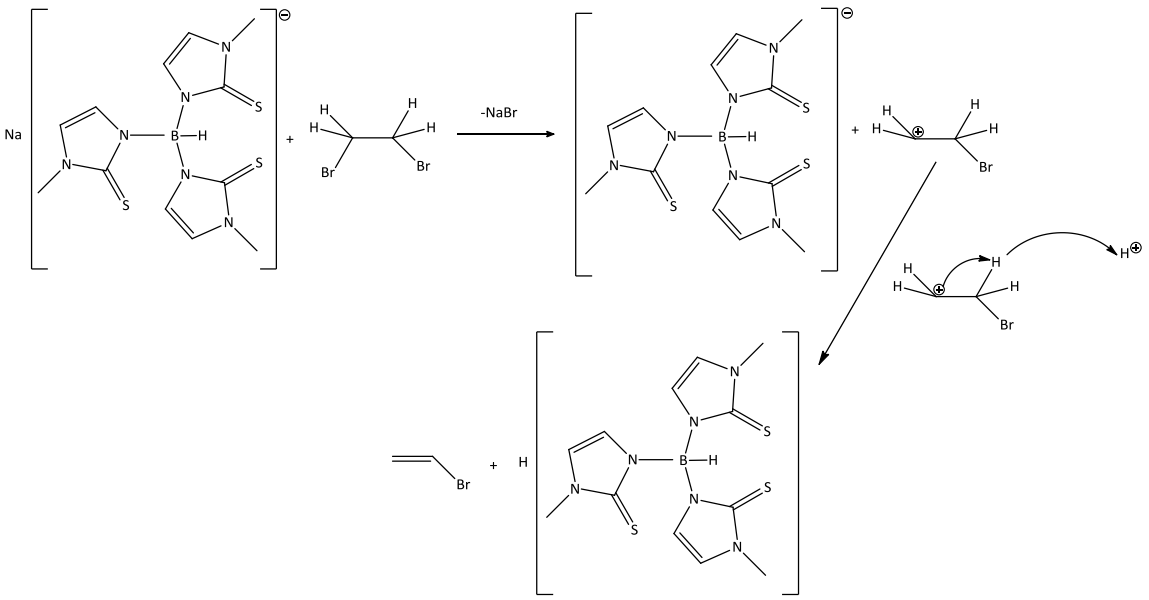

Scheme 3.2: Possible reaction mechanism of 1,2-dibromoethane with NaTm^{Me}.

To investigate the ring formation further, the methyl substituent on nitrogen was replaced with the phenyl group. These species were alkylated to produce the desired species with 1,3- diiodopropane and 1,10-diioddecane which explains that the ring closure reaction is preorganised.

The alkylated compounds discussed above are all adducts formed through reactions with electrophiles capable of forming stable bonds to sulfur. Reactions with electrophiles such as nitric oxide which do not support the formation of stable

adducts of sulfur have been investigated previously.[10] The major product isolated from these reactions was the borane adduct of DMF. This compound results from borohydride oxidation.[10] However, a second minor product was also isolated from the mixture which was found to be an unusual heterocycle (figure 2.5).[15]

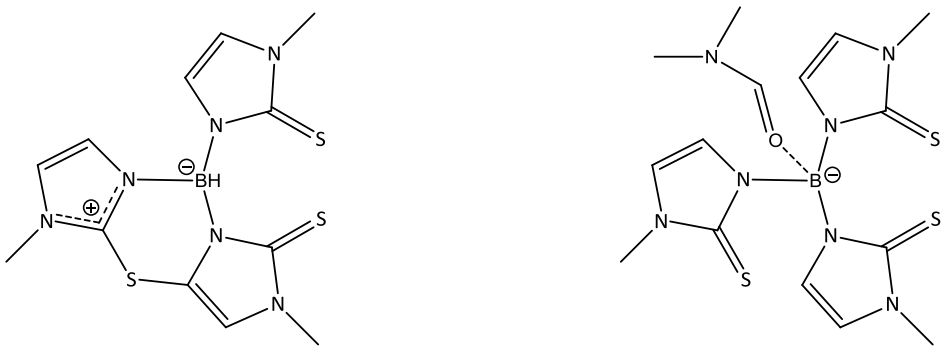

Figure 3.4: The crossbow product (left) and the DMF adduct (right) obtained by the reaction between $NaTm^{Me}$ and $NOBF_4$.[15]

The formation of the complex heterocycle (figure 3.4 left) results from the reaction of Tm^{Me} with an electrophilic oxidant. Molecular iodine is potentially a similar species which affords greater control of the reaction. The subsequent treatment of Tm^{Me} with molecular iodine generates the same heterocyclic product (figure 3.4) but in higher yield. This result indicates that there is a further reaction pathway available to soft scorpionates when challenged with mild oxidising agents. To further understand the chemistry of these reactions Tm^{Ph} anion was also subjected to oxidation with iodine and $NOBF_4$. However these reactions did not lead to the formation of the related Tm^{Me} based product. Although continuous attempts to crystallise and structurally characterise this material failed, the mass spectrum of the product (*m/z* = 505.1443 accurate mass, 100%) clearly suggested that the species obtained only contained two sulphur atoms.

From the related reaction of Tm^{Ph} with phosphorus tri-iodide (PI_3) a product was isolated (figure 3.5) which helped with the characterisation of the species isolated above. In this reaction oxidative desulphurisation of the Tm^{Ph} anion leading to ring closure is observed. This gives rise to a second polycyclic ring containing only two sulfurs and which carries an overall single positive charge. Under the anaerobic conditions prevailing in the reaction iodide is oxidised to form iodine and tri-iodide. The former forms a stable cationic adduct of polycyclic ring compound via the thione of the unmodified methimazole ring with the latter adopting the simpler role as the counter anion. Due to the weakness of the S-I_2 interaction it is unsurprising that the mass spectrum of this product is dominated by the molecular ion of the polycyclic cation (Tm^{Ph}-S; *m/z* = 505.1432 accurate mass, 100%). This observation is consistent with the elusive product discussed above for the reaction of Tm^{Ph} with electrophiles. From this premise it is possible to assign the other spectroscopic data from the product of this earlier reaction in such a way that the polycyclic cation (Tm^{Ph}-S) can also be identified as the product of Tm^{Ph} oxidation.

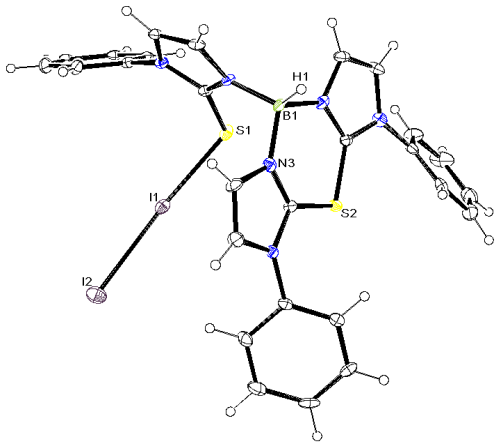

Figure 3.5: X-ray molecular structure of the polycyclic ring compound formed by the reaction of $NaTm^{Ph}$ with PI_3. The $[I_3]^-$ counteranion is omitted for clarity. Thermal ellipsoids are shown at a probability of 30%.

The treatment of $NaTm^{Ph}$ with molecular iodine leads to the formation of the same polycyclic ring compound (Tm^{Ph}-S). Repeated attempts to crystallise this material failed. However NMR spectroscopic analysis supports the presence of the polycyclic ring cation similar to that obtained from the reaction of $NaTm^{Ph}$ with PI_3 (figure 3.7).

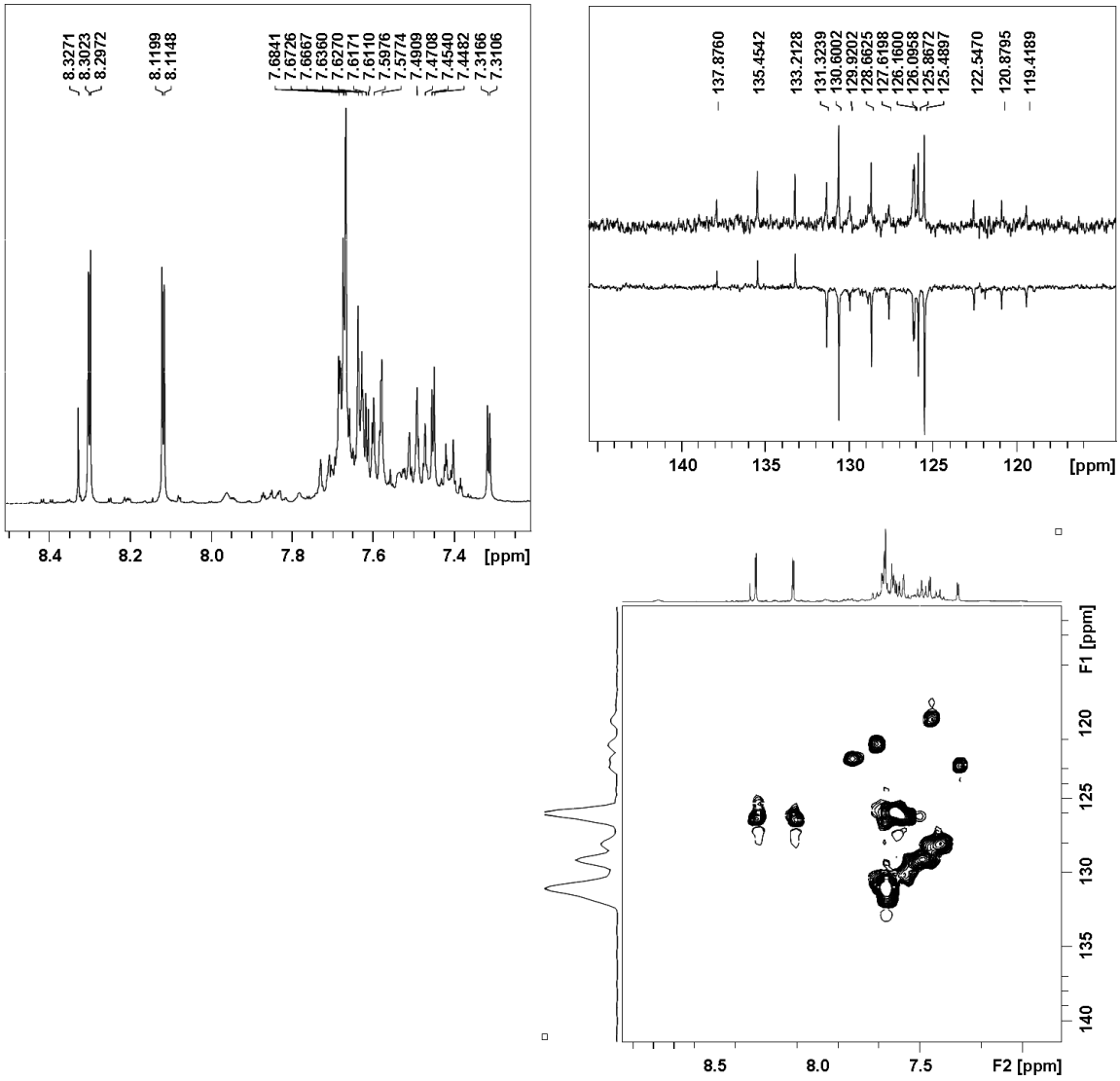

Figure 3.7: NMR spectrum study of $(Tm^{Ph}\text{-}S)I_3$; the polycyclic ring compound obtained by the reaction of $NaTm^{Ph}$ with molecular iodine. All the spectra were recorded by using 400 MHz and d^6-DMSO as solvent. Spectra were calibarated with respect to the solvent peaks. Only selected regions are showing.Top left is the ^1H NMR spectrum. Top right is 135 DEPT ^{13}C NMR and the bottom one is the $^1H/^{13}C$ correlation spectrum.

Iodine adducts of thiones are well known.[16-19] These are generally divided into three categories: (Type A) S-I^+ I^- (*d*/Å, I-I >2.8); (Type B) S-I-I (*d*/Å, I-I ~2.6-2.8 Å); and (Type C) S··I-I (*d*/Å, I-I <2.6 Å), where compounds are assigned to a category based on their corresponding S-I and I_2 bond distances. The compound reported above is cationic and while its bond lengths (*d*/Å S1-I1, 2.641; I1-I2, 2.9213) places it at the boundary between type A and B, when one considers the influence of the charge derived from the heterocycic ring a formulation of S-I^+ would seem appropriate.

The exact reaction mechanism of ring closure to form the two novel heterocycles discussed above is not clear. The proposed mechanism suggests that initially the electrophile (NO^+, I_2) forms an adduct at sulfur. For simple thiones these adducts of iodine can be stable (figure 3.6). In contrast S-nitrosation of thiones generate a reactive entity which leads to S-S coupling.[20] Since the soft scorpionates carries an overall negative charge it would seem that an intramolecular ring closure is favoured, which facilitates the formation of a borane centred heterocycle (figure 3.8).

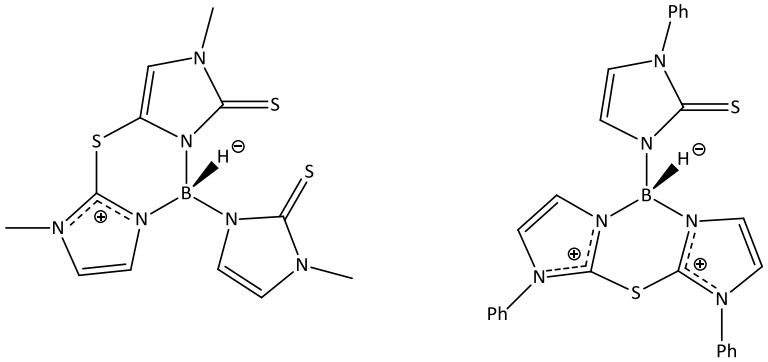

Figure 3.8: Borane centered hetrocycle formed by the reaction of soft scoprionates with NO^+ and iodine. Left is the neutral polycyclic compound formed from the reaction of Tm^{Me} anion with NO^+ and the right is the polycyclic cation formed by the reaction of Tm^{Ph} anion with NO^+.

It is interesting to note that the treatment of the two related soft scorpionates with the same reagents, $NOBF_4$, $NaTm^{Me}$ and $NaTm^{Ph}$ gives two different products. The earlier produced a polycyclic compound in which the ligand loses the proton from the methimazole ring (figure 3.4) being replaced by the bridging sulfur. In this species all three sulfurs are still present and the compound is neutral in charge, whereas in the case of Tm^{Ph} anion, a thioether bond is formed with the elimination of a sulfur from the methimazole unit which generates positive charge. Although this is not a common reaction for neutral thiones a related ring closure has been reported between thioimidazole and imidazoles.[21]

The reason why the two anions Tm^{Me} and Tm^{Ph} form different heterocycles can be explained. Studies on the conformations and dynamic behaviour of Tm^{R} indicate that there are four conformations of the uncoordinated anion (previously discussed in chapter 2). The most favoured species for Tm^{Me} and Tm^{Ph} have the anions in a conformation which aligns two thiones with the borohydride group with the remaining thione lying below the plane defined by the three nitrogens bonded to boron (**2:1**, figure 3.9). The electrostatic interactions between the B-H group and the thione act to protect the sulfur centres favouring a reaction between the thione below the N3 plane and the double bond in the methimazole unit (figure 3.8). Tm^{Ph} was also subjetcted to DFT and significantly no change in its conformational preference was found i.e the most stable form is the **2:1** form (figure 3.9, table 3.2).

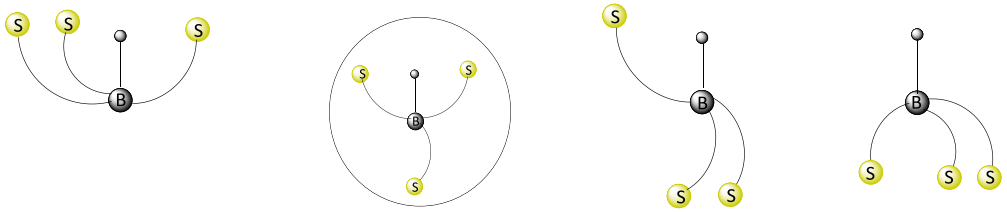

Figure 3.9: Simplified representation of conformations of Tm anion. TmMe figure was shown in chapter 2 (figure 2.15). Both Tm^{Me} and Tm^{Ph} anions are preferred stable conformation is **2:1** (circled in the figure) i.e. two methimazole units are pointing towards –BH and the third one is pointing away from –BH. The rottational energy barrier between **2:1** form and **1:2** form for Tm anion is not known but is so low so that the free rotation is possible.

Conformation	Tm^{Me} anion	Tm^{Ph} anion
3:0	-2015.022656 a.u. +2.90 kcal mol^{-1}	-2590.203662 a.u. +2.52 kcal mol^{-1}
2:1	-2015.027270 a.u. 0.00 kcal mol^{-1}	-2590.207686 a.u. 0.00 kcal mol^{-1}
1:2	-2015.027270 a.u. 0.00 kcal mol^{-1}	-2590.206445 a.u. +0.78 kcal mol^{-1}
0:3	-2015.004252 a.u. +14.44 kcal mol^{-1}	-2590.185739 a.u. +13.77 kcal mol^{-1}

Table 3.2: Comparison of total energy (a.u.) and relative enrgies (kcal mol^{-1}) of Tm^{Me} and Tm^{Ph} anions.

The mechanism thus does not rely on the conformation of the rings and thus must hinge on the electronic properties of the substiutenets on the hetertocyclic nitrogen. An analysis of the charges (Mulliken population) on the atoms in the thio-imidazole rings indicate that the substituent on the nitrogen have a minimal effect on electronic character of the parent scorpionate anions. This is not surprising as

the phenyl group does not adopt a conformation co-planar with the thio-imidazole ring in either the DFT analysis of the anion or any of its reported X-ray crystal structures.[22]

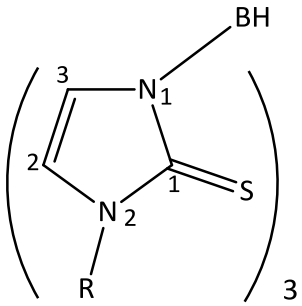

Figure 3.10: Numbering system used in the chapter.

	Tm^{Me}	Bm^{Me}imSMe			Tm^{Ph}	Bm^{Ph}im(Ph)SME		
		Ring A (Me)	Ring B (U)	Ring C (D)		Ring A (Me)	Ring B (U)	Ring C (D)
$H_{(B)}$	-0.04	-0.06			-0.04	-0.06		
B	+0.49	+0.47			+0.50	+0.46		
N1	-0.35, -0.35, -0.35	-0.30	-0.37	-0.36	-0.35, -0.38, -0.35	-0.29	-0.37	-0.36
N2	-0.34, -0.35, -0.34	-0.32	-0.34	-0.34	-0.42, -0.42, -0.41	-0.35	-0.41	-0.41
C1	+0.20, +0.22, +0.18	+0.18	+0.20	+0.16	+0.18, +0.20, +0.18,	+0.18	+0.18	+0.15
C2	-0.01, -0.01, -0.03	+0.02	-0.01	0.00	-0.02, -0.01, -0.03,	+0.02	-0.01	+0.01
C3	0.03, 0.04, 0.00	+0.02	0.00	0.00	+0.04, +0.04, +0.04,	+0.08	+0.13	0.00

Table 3.3: The charges (Mulliken population) on the thioimidazole rings of Tm^{Me}, Tm^{Ph} and their mono-methylated adducts Bm^{Me}imSMe and Bm^{Ph}imSMe (im denotes the alkylated thio-imidazole).‡ The numbering system follows that shown in figure 3.8

DFT analysis of the charges on the atoms as a result of the alkylation of a single thione (figure 3.10, table 3.3) demonstrate the expected change occuring at sulfur as the thione changes to a thioether. The calculated charges on the thioimidazole rings lying below the BN_3 plane remain similar despite alkylation suggesting that these rings are the spectators in the ring closure reaction. By virtue of the low charge on the C_3 atom (table 3.3) this pathway is available to Tm^{Me} (scheme 3.3). However, for Tm^{Ph} the charge calculated on this atom is found to be significantly higher (+0.13) and consequently ring closure between C_3 and the thione is no longer favourable. Instead ring formation occurs by the reaction of the thione on the thione. This analysis explains why we do not observe any neutral crossbow product in the reaction mixtures derived from Tm^{Ph}. However, it does not explain why the polycyclic cation is absent in the reactions of Tm^{Me}. These are unique heterocycles which are of great interest. Greater clarity regarding the ring closure mechamisms will only become available as new species are reported.

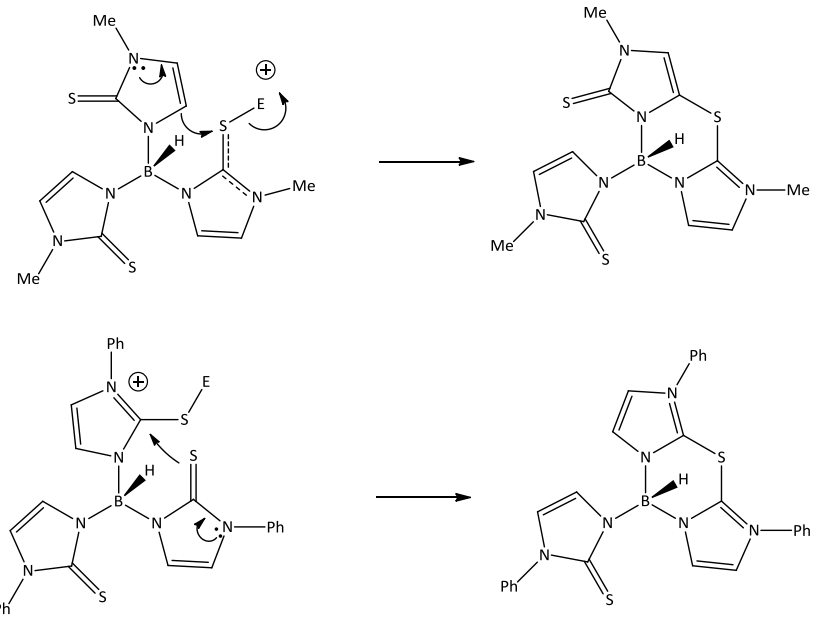

Scheme 3.3: Proposed reaction mechanism of NO^+ with Tm^{Me} anion (top) and Tm^{Ph} anion (bottom).

Thus the formation of the alkyl adducts and polycyclic rings were an important step in the discovery of a range of unusual polycyclic rings. This chemistry suggests that there may be futher interesting chemistry between Tm^R and oxidising agents.

3.4. Conclusion

Scorpionates have been popular ligands for nearly fifty years. The advent of soft scorpionates generated new metal complexes and reactivities. The chemistry described here extends their chemistry by forming novel cations and unusal polycyclic heterocycles. Using the lower halides we have been able to increase the efficiency of this reaction and consequently extend this series of multi-ring heterocyclic compounds. With mild oxidising agents like NO^+ and iodine, Tm^R generate different polycyclic heterocycles. The treatment of other soft scorpionates with other mild oxidising agents is an area of chemistry which should be explored futher.

3.5. References:

1. Spicer, M. D.; Reglinski, J. *Eur. J. Inorg. Chem*. **2009**, 1553-1574.
2. Mohamed, A. A.; Rabinovich, D.; Fackler, J. P. *Acta Crystallogr., Sect. E,* **2002**, *58*, m726.
3. Patel, D. V.; Mihalcik, D. J.; Kreisel, K. A.; Yap, G. P. A.; Zakharov, L. N.; Kassel, W. S.; Rheingold, A. L.; Rabinovich, D. *Dalton Trans.* **2005**, 2410-2416.
4. Dodds, C. A.; Garner, M.; Reglinski, J.; Spicer, M. D. *Inorg. Chem.* **2006,** *45,* 2733-2741.
5. Bailey, P. J.; Lorono-Gonzales, D. J.; McCormack, C.; Parsons, S.; Price, M. *Inorg. Chim. Acta* **2003**, *354*, 61- 67.
6. Graham, L. A.; Fout, A. R.; Kuehne, K. R.; White, J. L.; Mookherji, B.; Marks, F. M.; Yap, G. P. A.; Zakharov, L. N.; Rheingold, A. L.; Rabinovich, D. *Dalton Trans.* **2005**, 171-180.
7. Bailey, P. J.; Budd, L.; Cavaco, F. A.; Parsons, S.; Rudolphi, F.; Sanchez-Perucha, A.; White, F. J. *Chem. Eur. J*. **2010**, *16*, 2819-2829.
8. Crossley, I. R.; Hill, A. F.; Humphery, E. R.; Smith, M. K.; Tshabang, N.; Willis, A. C. *Chem Commun*. **2004**, 1878-1879.
9. Rajasekharan-Nair, R.; Moore, D.; Chalmers, K.; Wallace, D.; Reglinski, J.; Spicer, M. D. *Chem. Eur. J*. DOI: 10.1002/ Chem.201202314
10. Schwable, M.; Andrikopoulos, P. C.; Armstrong, D. R.; Reglinski, J.; Spicer, M. D. *Eur. J. Inorg. Chem*. **2007**, 1351-1360.
11. Garner, M.; Reglinski, J.; Cassidy, I.; Spicer, M. D.; Kennedy, A. R. *Chem Commun*. **1996**, 1975-1976.
12. Sheldrick, G. M. *Acta Crystallogr*. **2008**, *A64*, 112-122.
13. Altomare, A.; Cascarano, G.; Giacovazzo, C.; Gualardi, A. *J. Appl. Crystallogr.* **1993,** *26*, 343-350.
14. Farrugia, L. J. *J. Appl. Crystallogr*. **1999,** *32*, 837.
15. Schwalbe, M.; Beirnat, A.; Reglinski, J.; Spicer, M. D. Unpublished results.

16. Freeman, F.; Ziller, J. W.; Po, H. N.; Keindl, M. C. *J. Am. Chem. Soc*. **1988**, *110*, 2586-2591.
17. Bigoli, F.; Deplano, P.; Mercuri, M. L.; Pellinghelli, M. A.; Sabatini, A.; Trogu, E. F.; Vacca, A. *J. Chem. Soc. Dalton Trans.*, **1996**, 3583-3589.
18. Corban, G. J.; Hadjikakou, S. K.; Hadjiliadis, N.; Kubicki, M.; Tiekink, E. R. T.; Butler, I. S.; Drougas, E.; Kosmas, A. M. *Inorg. Chem.* **2005**, *44*, 8617- 8627.
19. Isaia, F.; Aragoni, M. C.; Arca, M.; Desmartin, F.; Devillanova, F. A.; Floris, G.; Garau, A.; Hursthouse, M. B.; Lippolis, V.; Medda, R.; Oppo, F.; Pira, M.; Verani. G. *J. Med. Chem.*, **2008**, *51*, 4050-4053.
20. Amado, S.; Dicks, A. P.; Williams, D. L. H. *J. Chem. Soc. Perkin Trans 2*. **1998**, 1869-1875.
21. Saczewski, F.; Gdaniec, M. *J. Chem. Soc. Perkin Trans.* **1992**, 47-50.

Chapter 4

An investigation on the stability of mercaptobenzothiazole based soft scorpionate (Tbz) complexes

4.1 Introduction

Interest in the methimazole based soft scorpionate anions has led to the use of other imine-thione heterocycles in the synthesis of further ligand systems. Amongst the earliest alternative donor species were hydro*tris*(mercaptobenzothiazolyl)borate (Tbz) and hydro*tris*(thiazolyl)borate (figure 4.1, Ttz).[1,2] However, since the initial report on these species, there have been a few reports on their chemistry. The initial study on Tbz included the synthesis of a thallium complex (figure 4.2) and this remained the only known complex of this anion until Baba *et al.* reported on the synthesis, structure and magnetic properties of a cobalt complex.[3] In 2003 Soares *et.al*. reported the synthesis of the related *tetrakis*(thiazolyl)borate anion.[4] But again to date no metal complexes of this species have been reported.

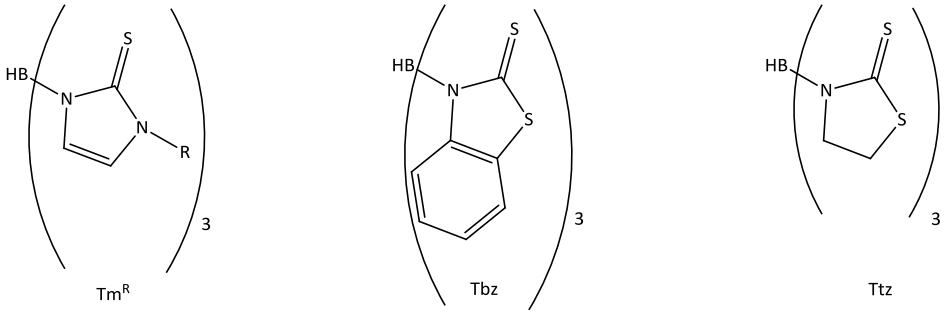

Figure 4.1: Pictorial representation of the soft scorpionates, Tm, Tbz and Ttz

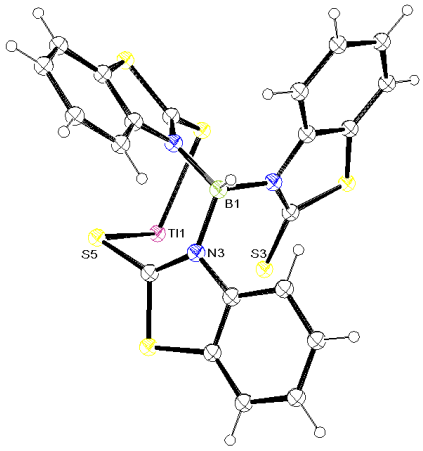

Figure 4.2: Molecular structure of hydro*tris*(mercaptobenzothiazolyl)boratothallium(I).[1] Solvent molecules are omitted for clarity. Thermal ellipsoids are shown at a probability of 30%.

Despite the ease with which these anions can be prepared, neither of these ligands has received much attention. The data presented above (Chapter 2) on the stability of scorpionate anions during alkylation and on the nature of the B-N bond may provide a reason for their lack of utility. However, the results discussed earlier also suggest that when complexed to a large electron rich metal (e.g. thallium), the resulting complex can be stable.[1] In contrast when complexed with strong, small Lewis acidic metals, the internal B-N bond will elongate and ligand decomposition will be promoted. This study seeks to explore the chemical consequences of the DFT study reported in chapter 2 by focusing on the chemistry of Tbz.

4.2 Experimental section

All chemicals used were commercially available and used without any purification. NaTbz was prepared in a slightly modified procedure to that reported in the literature.[1] NMR spectra were recorded using a Bruker AV500 or Bruker DPX400. All spectra obtained were referenced to the residual solvent peaks. IR spectra were recorded as KBr discs using a Nicolet Avatar 360 FT-IR spectrometer. Mass spectra were recorded by MALDI analysis using a Kratos AXIMA-CFR spectrometer. Crystals obtained were coated in mineral oil and mounted on glass fibres or a glass loop. Data were collected at 123K on Oxford diffraction diffractometer using graphite monochromated Mo-Kα radiation. The heavy atom positions were determined by Patterson methods and the remaining atoms located in the difference electron density maps. Data were solved using the programs Shelx 97[5] and Sir 92[6] using the Wingx graphical[7] interface with all the non-hydrogen atoms anisotropic. Hydrogen atoms are placed as a mixture of independent and constrained refinement in the calculated positions around the parent atoms.

4.2.1 Preparation of sodium hydro*tris*(mercaptobenzothiazolyl)borate (NaTbz)

2-mercaptobenzothiazole (13 g, 0.78 mmol) and sodium borohydride (1.01 g, 0.26 mmol) were placed in a dry 100ml round bottom flask fitted with an air jacket and heated in an oil bath with continuous stirring (see experimental setup 1). The mixture was heated to 160^{o}C releasing hydrogen gas as the mixture melts. The temperature was raised slowly 180-185^{o}C being maintained at this temperature for a further 30 mins. The temperature was slowly raised to 190^{o}C and held there for an hour. The hydrogen gas evolved was measured throughout to ensure that three molar equivalent of gas was released. The mixture was allowed to cool to room temperature to give a hard yellow mass. A 1:1 v:v mixture of chloroform and THF (20 ml) was added and the mixture stirred vigorously overnight to remove any un-reacted mercaptobenzothiazole. The yellow suspension formed was filtered by vacuum and the powder washed a further three times with 10 ml aliquots of 1:1 $CHCl_3$/THF. The yellow residue thus obtained was washed with methanol (20 ml) and suction filtered to give the desired product. The material obtained was sufficiently pure for further use. However pure crystalline NaTbz ($Na(C_{21}H_{13}B_1N_3S_6).1.5\ H_2O$) can are obtained by extracting NaTbz into chloroform. The extract is filtered through celite and recrystallised by vapour diffusion with diethyl ether. Anal. calcd for

$Na[B(C_{21}H_{16}N_3S_6)].3H_2O$: C, 44.11; H, 3.48; N, 6.68%. Found: C, 44.23; H, 3.87; N, 6.73%. MALDI-MS $[Tbz]^-$: 512 (5%), 166 (100%). Accurate mass predicted 511.96778; found: 511.96835. ^{1}H-NMR (500 MHz, Acetone δ): δ = 7.05 (br, 2H), 7.35 (br, 2H). ^{13}C-NMR (1024 Scans, Acetone) δ = 195, 146.9, 130.8, 126.6, 124.4, 120.1, 115.6 ppm. FT-IR (KBr, cm^{-1}): 750 (C=S) -BH stretch is not observed.

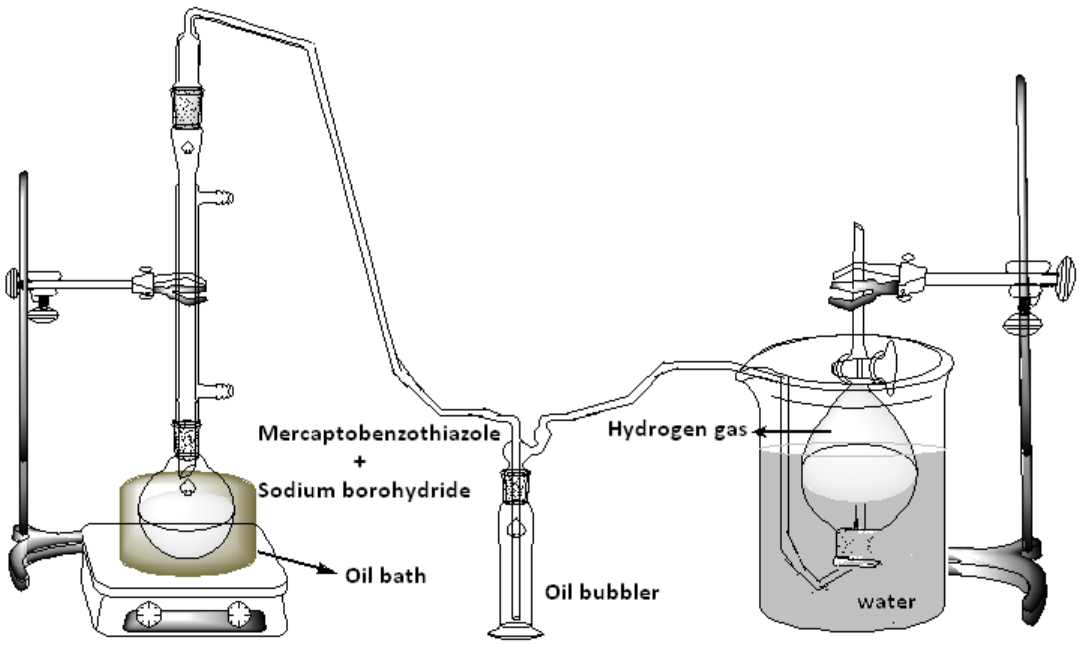

Experimental setup 1: Experimental setup for the preparation of soft scorpionate ligands by melt reaction.

4.2.2 Preparation of κ^3-S,S,S-hydro*tris*(mercaptobenzothiazolyl)borato-iodomercury(II), [HgTbzI]:

Mercuric iodide (0.1135 g, 0.25 mmol) and NaTbz (0.133 g, 0.25 mmol) were stirred overnight in 20 ml THF/$CHCl_3$ (1:1 by volume). A yellow suspension formed. The solid was collected by filtration and extracted with minimum amount of DMF. The product was extracted into DMF and crystallised by the vapour diffusion with diethyl ether. The crystalline mass was a mixture

of products which were separated manually for X-ray crystallographic analysis. The remaining spectroscopic analyses were carried out with the bulk of the sample. An explanation is given in the text (section 4.3.1). MALDI-MS $[C_{21}H_{13}N_3S_5B]^+$: 477 (100%). ^{1}H-NMR (400 MHz, DMSO): δ = 8.85 (d, 1H), 8.5 (d, 2H), 7.87 (t, 1H), 7.85 (t, 2H), 7.80 (d, 1H), 7.72 (t, 2H), 7.63 (t, 2H), 7.55 (t, 1H). ^{13}C-NMR (100MHz, DMSO): δ = 169.60, 145.62, 143.26, 130.67, 130.06, 129.12, 128.32, 128.21, 125.28, 124.70, 122.45, 116.20, 114.94 ppm. FT-IR (KBr, cm^{-1}): 2499 (B-H), 748 (C=S), 727 (C-S).

4.2.3 The analysis of the reaction of mercuric iodide with NaTbz using NMR

NaTbz (0.0155 g, 39.1 μmol) was dissolved in d6-DMSO (0.75 ml) and the ^{1}H NMR spectrum recorded. A solution of HgI_2 (0.0139 g, 30.6 μmol) in d6-DMSO (0.75 ml) was then introduced into the NMR tube. The sample was thoroughly mixed and sample placed in the magnet. Spectra (16 scans) were recorded at 15 mins time interval time for 3 hours and then daily for a further five days. The spectra were calibrated to the residual solvent (resonance position and integral) for display.

4.2.4 Preparation of [Tbz-S][SbTbzI$_3$]

A solution of antimony triiodide (0.13 g, 0.26 mmol) in 10 ml THF/$CHCl_3$ (1:1 v:v) was stirred with NaTbz (0.1441 g, 0.27 mmol) in 10ml THF/ $CHCl_3$ (1:1 v:v). An immediate blood red coloured solution formed which changes to a deep dark coloured on standing. A precipitate formed which was collected and extracted with DMF. The product was crystallised by the slow vapour diffusion of the DMF extract with diethyl ether. A mixture of red and yellow crystalline materials were obtained. These were separated manually for X-ray crystallographic analysis. However all the remaining spectroscopic analyses were carried out with the bulk of the sample. An explanation is given in the text (section 4.3.2). MALDI-MS $[bz]^-$: 478 (100%). ^{1}H-NMR (400 MHz, DMSO): δ = 8.85 (d, 1H), 8.5 (d, 2H), 7.87 (t, 1H), 7.85 (t, 2H), 7.80 (d, 1H), 7.72 (t, 2H), 7.63 (t, 2H), 7.55 (t, 1H). ^{13}C-NMR (100MHz, DMSO): δ = 169.60, 145.62, 143.26, 130.67, 130.06, 129.12, 128.32, 128.21, 125.28, 124.70, 122.45, 116.20, 114.94 ppm. FT-IR (KBr, cm^{-1}): 2494 (B-H), 753 (C=S), 722 (C-S).

4.2.5 The analysis of the reaction of antimony iodide with NaTbz using NMR

NaTbz (0.0108 g, 20.3 μmol) was dissolved in d6-DMSO (0.75 ml) and the ^{1}H NMR spectrum recorded. A solution of SbI_3 (0.0105 g, 20.9 μmol) in d6-DMSO (0.75 ml) was prepared and introduced into the NMR tube. The sample was thoroughly mixed and sample placed in the magnet. Spectra (16 scans) were recorded at 15 mins time interval time for 3 hours and then daily for a further five days. The spectra were calibrated to the residual solvent (resonance position and integral) for display.

4.2.6 Preparation of $[Bi(DMF)_8Bi_3I_9]$

A solution of bismuth iodide (0.1444 g, 0.24 mmol) in 20 ml acetone was stirred overnight with NaTbz (0.1405 g, 0.26 mmol). The deep red suspension was subjected to gravity filtration to give an orange red solution. The solvent was removed to give a deep purple residue. The material was recrystallised by the slow vapour diffusion of the product in DMF with diethyl ether. A mixture of products was obtained, which were separated manually for X-ray analysis to obtain $[Bi(DMF)_8][Bi_3I_9]$. However all the remaining analysis were carried out with the bulk of the sample. MALDI-MS $[C_7H_5NS_2]^-$: 166 (100%). ^{1}H-NMR (500 MHz, Acetone): δ = 8.03 (s, 1H), 2.82 (s, 3H), 2.98 ppm (s, 3H). FT-IR (KBr, cm^{-1}): 1624(C=O)

4.2.7 Reaction of bismuth iodide with NaTbz in chloroform

A solution of bismuth iodide (0.1464 g, 0.25 mmol) in 10 ml chloroform was stirred with a suspension of NaTbz (0.2671 g, 0.50 mmol) in 10 ml chloroform. A dark ash coloured suspension formed which was filtered to give a deep pink solution. The solvent was removed to give an orange residue. Vapour diffusion of a solution of the product in DMF with diethyl ether gave small orange red coloured crystals. Anal. calcd for $(H_3O)[C_{21}H_{13}B_1Bi_1N_3S_6I_3]$: C, 22.53; H, 1.44; N, 3.76%. Found: C, 25.07; H, 1.07; N, 5.47%. MALDI-MS $[C_{21}H_{13}N_3S_5B]^+$: 477.59 (100%), $[C_{21}H_{13}N_3S_6B_1Bi]^-$: 716 (100%), $[C_7H_5NS_2]^-$: 166.9 (100%). ^{1}H-NMR (400 MHz, DMSO): δ = 7.97 (br, 1H), 7.95 (s, 1H), 7.37 (br, 2H), 7.26 (br, 1H), 2.89 (s, 3H), 2.72 ppm (s, 3H). FT-IR (KBr, cm^{-1}): 748 (C=S), 722.62 (C=S), -BH stretch cannot seen in the spectrum. As yet this species does not have an identified cation to balance the $[TbzBI_3]$ anion. The ^{1}H NMR spectrum does not support the presence of an organic cation (i.e. dimethylamine, mercaptobenzothiazole) and the inference is

that a small highly disordered cation (e.g. H_3O^+) is present in the voids between the anionic layers in the crystal lattice.

4.2.8 Preparation of $[Co(Bz\text{-}S)_2Br_2]$

A solution of cobalt bromide (0.2185 g, 1 mmol) in 50 ml acetone was refluxed with NaTbz (0.5330 g, 1mmol) for 2 hours. The green suspension was subjected to gravity filtration to give a blue solution. The solution was reduced in volume and the resulting liquor filtered through celite. The resulting solution was crystallised by vapour diffusion with diethyl ether. Blue coloured crystals were collected from the mixture which were separated manually and subjected to analysis by X-ray methods. MALDI-MS $[C_7H_5NS_2]^-$: 166 (100%).

4.2.9 Preparation of $[CoBz_2Br_2]$

A solution of cobalt bromide (0.2181 g, 1 mmol) in 50 ml acetone was refluxed with 2-mercaptobenzothiazole (0.1682 g, 1 mmol) for 2 hours. The light green suspension was filtered to give a blue coloured solution. The green coloured crystals were obtained by the slow vapour diffusion of this acetone solution with diethyl ether. Found: C, 30.51; H, 2.0; N, 4.73%. Anal. Calcd for $Co(C_7H_5NS_2)_2Br_2$, C, 30.40; H, 1.82; N, 5.07%. MALDI-MS $[C_7H_5NS_2]^-$: 166 (50%). FT-IR (KBr, cm^{-1}): 753 (C-S)

	HgTbzI	(Tbz-S)(HgI_3)	(Tbz-S)I	(Tbz-S)($SbTbzI_3$)	$BiTbzI_3$	Co(bz-S)Br_2	Co(bz)Br_2
Empirical formula	$C_{21}H_{13}BHgN_3S_6I$	$C_{21}H_{13}BHgN_3S_5I_3$	$C_{21}H_{13}BN_3S_5I$	$C_{42}H_{26}B_2N_6S_{11}SbI_3$	$C_{21}H_{13}BBiN_3S_6I_3$	$C_{14}H_{10}Br_2$ CoN_2S_2	$C_{14}H_{10}Br_2CoN_2S_4$
FW	837.44	1059.28	604.88	1490.38	1099.64	488.77	552.71
Crystal system	Monoclinic	Triclinic	Trigonal	Triclinic	Triclinic	Monoclinic	Monoclinic
Space group	P 2_1/c	P -1	R -3	P -1	P -1	P 2/n	P 2_1
a/Å	10.0750(6)	9.6385(7)	31.7240(50)	10.9829(6)	10.1400(40)	7.7650(50)	15.8210(50)
b/ Å	12.7100(8)	12.7847(8)	31.7240(50)	22.9779(12)	10.7790(40)	6.9370(50)	29.0700(50)
c/ Å	19.6116(10)	16.1011(10)	12.6180(50)	24.9438(14)	21.3920(80)	14.4480(50)	7.9280(50)
α/°	90.0	98.895(5)	90.000(5)	88.713(4)	81.103(15)	90.000(5)	90.000(5)
β/°	90.334(4)	105.408(6)	90.000(5)	87.356(5)	82.795(15)	95.111(5)	90.636(5)
γ/°	90.0	105.274(6)	120.000(5)	83.000(5)	78.886(16)	90.000(5)	90.000(5)
Z	4	3	6	6	2	4	4
V/A^3	2511.29(3)	1790.56(62)	10997.58(370)	6240.44(41)	2252.62(91)	775.16(9)	3645.99(27)
μ_{calc}/mm^{-1}	7.874	7.199	1.752	3.489	6.251	6.523	2.890
No. Reflns Measd	7703	17446	15739	54842	28662	5238	12290
No. Unique reflns	4817	7714	5269	21649	10192	1929	6261
No Observed reflns	4309	5699	4291	11853	8739	1208	3735
No. Parameters	301	354	284	1306	321	100	369
R^a (1>2σ(I))	0.022	0.080	0.036	0.134	0.061	0.029	0.108
$R_w{}^b$ (all reflns)	0.045	0.267	0.103	0.367	0.163	0.048	0.245
GOF	1.008	1.045	1.063	1.065	1.059	0.805	1.172

4.3 Results and Discussion

NaTbz was prepared by a solvent free melt reaction employing mercaptobenzothiazole and sodium borohydride in a 3:1 mol:mol ratio as previously reported in the chapter 2. The complex was crystallised by vapour diffusion of a chloroform solution of NaTbz with diethyl ether (figure 4.3). The structure obtained shows the Tbz ligand coordinated in the k^3-S,S,S conformation.

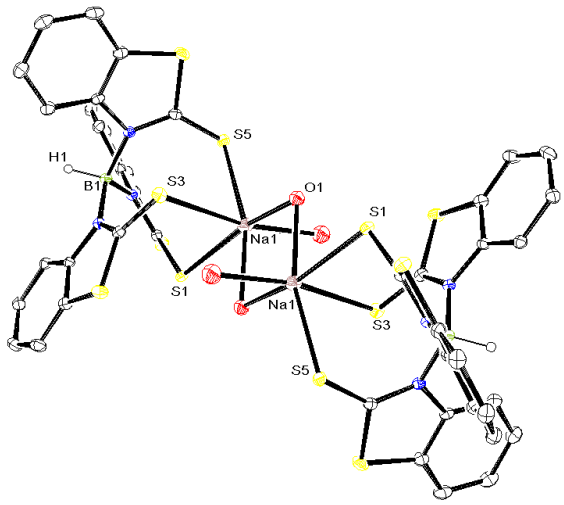

Figure 4.3: Molecular structures of {NaTbz(OH_2)}μ-(OH_2)$_2$. Hydrogen atoms are omitted for clarity. Thermal ellipsoids are shown at 30% probability. The metrical parameters and structural analysis can be found in chapter 2

4.3.1 Reaction of mercuric iodide with NaTbz

The initial report on the chemistry of NaTbz indicated that complexes of the lower main group could be generated.[1] This hypothesis is supported by DFT analysis and as such we began this study by challenging NaTbz with antimony, mercury and bismuth. Reacting NaTbz with mercuric iodide produces the desirable product HgTbzI (κ^3-S,S,S hydro*tris*(mercaptobenzothiazolyl)borato-iodomercury (II) figure 4.4) in a very low yield. This species is manually isolated with some difficulty from a mixture of yellow crystalline products.

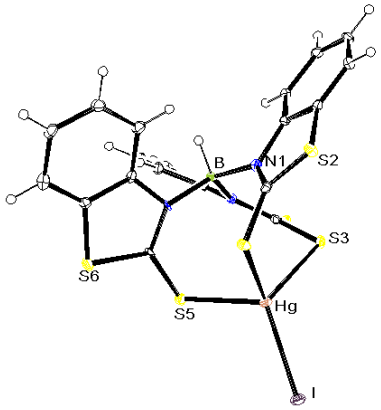

Figure 4.4: Molecular structure of HgTbzI (hydro*tris*(mercaptobenzothiazolyl)borato-iodomercury(II)). Thermal ellipsoids are shown at a probability of 30%. The metrical parameters for this species can be found in table 4.1

The molecular structure clearly indicates the successful formation of HgTbzI. Soft scorpionates of mercury(II) have been reported previously and there are currently fifteen structures in the crystallographic database.[8-13] Of particular interest to this study is the iodide complex of Hg(II)Tm^{tBu} reported by Melnick and Parkin (figure 4.5).[11] A brief comparison of these two complexes is given in table 4.2. It can be seen that the metrical parameters of these two species are roughly comparable. The iodine ligand in both complexes is found at an angle (~10^{o}) to the notional H-B-M axis. Furthermore, the B-N bond distances come within a small range (1.552(2) - 1.559(2) Å) in both complexes and thus are not significantly different. The major difference between these two complexes is found in the S-Hg-S angles. Unlike the Tm^{tBu} anion, Tbz anion incorporates an inflexible aryl ring to the rear of the thio-imidazole which, due to its inflexible shape, restricts the positioning of the ring at the boron centre forcing the S-Hg-S angle to slightly higher values (~102^{o} Vs 99^{o}).

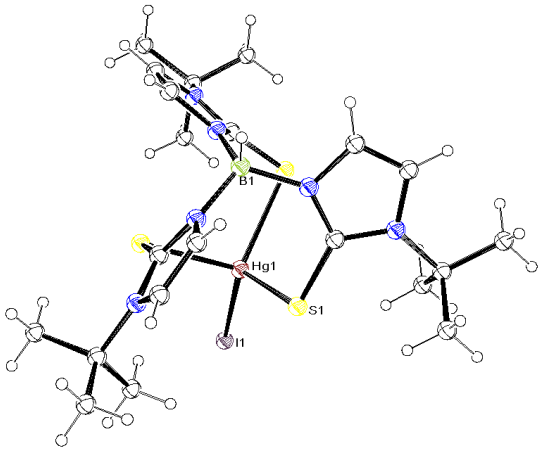

Figure 4.5: Molecular structure of $HgTm^{t\text{-}Bu}I$ {(hydro*tris*(tert-butylthioimidazolyl)borate)-iodomercury (II)} complex.[11] Thermal ellipsoids are shown at a probability of 30%. The metrical parameters for this species can be found in table 4.1.

	HgTbzI	$HgTm^{t\text{-}Bu}I$
Hg-S	2.579(1) 2.625(1) 2.547(1)	2.577(1) 2.565(1) 2.587(1)
Hg-I	2.6884(4)	2.6873(5)
∠B-Hg-I	168.22	170.57
∠S-Hg-I	127.07(3) 107.78(3) 114.10(3)	118.19(3) 125.89(3) 110.44(3)
∠S-Hg-S	101.99(4) 101.75(4) 100.86(4)	98.34(4) 98.88(4) 100.65(4)

Table 4.2: A comparison of some selected bond lengths (Å) and bond angles (^{o}) of HgTbzI and $HgTm^{t\text{-}Bu}I$ complexes.[11]

The major product in the mixture (~70%) was found to be another unusual polycyclic cation (figure 4.6). Similar to the product derived from the oxidation of Tm^{Ph} (c.f. chapter 3, figure 3.5), ring closure in this species was achieved at the expense of a sulfur atom. Both rings are planar with a central six membered heterocyclic ring which contains boron, sulphur, nitrogen and

carbon atoms. A comparison of the key bond lengths are given in Table 4.3 where it can be seen that there is great similarity between the core BN_2C_2S rings in both heterocycles (figure 4.7). Heterocyclic rings of this type have never been reported previously and this chemistry would seem to have generated a new organic system.

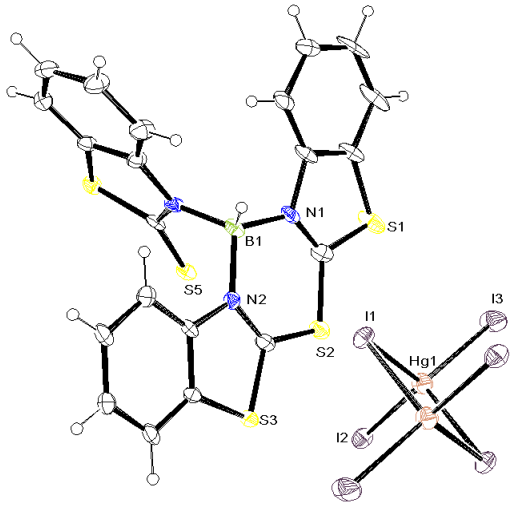

Figure 4.6: The molecular structure of the major product obtained from the reaction of HgI_2 and NaTbz reaction. The second polycyclic cation and solvent molecules are omitted for clarity. Thermal ellipsoids are shown at a probability of 30%.

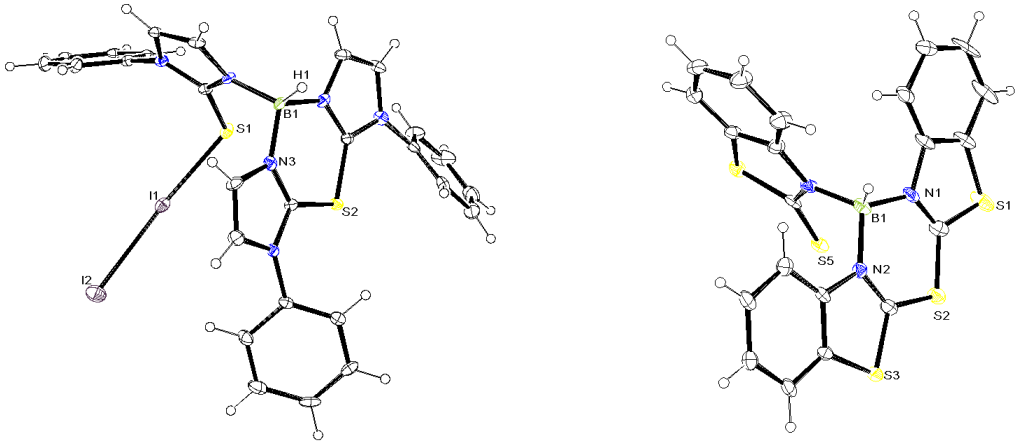

Figure 4.7: The molecular structure of polycyclic cation obtained by the reaction of $NaTm^{Ph}$ with PI_3 (left) and the polycyclic cation obtained from the mercuric iodide reaction with NaTbz. Counter ions are omitted for clarity. Thermal ellipsoids are shown at a probability of 30%.

	$[Tbz\text{-}S]^+$ (Å)	$[(Tm^{Ph}\text{-}S)SI_2]^+$ (Å)
B-N	1.562(6) 1.551(5) 1.559(6)	1.55(1) 1.55(1) 1.54(1)
C=S	1.752(4) 1.747(5) 1.660(5)*	1.740(8) 1.736(8) 1.715(8)**
C-N(B)	1.368(7) 1.320(6) 1.323(5)*	1.321(9) 1.325(9) 1.34(1)**
C-N(R) C-S(hetero)	1.741(4) 1.721(4) 1.723(4)*	1.34(1) 1.35(1) 1.37(1)**

Table 4.3: A structural comparison of the polycyclic rings formed using the Tbz and Tm^{Ph} anions. * indicates the free heterocycle and ** indicates the heterocycle to which is coordinated with an iodine molecule.

The formation of soft scorpionate derived polycyclic cations was discussed in Chapter 3. In these instances ring closure was effected by either olefin attack on an alkylated thione or a thione attack at the alkylated thione. Tbz contains an aryl moiety which blocks the pathway open to Tm^{Me}. Thus ring closure is forced to occur at the thiones using a similar route to that employed by Tm^{Ph} i.e. desulfurisation.

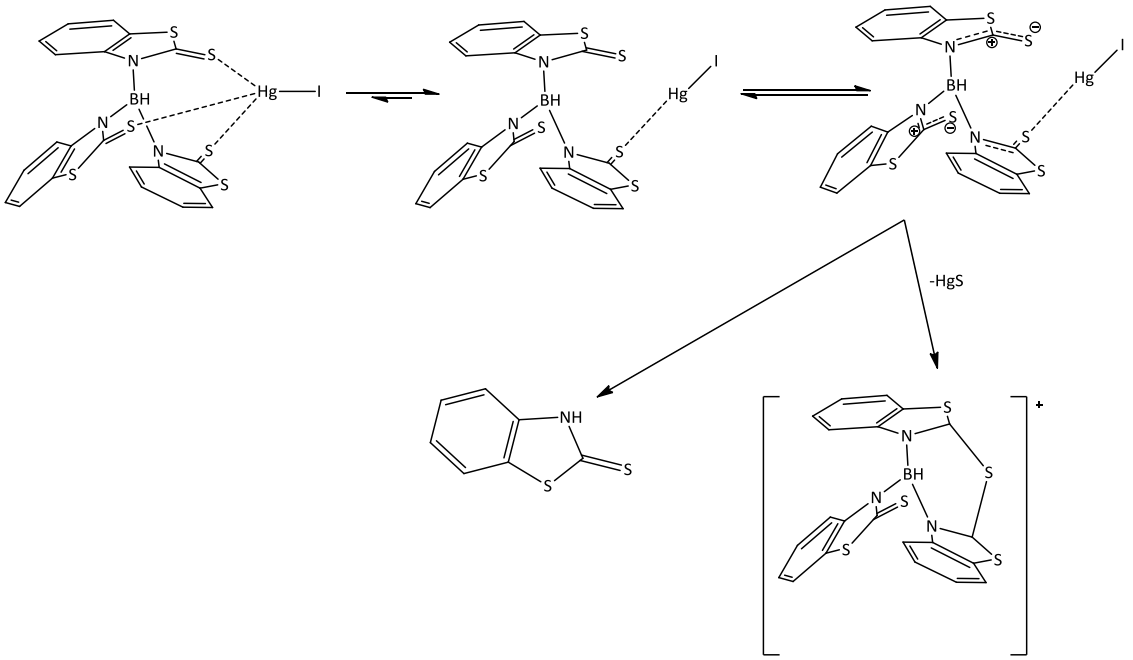

Scheme 4.1: The possible reaction mechanism for the formation of the polycyclic ring compound during the Tbz metalation reaction.

The study of Melnick and Parkin demonstrated that the $HgTm^{tBu}I$ adopts two forms in solution i.e. the κ^3-S,S,S and κ^1-S forms.[11] Considering the structural similarities between $HgTm^{t\text{-}Bu}I$ and HgTbzI (table 4.3) it is not unreasonable to suggest that a similar equilibrium exists here. Indeed from table 4.2 it is clear that one of the Hg-S bonds is much stronger (2.547(1) Å) than the other two (2.579(1) Å and 2.625(1) Å). It is postulated that in the κ^1-S form the un-coordinated sulphurs assume the role of the nucleophile to the coordinated thione which due to its attachement to the metal is more prone to attack from an adjacent thione ring. This promotes ring closure. The proposed mechanism is summarised in scheme 4.1. During this process the B-N bond distance increases. This modification leads to the decomposition of the complex to mercaptobenzothiazole via an alternative pathway (figure 4.7).

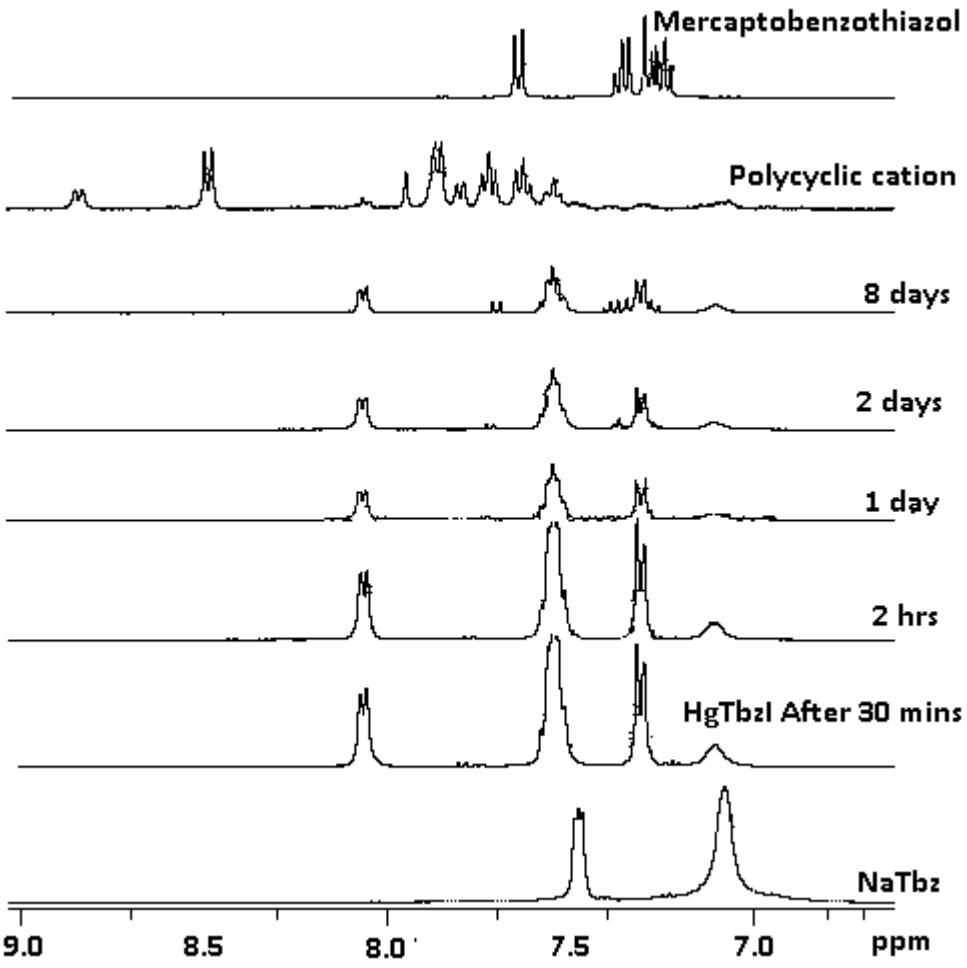

Figure 4.7: The NMR spectra collected for the reaction mixture of NaTbz and HgI_2 in d_6-DMSO. Bottom: NaTbz in d_6-DMSO. Middle: Spectra recorded from the mixture at the stipulated times (only selected spectra are shown) Top: NMR spectra of polycyclic ring and 2-mercaptobenzothiazole. All resonances are calibrated to the solvent peak d_6 -DMSO.

A kinetic NMR spectroscopic study of the reaction of NaTbz and HgI_2 was performed (figure 4.7). Prior to the addition of HgI_2 the spectrum of NaTbz has its familiar form i.e. two broad resonances indicative of the slow tumbling of the mercaptobenzothiazole rings about the boron. Immediately after the addition of HgI_2 resonances (in a ratio 1:2:1 derived from the four protons on the aryl ring) which can be assigned to k^3-S,S,S-HgTbzI are clearly visible in the spectrum. However, as the reaction proceeds the resonances assigned to k^3-S,S,S-HgTbzI diminish and new resonances appear. These are assigned to 2-mercaptobenzothiazole and the

polycyclic cation. Concurrent with these observations a yellow precipitate forms in the NMR tube. On isolation and analysis this material is identified as the polycyclic ring compound. This study supports the view that while HgTbzI is the primary product it is not stable in solution. Indeed similar to the synthetic study, the reaction of NaTbz and HgI_2 produces a complex mixture of species i.e. HgTbzI, a polycyclic cation and 2-mercaptobenzothiazole.

4.3.2 Reaction of Antimony iodide with NaTbz

Similar to the reactions above using mercuric iodide, the reaction of antimony iodide with NaTbz produced a mixture of products. These compounds again crystallised concurrently. However, in this instance, the difference in colour (red and yellow) made separation of the species easier. The red coloured crystals were identified as a SbTbz complex. However, unlike the mercury, antimony generates a more unusual complex of Tbz (figure 4.8).

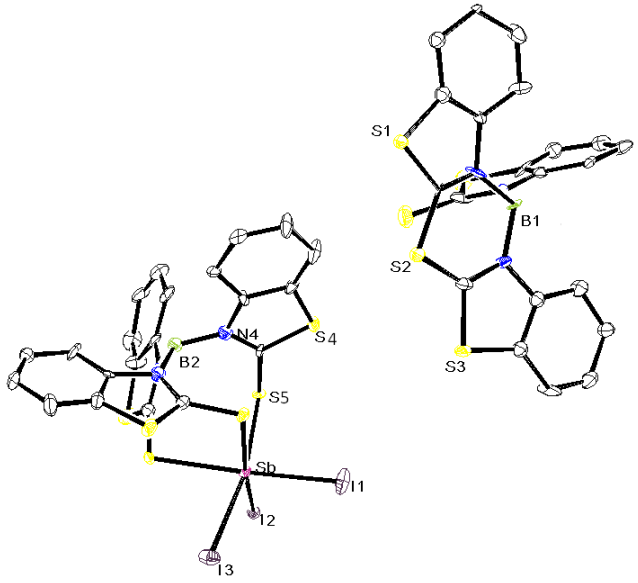

Figure 4.8: The molecular structure of the hydro*bis*(mercaptothiazolyl)benzoimidazolylboron cation hydro*tris*(mercaptobenzothiazolyl)boratotriodoantimonate(III) anion. Hydrogen atoms and solvent molecules are omitted for clarity. Thermal ellipsoids are shown at a probability of 30%. The R factor for this species is higher than desired (R= 13.40). However, the connectivity of the atoms is beyond doubt.

The product is a salt containing a polycyclic cation and a unique anionic lower main group scorpionate. Thus the antimony is not only complexed to the scorpionate in a κ^3-S,S,S mode, it remains complexed to three iodides. Soft scorpionate antimony complexes were first reported in 2006.[14] The majority of these complexes are five coordinated. There is, however, one known six coordinated antimony complex i.e. (μ-iodo)-*bis*(hydro*tris*(3-methyl-2-thioxoimidazolyl)borato-S,S',S'')-diiodo-di-antimony (III) in which two iodine molecules act as a bridge between two antimony centres (figure 4.9). Although this species is six coordinated the geometry at antimony is heavily distorted. Thus the Tbz species isolated here is unique not just because it is anionic but also because there is little distortion about the antimony.

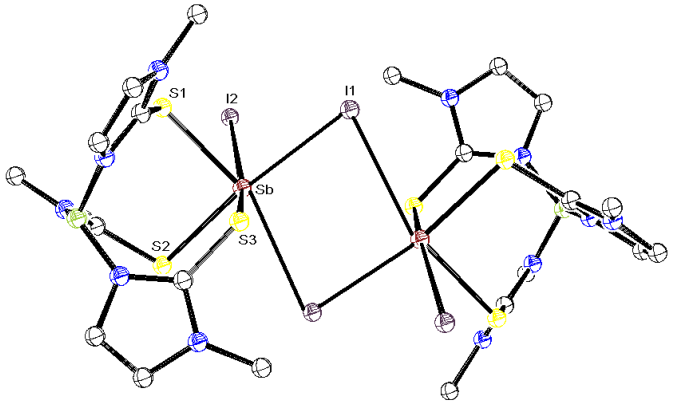

Figure 4.9: The molecular structure of (μ-iodo)-*bis*(hydro*tris*(3-methyl-2-thioxoimidazolyl)borato-S,S',S'')-diiodo-di-antimony (III).[14] Hydrogen atoms are omitted for clarity. The bond angles (°) of S2-Sb-I1, S2-Sb-S3, S3-Sb-I2 and I2-Sb-S1 are 165.12(2), 91.80(3), 162.55(2), and 73.67(2) respectively. Thermal ellipsoids are shown at a probability of 30%.

Similarly to the chemistry of mercury, the other major product (yellow product) was found to be a simple iodide salt of the complex polycyclic cation (figure 4.10). The ease of its identification (yellow, red) made its isolation possible. Thus, from this mixture we were able to manually isolate sufficient material for analysis by NMR spectroscopy and mass spectrometry (but not elemental analysis) which allows us to decipher the NMR spectra of the mixtures obtained from the reactions with mercuric and antimony salts (figure 4.7, 4.11).

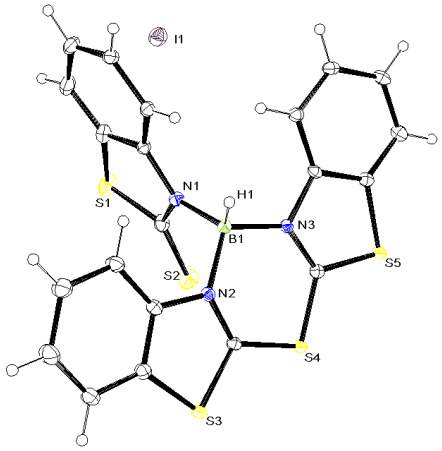

Figure 4.10: The polycyclic ring product isolated from the reaction of antimony triiodide with NaTbz. Thermal ellipsoids are shown at a probability of 30%.

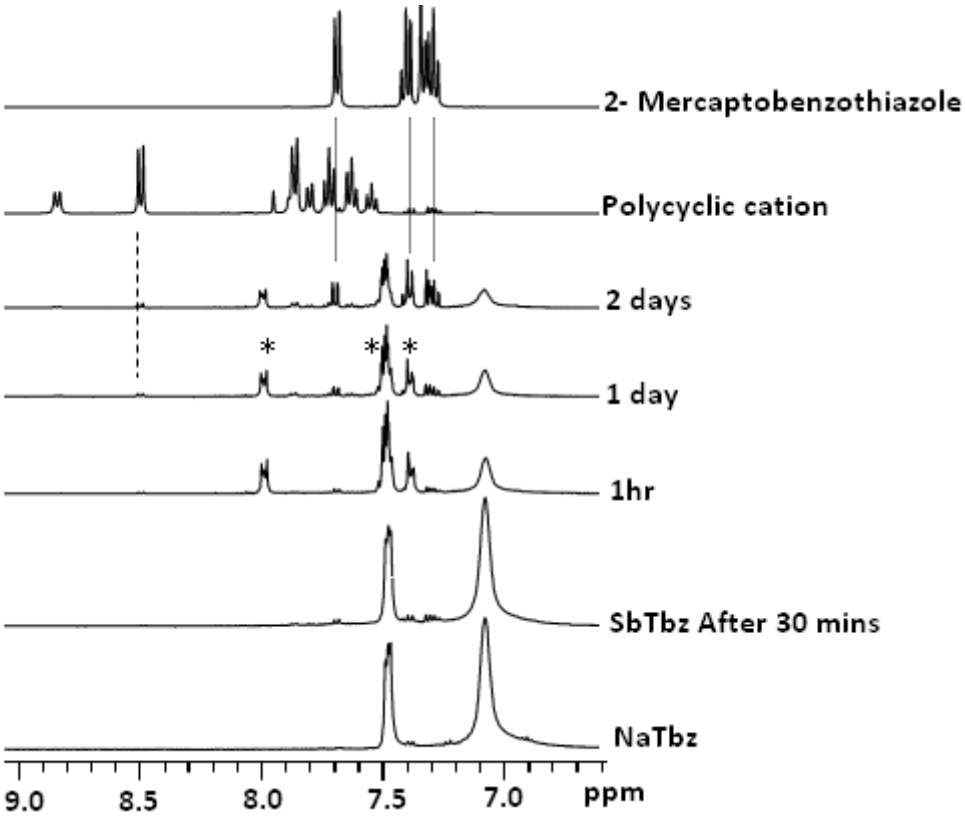

Figure 4.11: The NMR spectra derived from the reaction mixture of NaTbz and SbI_3 in d_6-DMSO. Bottom: NaTbz in d_6-DMSO. Middle: Spectra recorded from the mixture at the stipulated times (only selected spectra are shown) Top: NMR spectra of polycyclic ring and 2-mercaptobenzothiazole. All resonances are calibrated to the solvent peak DMSO.

In an attempt to decipher the sequence of events occurring in these reactions we again resorted to a rudimentary kinetic study of the antimony system using NMR spectroscopy (figure 4.11). In contrast to the mercury reaction the formation of $SbTbzI_3$ does not seem to be rapid. After 30 minutes the Tbz anion still dominates the spectrum. After this time resonances which can be assigned to $SbTbzI_3$ appear. Again they adopt a 1:2:1 pattern with the lines resolving in a manner which is consistent with a coordinated Tbz. It is interesting to note that the mercury complex is more stable than the antimony complex and that the resonances derived from the polycyclic heterocycle and mercaptobenzothiazole are more prominent in the NMR spectra of the antimony reaction (figure 4.11). Again the NMR spectroscopic analysis supports the view that from the outset mixtures form and that the desired Tbz complexes have a limited lifetime in solution.

4.3.3 Reaction of Bismuth iodide with NaTbz

To conclude the analysis of the lower main group species with Tbz, we turned our attention to bismuth. There is some evidence to support the view that with bismuth iodide, Tbz forms a complex analogous to that obtained with antimony except that in this case we have been unable to find a cation during the refinement of the X-ray structure due to the poor quality of the crystals and the data sets. (figure 4.12).

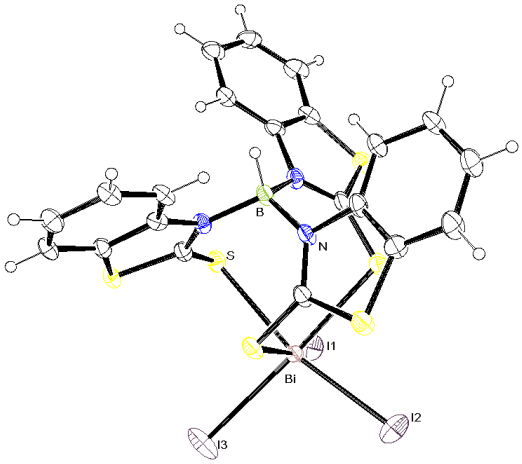

Figure 4.12: The molecular structure of $[Bi(Tbz)I_3.]^-$. Despite the low R value (6.14%) the structure solution is not complete as the counter cation has not been found. The hkl file for the solution shown was SQUEEZED in PLATON to remove the disordered cations/solvent. On packing, the gross structure clearly shows the layers which contain the $Bi(Tbz)I_3$ anion. The layers in between these species, which should contain the cation, are heavily disordered. Although evidence exists for the presence of DMF, as yet we have been unable to identify a cation in this space. It should be noted that the hydrogen bonded to the boron is found. Furthermore, the three iodine sites do not respond to attempts to distribute two iodines over the three sites. Finally, the Bi-I (2.948 Å, 2.997 Å, 3.007 Å), Bi-S (2.883 Å, 2.914 Å, 2.920 Å) and S-C (1.689 Å, 1.693 Å, 1.704 Å) are in line with that expected.

The structure although very poor does not support the formation of a similar complex to that found with antimony i.e. one which contains the polycyclic cation. Protracted efforts to refine this synthesis were unsuccessful. Indeed a number of attempts generated a simple DMF adducts of bismuth (figure 4.13) which confirmed the sensitivity of the reaction.

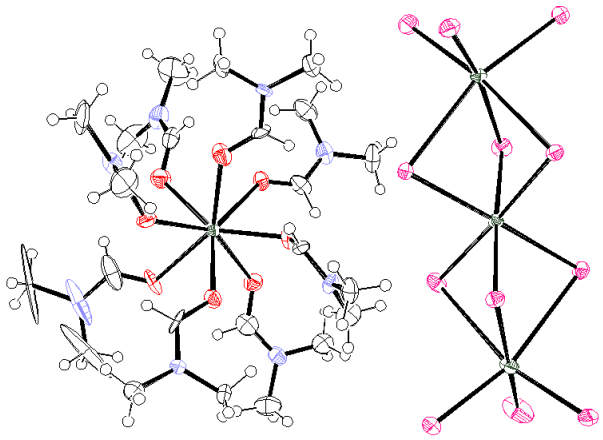

Figure 4.13: The molecular structure of $[Bi(DMF)_8)]$ $[Bi_3I_9]$. Since the R value (16%) is a little high, metrical parameters are not available. But it clearly shows the connectivity of atoms.

4.3.4 Reaction of Cobalt bromide with NaTbz

The main group studies support the view that there are stability issues with Tbz complexes. Consequently the recent report of Baba *et al.* detailing the synthesis of *bis*(hydro*tris*(2-mercaptobenzothiazolyl)borate)cobalt(II) was intriguing. This species was made in low yield by diffusion methods. This approach relies on the insolubility of the product which favours the formation of crystalline materials as the reaction proceeds. Repeated attempts to make Co(Tbz)Br by rational methods failed. Instead we obtained species such as *bis*(1,3-benzothiozole)*bis*bromocobalt(II) (figure 4.14) along with a mixture of unidentified decomposition products.

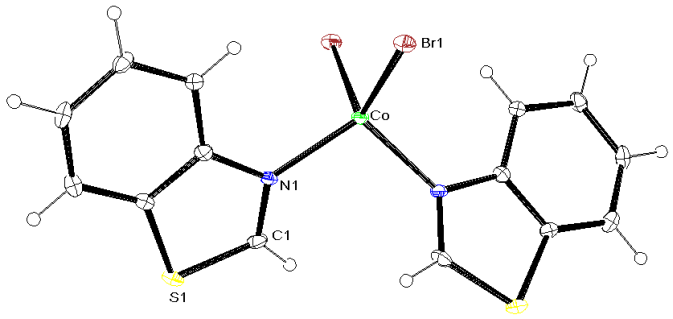

Figure 4.14: The molecular structure of *bis*(1,3- benzothiozole)*bis*bromocobalt(II). The thermal ellipsoids are shown at a probability of 30%.

Not only do we observe complete decomposition of the ligand we also observe the elimination of the sulphur from the 2-position of Tbz anion. The initial observation is consistent with the DFT analysis. However, the loss of sulphur suggests that other reaction pathways are in progress. Before leaving this chemistry, it was decided to revisit the simple reaction of mercaptobenzothiazole and cobalt bromide. This reaction leads to the formation of the expected simple adduct (figure 4.15) with no evidence of the loss of sulfur. The reaction of cobalt bromide and mercaptobenzothiazole illustrates that the elimination of sulphur is not occurring with the 2-mercaptobenzothiazole. It is more likely that loss of sulfur is occurring during ligand decomposition.

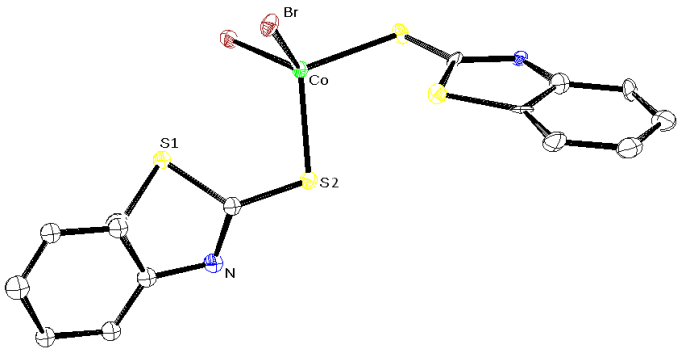

Figure 4.15: The molecular structure of *bis*(2-mercaptobenzothiazole)cobalt(II) bromide. Hydrogen atoms are omitted for clarity. Thermal ellipsoids are shown at a probability of 30%.

Previous studies using DFT analysis of the scorpionate anions suggest that the B-N bond distance is very important for the stability of the ligands (see Chapter 2). Since the ligand, Tbz, itself lies at the upper limit (1.552(2)Å to 1.559(2)Å) of this series, hard metals are not expected to produce stable complexes. The hardest metal which forms a stable complex of Tbz is the cobalt complex reported by Baba *et al.*[3] However this species was prepared by a route which, due to solubility, favours the primary adduct. Thus the general stability of metal complexes of first row transition metals is not promising. This prediction also encompasses the Ttz anion. Soft metals (mercury, antimony or bismuth) are known to form strong coordinate bonds with sulphur. However, even these metals would seem incapable of producing stable metal complexes. The study of Baba *et al.* suggest that eventually a synthesis of these species might be identified. However, the utility of a complex which is unstable in solution must be questioned. These issues may affect the new soft scorpionates being produced and it will be interesting to witness the progress of this chemistry over the coming years.

4.4 Conclusion

Investigation of the chemistry of the Tbz anion suggests that the synthesis of its metal complexes is not straight forward. However, the main purpose of this study was to investigate the predictions made using DFT analysis regarding this system (chapter 2). In general these predictions are sound and as predicted the anion remains prone to rearrangement. While the interest in these species as ligands in inorganic chemistry would be best abandoned, there is scope to investigate decomposition reaction further as it may be a rich source of new heterocyclic compounds.

4.5 References

1. Ojo, J. F.; Slavin, P. A.; Reglinski, J.; Garner M.; Spicer, M. D.; Kennedy, A. R.; Teat, S. J. *Inorg. Chim. Acta* **2001**, *313*, 15-20.
2. Pettinari, C. *Scorpionates II: Chelating borate ligands, Imperial College Press*. **2008**.
3. Baba, H.; Naka, M.; *Inorg. Chem. Commun*. **2012**, *17*, 177-179.
4. Soares, L.F.; Menezes, D. C.; Silva, R. M.; Doriguetto, A. C.; Ellena, J.; Mascarenhas, Y. P.; Castellano, E. E. *Polyhedron* **2004**, *23*, 205-209.
5. Sheldrick, G. M. *Acta Crystallogr. A64*, **2008**, 112-122.
6. Altomare, A.; Cascarano, G.; Giacovazzo C.; Gualardi, A. *J. Appl. Crystallogr.* **1993**, 26, 343-350.
7. Farrugia, L.J. *J. Appl. Crystallogr*. **1999** *, 32,*837.
8. Cassidy, I.; Garner, M.; Kennedy, A. R.; Potts, G. B. S.; Reglinski, J.; Slavin, P. A.; Spicer, M. D. *Eur. J. Inorg. Chem.* **2002**, 1235-1239.
9. Alvarez, H, M.; Tran, T. B.; Richter, M. A.; Alyounes, D. M.; Rabinovich, D.; Tanski, J. M.; Krawiec, M. *Inorg. Chem.* **2003**, *42*, 2149-2156.
10. Melnick, J. G.; Yurkrwich, K.; Parkin, G. *J. Am. Chem. Soc*. **2010**, *132*, 647-655.
11. Melnick, J. G.; Parkin, G. *Science* **2007**, *317*, 225-227.
12. Cetin, A.; Ziegler, C. J. *Dalton. Trans*. **2006**, 1006-1008.
13. White, J. L.; Tanski, J. M.; Rabinovich, D. *J. Chem. Soc., Dalton. Trans*. **2002**, 2987-2991.
14. Dodds, C. A.; Reglinski, J.; Spicer, M. D. *Chem. Eur. J*. **2006**, *12*, 931-939.

Chapter 5

An investigation on the stability of the metal –hydride bond in soft scorpionate ruthenium complex.

5.1 Introduction:

For many years nitric oxide was thought of as a poisonous substance produced by the incomplete combustion of the fuel and oxidation of ammonia.[1] In the early 1900's research suggested that nitric oxide was of some importance in biology. As early as 1916 Mitchell *et al*. had suggested that nitric oxide could be produced in mammalian biochemistry. These observations were confirmed by Tannenbaum *et al.* in 1928.[2] However it was not until the 1980's that the importance of nitric oxide in signal transduction and cytotoxicity was revealed.[2] At this time there was a resurgent interest in the coordination chemistry of nitric oxide.[1, 2] In 1992 nitric oxide was named as the molecule of the year by the journal *Science*.[2, 3] A range of biological activities including digestion, blood pressure regulation and antimicrobial activity are mediated by nitric oxide in mammals.[3] Nitric oxide is produced in a wide range of cells in the body depending on function. Nitric oxide produced in neurons plays a key role in the neurotransmission, whereas when produced in the macrophages it has an anti-microbial role.[2] The chemistry and patho-physiology of nitric oxide is still an expanding area of interest. Its generation/supplementation in atherosclerosis is of value by dilating the surrounding blood vessels thus increasing blood flow to heart.[4] In certain cases e.g. hypotension (low blood pressure) it is important to control or minimise the production of nitric oxide. It is evident that agents which can regulate nitric oxide are of great clinical interest.

Ruthenium complexes have distinct advantages as a vehicle for nitric oxide in biology. Not only does ruthenium readily form stable complexes with nitric oxide (i.e. *in-situ* scavenging),[5, 6] depending on the ligands employed, Ru-NO complexes can be synthesized which are useful for photolytic generation of nitric oxide.[7] One of the major applications of soft scorpionates has been in modeling bioactive molecules.[8, 9, 10] The presence of soft sulfur donors in Tm^R and Bm^R have marked these ligands as ideal for applications in the bioinorganic chemistry. Considering the activity of ruthenium

with nitric oxide either as a scavenger or as Ru-NO complexes as a source of nitric oxide, it would seem timely that the behavior of ruthenium soft scorpionates in the presence of nitric oxide should be investigated. There have been a number of reports on ruthenium soft scorpionate complexes.[11] In most cases the complexes are not entirely appropriate for biological use incorporating cumene, cyclopentadienyl or DMSO ligands to satisfy the remain coordination sites.[11, 12, 13] Wang *et al.* has shown that ruthenium can adopt a range of coordination modes with soft scorpionates including the κ^3-H,S,S mode.[13] Thus it has been demonstrated that the electrostatic metal-hydrogen-boron interaction is available in ruthenium chemistry. The importance of M-H-B bond in the bioinorganic chemistry of soft scorpionates has been discussed by Santos *et al.* They have been developing technetium and rhenium complexes of the soft scorpionates as radiopharmaceuticals.[14] These complexes contain the familiar M····H-B interaction. Furthermore, they have shown that this interaction is susceptible to displacement when challenged with π- acceptors (e.g. nitriles, phosphines, etc. figure 5.1).[10, 14]

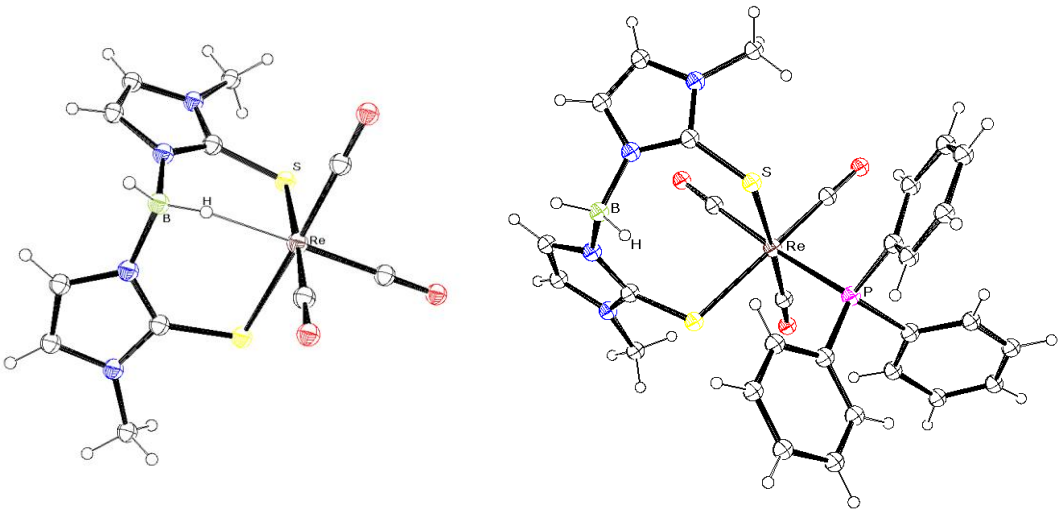

Figure 5.1: Molecular structure of tricarbonyl dihydro bismethimazolylborate rhenium (I) complex (left) and tricarbonyl dihydro bismethimazolylborate triphenyl phosphine rhenium (I) complex (right). The molecular structure clearly illustrates that metal hydride interaction could be replaced by triphenyl phosphine; a π- acceptor.

The Strathclyde group has an established interest in the chemistry of soft scorpionate complexes which include nitric oxide as ligand.[15] Considering the potential of ruthenium species in biology and medicine it seemed prudent to investigate the interaction of nitric oxide with ruthenium soft scorpionates

5.2 Experimental section

All chemicals used were commercially available and used without any purification. $NaBm^{Me}$ [16], $Ru(DMSO)_4Cl_2$ [17] and $RuNOCl_3$ [18] were prepared as per literature. NMR spectra were recorded using a Bruker AV500. All spectra obtained were referenced to the residual solvent peaks. IR spectra were recorded as KBr discs using a Nicolet Avatar 360 FT-IR spectrometer. Mass spectra were recorded using a Thermo Finnigan LCQDuo by electrospray ion trap. UV-Vis spectra were recorded using a Thermo Spectronic Unicam UV 300 and all the electrochemistry experiments were carried out using a Potentiostat/ Galvinostat Model 263A instrument by using DMF (dried over activated molecular sieve and vacuum distilled) and 0.1M $(tBu)_4NBF_4$ was used as electrolyte. A glassy carbon electrode was used as the working electrode. Platinum wire and silver wire are used as counter and reference electrode respectively. Crystals obtained were coated in mineral oil and mounted on glass fibres or a glass loop. Data were collected at 123K on Oxford diffraction diffractometer using graphite monochromated Mo-Kα radiation. The heavy atom positions were determined by Patterson methods and the remaining atoms located in the difference electron density maps. Data were solved using Shelx 97 [19] and SIR 92 [20] using the graphical interface, Wingx [21]. All non-hydrogen atoms are anisotropic. The hydrogen atoms are placed as a mixture of independent and constrained refinement in the calculated positions around the parent atoms.

5.2.1 Preparation of κ^3-H,S,S-bis(dihydrobis(methimazolyl)borato) ruthenium(II), $[Ru(II)(Bm^{Me})_2]$

$[Ru(DMSO)_4Cl_2]$ (0.0661 g, 0.13 mmol) in 20 ml acetonitrile was refluxed for 90 minutes with $NaBm^{Me}$ (0.0682 g, 0.26 mmol). The deep red solution obtained was collected by gravity filtration and reduced in volume to 2ml. X-ray quality crystals were obtained by the vapour diffusion of this solution with diethyl ether. Yield 95%. Anal. Calcd for $C_{16}H_{24}N_8B_2RuS_4$. C, 33.15; H, 4.18; N, 19.34%. Found: C, 33.41; H, 3.91; N, 19.34%. ^1H NMR (DMSO, 500 MHz): δ = 7.18 (d, 2H, CH), 7.13 (d, 2H, CH), 6.98 (d , 2H, CH), 6.97 (d ,

2H, CH), 3.53 (s, 6H, CH_3), 3.44 ppm (s, 6H, CH_3). FTIR [ν/cm^{-1} (KBr)]: 2376, 2049 (B-H), 737 (C=S). (EI; m/z) $[Ru(Bm^{Me})(mt)+H]^+$ 452 (100%), $[Ru(Bm^{Me})_2+Na]^+$ 603 (90%), $[Ru(Bm^{Me})_2-2H]^+$ 575 (75%) $[Ru(Bm^{Me})_2(mtB)]^+$ 464 (55%). λ_{max} (DCM) 398nm

5.2.2 Preparation of κ^3-H,S,S-bis(dihydrobis(methimazolyl)borato) ruthenium(III) tetrafluoroborate, $[Ru(III)(Bm^{Me})_2]BF_4$

$[Ru(Bm^{Me})_2]$ in 10 ml DCM was mixed with 1 equivalent of NO as $NOBF_4$, $NO^{\cdot}$ or NOBr. An immediate purple colour was formed. The compound was isolated by the addition of diethyl ether. The ether was removed under a stream of air. X- ray quality crystals could be obtained by the slow evaporation of the material in methanol Yield 57%. Anal. Calcd for $(C_{16}H_{24}N_8B_3RuS_4F_4)(H_2O)_2$. C, 27.34; H, 4.02; N, 15.95%. Found: C, 27.57; H, 3.53; N, 15.87%. FTIR [ν/cm^{-1} (KBr)]: 2438, 2049 (B-H), 727.74 (C=S). (EI; m/z) $[Ru(Bm^{Me})(mt)+H]^+$ 575 (100%), $[Ru(Bm^{Me})_2-2H]^+$ 452 (80%) λ_{max} (DCM) 553nm and 711nm.

5.2.3 Attempted preparation of bis(dihydrobis(methimazolyl)borato) nitrosyl ruthenium (II)

An aqueous solution of $RuNOCl_3$ in 10ml water (1g, 0.4209 mmol) was mixed with a solution of (0.221g, 0.842mmol) $NaBm^{Me}$ in 10 ml water. An immediate colour change was observed. The solution was stirred overnight and then filtered by gravity to collect the filtrate. The volume of solvent was reduced to about 5-10 ml. Slow evaporation of this solution gave X-ray quality crystals (0.0473 g). Anal. Calcd for $(Na_2[Ru(C_4H_6N_2S_1)_3(C_4H_5N_2S_1)NOCl]Cl_3)$. C, 24.81; H, 2.99; N, 16.28%. Found: C, 24.46; H, 3.64; N, 15.76 %. ^{1}H NMR (DMSO, 500 MHz)) δ = 13.96 (br, 3H, NH), 7.64 (s, 4H, CH), 7.5 (s, 4H, CH),) 3.79 ppm (s, 12H, CH_3). FTIR [ν/cm^{-1} (KBr)]: 1841 (N≡O) 759 (C-S). (EI; m/z) $[Ru(mt\text{-}H)_2]^+$ 328 (100%), $[Ru(mt\text{-}H)_2NO]^+$ 357 (75%).

	$[Ru(Bm^{Me})_2]$	$[Ru(Bm^{Me})_2]BF_4$	$[RuNOCl(mtH)_4]Na_2Cl_4$
Empirical formula	$C_{16}H_{24}B_2N_8Ru_1S_4$	$C_{16}H_{24}B_3F_4N_8Ru_1S_4$	$C_{16}H_{23}Cl_4N_9Na_2O_1Ru_1S_4$
FW	579.17	666.16	773.95
Crystal system	Trigonal	Triclinic	Monoclinic
Space group	P 6_1	P-1	C 1 2/c 1
a/Å	12.9827(6)	9.5360(50)	16.2736(3)
b/ Å	12.9827(6)	10.8680(50)	8.9653(2)
c/ Å	29.7669(14)	13.2060(50)	20.2682(4)
α/°	90	75.112(5)	90
β/°	90	89.740(5)	91.663(2)
γ/°	120	88.166(5)	90
Z	8	2	4
V/A^3	4345.04(3)	1322.00(21)	2955.84(2)
μ_{calc}/mm^{-1}	0.859	0.966	1.227
No. Reflns Measd	13527	14067	9787
No. Unique reflns	5646	5739	3644
No Observed reflns	4650	4676	3226
No. Parameters	324	354	180
R^a (1>2σ(I))	0.045	0.042	0.055
$R_w{}^b$ (all reflns)	0.106	0.100	0.156
GOF	1.006	1.065	0.994

5.3 Results and Discussions:

Ruthenium(II) κ^3-H,S,S-bis-dihydrobis(methimazolyl)borate was prepared by heating to reflux a mixture of $[Ru(DMSO)_4Cl_2]$ and $NaBm^{Me}$ in acetonitrile to give a reddish brown product. Structural analysis (figure 5.1) reveals the expected κ^3-H,S,S configuration with the hydrides lying *cis* to one another.

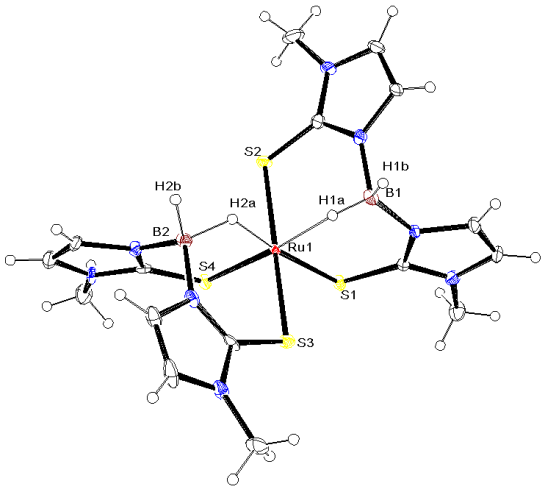

Figure 5.2: The molecular structure of $[Ru(Bm^{Me})_2]$. Solvent molecules are omitted for clarity. Thermal ellipsoids are shown at 30% probability.

The subsequent treatment of $[Ru(Bm^{Me})_2]$ with a stoichiometric amount $NOBF_4$ leads to the formation of a purple product, $[Ru(Bm^{Me})_2]BF_4$. Structural analysis of this cation shows that the donor set around the metal centre has not changed on oxidation apart from the minor alterations in bond lengths and angles on oxidation (table 5.1). These are in line with what is expected on moving from Ru^{2+} to Ru^{3+}. A similar result is obtained if the source of nitric oxide is changed to NOBr or gaseous NO. Thus, irrespective of the source of nitric oxide, this species acts as a mild oxidising agent for this ruthenium soft scorpionate. This is consistent with the studies above (Chapter 3)

where nitrosation of a thione leads to oxidative ring closure to form a cationic polycyclic heterocycle.

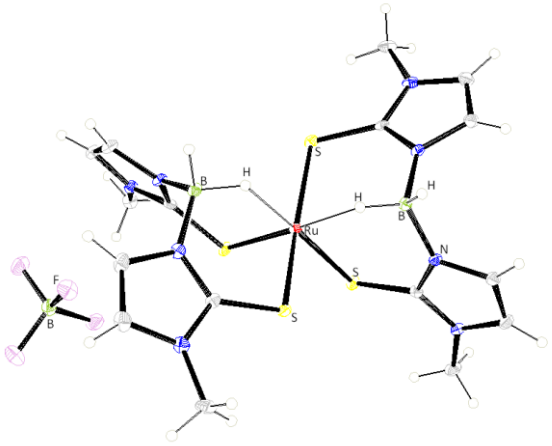

Figure 5.3: Molecular structure of $[Ru(Bm^{Me})_2]BF_4$. The tetrafluoroborate is included to confirm the ionic nature of the product. The solvated water molecule is omitted for clarity. Thermal ellipsoids are shown at a probability of 30%.

Distance/Å	$[Ru(Bm^{Me})_2]$	$[Ru(Bm^{Me})_2]BF_4$
B-N	1.5469(1), 1.5578(1), 1.5420(1), 1.5426	1.5351(4), 1.5441(8), 1.5380(7), 1.5414(5)
Ru-S	2.3622(1), 2.3669(1), 2.3694(1), 2.3717(1)	2.3292(8), 2.342(1), 2.334(1), 2.3447(9)
C=S	1.689(6), 1.7020(1), 1.722(6), 1.6978(1)	1.7227(5), 1.7166(5), 1.7204(7), 1.7128(6)
B-H	1.35(5), 0.92(6)	1.1422(4), 1.1051(4)
$B\text{-}H_{Ru}$	1.28(5), 1.05(5)	1.1455(5), 1.0440(3)
$C\text{-}N_{Me}$	1.3554(1), 1.3395(1), 1.362(7), 1.3518(1)	1.3392(4), 1.356(5), 1.3489(4), 1.3507(5)
$C\text{-}N_B$	1.362(7), 1.3362(1), 1.3390(1), 1.3638(1)	1.3422(6), 1.3409(5), 1.3436(4), 1.3485(4)
∟H-Ru-H	77.2(19)	85.0(17)
∟S-Ru-S	178.67(5), 86.87(4), 93.28(4), 85.68(5)	168.36(4), 90.53(4), 96.73(4), 84.1(16)

Table 5.1: A comparison of selected metrical parameters of $[Ru(Bm^{Me})_2]$ and $[Ru(Bm^{Me})_2]^+$.

Vibrational analysis is perhaps more responsive (c.f. X-ray analysis, table 5.1) to the structural changes which occur. Thus although the band associated with the bridging hydride remains unchanged (2049 cm^{-1}) on moving from Ru(II) to Ru(III), the band associated with terminal υ(B-H) shifts to higher frequency (~60 cm^{-1}) indicating a shortening of the B-H bond in response to the increased charge.

Electrochemical analysis of the species $[Ru(Bm^{Me})_2]^+$ in DMF indicates that there is a quasi reversible redox reaction with an E^0 of 40mV (Vs Ag/AgCl).

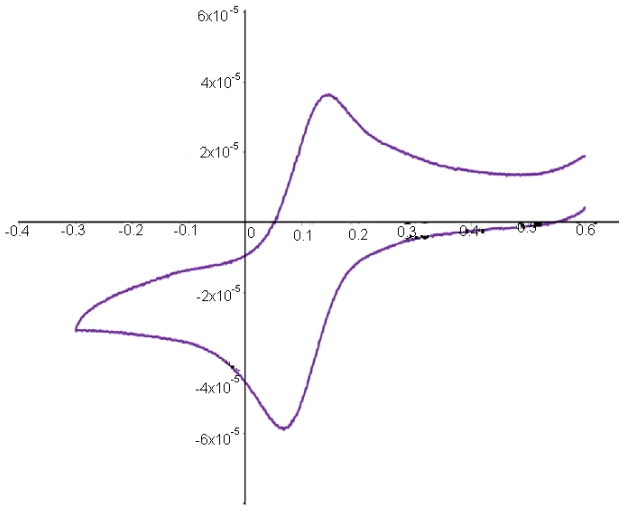

Figure 5.4: Cyclic voltammogram of $[RuBm^{Me})_2]^+$. The E^0 value of Ru^{2+}/Ru^{3+} couple is calculated to be 40mV (Vs Ag/AgCl).

The reaction of nitric oxide with $[Ru(Bm^{Me})_2]$ occurs on a modest timescale (~5 mins) which allows time to interrogate the reaction using visible spectrophotometry (figure 5.4). However, it is difficult to control the amounts of nitric oxide being added and typically an excess is present, irrespective of its source ($NOBF_4$, NO, NOBr). Thus we observe secondary reactions i.e. decomposition. The band at 430 nm derived from the orange $[Ru^{II}(Bm^{Me})_2]$ is quickly replaced by a pair of bands (550, 680 nm) derived from the purple $[Ru^{III}(Bm^{Me})_2]^+$. On standing however, the colour fades and a yellow product

is obtained. Although we have been unable to confidently identify the nature of this species, the spectroscopic data supports the formation of a [Ru(Bm^{Me})] adduct of methimazole consistent with the complexes reported by Jiménez-Tenorio.[22]

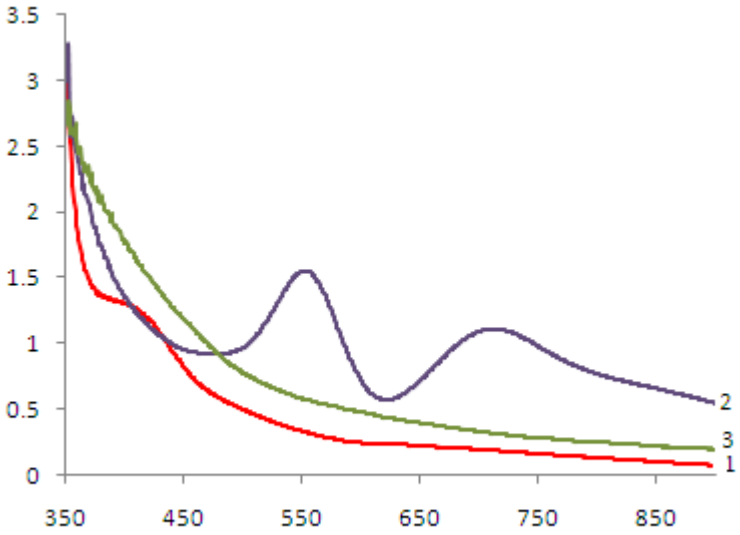

Figure 5.5: The UV-Visible spectrum (350- 900nm; in DCM) of Ru(Bm^{Me})$_2$ (1 red), [Ru(Bm^{Me})$_2$]$^+$ produced by the addition of $NOBF_4$ (2. Purple, 5 mins) and the degradation product which forms on standing (3. Green, 15 mins).

The inability of [Ru(Bm^{Me})$_2$] to scavenge nitric oxide and form adducts is disappointing. We thus resorted to other routes for a synthesis of [Ru(Bm^{Me})$_2$] nitric oxide adducts. Fletcher *et al.* have reported the synthesis of ruthenium nitrosyl chloride which would allow the introduction of the Bm^{Me} and nitric oxide ligands in the reverse order.[18] Approaching the synthesis in this manner we obtained [Ru-(mtH)$_3$(mt)NOCl]$^+$ (mt= methimazole, figure 5.5). The charge is balanced by an unusual Na_2Cl_3 anion which forms ribbons within the structure and where the sodium atoms are observed to interact with the deprotonated methimazole ring.

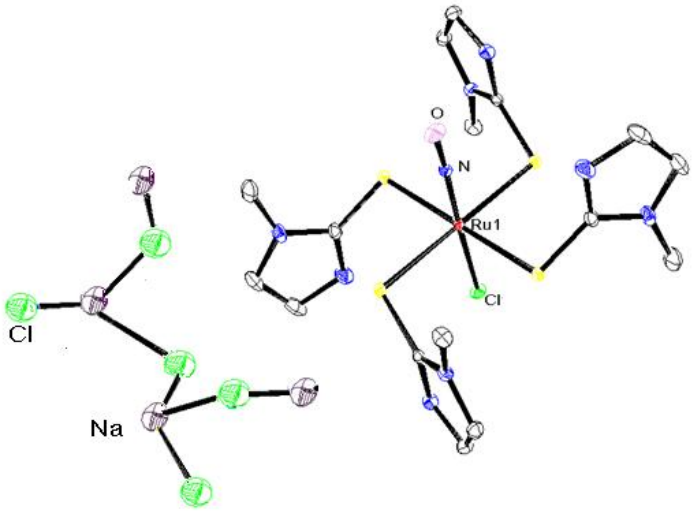

Figure 5.6: Molecular structure of $Na_2[Ru(mtH)_3(mt)(NO)Cl]Cl_3$. Counter ions are omitted for clarity. Thermal ellipsoids are shown at a probability of 30%. Selected bond lengths (Å) and angles (°) Ru-S(1) 2.4326(10), Ru-S(2) 2.4506(10), Ru-N 1.828(11), Ru-Cl 2.270(4), N-O 1.137(11); Ru-N-O 177.4(10), N-Ru-Cl 177.5(3). The sodium chloride ribbon in the above picture is not 100% refined.

We have been unable to combine nitric oxide and Bm^{Me} within the coordination sphere of ruthenium. It is notable that in the reactions used to synthesis ruthenium nitrosyl adducts of the tris(pyrazolyl)borates (Tp), two products are obtained namely $[RuCl_2\{BH(3,5\text{-}Me_2Pz)_3\}(NO)]$ (3,5-Me_2Pz = 3,5-dimethyl-1-pyrazolyl) and $RuCl_3(NO)(3,5\text{-}Me_2PzH)_2$. The former, the desired complex which contains Tp and nitric oxide, is obtained only in low yield.[23] The latter species is obtained in high yield and is also believed to form via intramolecular re-arrangement. Significantly, Ortis *et al.* were more successful in making ruthenium nitrosyl complex of scorpionates were the bridgehead atom is carbon and not boron.[24] It is evident that there are problems balancing the properties of ligand and ruthenium as other metals (Mo, W and Ni) are capable of supporting boron based soft scorpionates which include nitric oxide in the coordination sphere of the metal moiety.[15,25,26]

5.4 Conclusion:

A Ruthenium(II) κ^3-H,S,S-bis(dihydrobismethimazolyl)borate complex had been prepared and fully characterised. The efficiency of this complex as a nitric oxide scavenger has been tested using various nitric oxide sources such as NO, $NOBF_4$ and NOBr. The formation of nitrosyl adducts does not seem possible by these routes and it would seem that the ruthenium complex enters into a simple redox reaction with nitric oxide where nitric oxide acts as an oxidising agent. The corresponding Ru(III) i.e. the ruthenium(III) κ^3-H,S,S-bis(dihydrobismethimazolyl)borato cation was isolated and structurally characterised. Alternative routes to include both ruthenium and nitric oxide in the same coordination sphere lead to the decomposition of the ligand system. The comparison with the carbon bridgehead ruthenium scorpionates suggests that nitric oxide adducts should form. Similarly previous studies on boron bridgehead soft scorpionates show that the ligand system is capable of co-existing with nitric oxide.[15] This suggests the there is an incompatibility of nitric oxide and the metal when the metal is placed in a soft coordination environment.

5.5 References:

1. McCleverty, J. A. *Chem. Rev*. **2004**, *104*, 403-418.
2. Rosselli, M.; Keller, P. J.; Dubey, R. K. *Human reprod. Update* **1998**, *4*, 3-24.
3. Culotta, E.; Koshland Jr, D. E. *Science* **1992**, *258*, 1862-1865.
4. Napoli, C.; Ignarro, L. J. *Nitric Oxide: Biology and Chemistry* **2001**, *5*, 88-97.
5. Marmion C. J.; Cameron, B.; Mulcahy, C.; Fricker, S. P. *Curr. Top. Med. Chem*. **2004**, *4,* 1585-603.
6. Hutchings, S. R.; Song, D.; Fricker, S. P.; Pang, C. C. Y. *Eur. J. Pharmacol*. **2005**, *528,* 132-136.
7. Fry, N. L.; Mascharak, P. K. *Acc. Chem. Research* **2011**, *44*, 289-298.
8. Trofimenko, S. *Scorpionates The coordination chemistry of polypyrazolylborate ligands, Imperial College Press.* **1999.**
9. Pettinari, C. *Scorpionates II: Chelating borate ligands, Imperial College Press*. **2008**.
10. Reglinski, J.; Spicer, M. *Curr. Bioact. Compd.* **2009**, *5*, 264-276.
11. Bailey, P. J.; Lorono-Gonzales, D. J.; McCormack, C.; Parsons, S.; Price, M. *Inorg. Chim. Acta* **2003**, *354*, 61-67.
12. Saito, T.; Kuwata, S.; Ikariya, T. *Chem. Letters* **2006**, *35*, 1224-1225.
13. Wang, X.; Shi, H.; Wu, F.; Zhang Q. *J. Mol. Struct*. **2010**, *982*, 66-72.
14. Garcia, R.; Paulo, A.; Santos, I. *Inorg. Chim. Acta* **2009**, *362*, 4315-4327.
15. Schwalbe, M.; Andrikopoulos, P. C.; Armstrong, D. R.; Reglinski, J.; Spicer, M. D. *Eur. J. Inorg. Chem.* **2007**, 1351-1360.
16. Kimblin, C.; Bridgewater, B. M.; Hascall, T.; Parkin, G. *Dalton Trans.* **2000**, 891-897.

17. Evans, I, P.; Spencer, A.; Wilkinson , G. *J. Chem. Soc., Dalton Trans*. **1973**, 204-209.

18. Fletcher, J. M.; Jenkins, I. L.; Lever, F. M.; Martin, F. S.; Powell, A. R.; Todd R. *J. Inorg. Nucl. Chem*. **1955**, *1*, 378-401.

19. G. M. Sheldrick (2008) *Acta Cryst*. A64, 112-122.

20. A. Altomare, G. Cascarano, C. Giacovazzo and A. Gualardi, (1993) *J. Appl. Crystallogr*. 26, 343-350.

21. L.J. Farrugia, *J. Appl. Crystallogr*. 32 (1999) 837.

22. Jiménez-Tenorio, M.; Puerta, C. M.; Valerga P. *Organometallics* **2009**, *28*, 2787-2798.

23. Onishi, M. *Bull. Chem. Soc. Jpn*. **1991**, *64*, 3039-3045.

24. Ortiz, M.; Penabad, A.; Diaz, A.; Cao, R.; Otero, A.; Antiñolo, A.; Lara, A. *Eur. J. Inorg. Chem*. **2005**, 3135-3140.

25. Maffett, L. S.; Gunter, L.; Kreisel, K. A.; Yap, G. P. A.; Rabinovich, D. *Polyhedron* **2007**, *26*, 4758-4764.

26. Abernethy, R. J.; Foreman, M. R. St-J.; Hill, A. F.; Tshabang, T.; Willis, A. C.; Young, R. D. *Organometallics* **2008**, *27*, 4455-4463.

Chapter 6

Buried Volume analysis of soft scorpionate ligands

6.1 Introduction:

During the analysis of the many studies on the coordination chemistry and reactivity of the pyrazolyl borates it became apparent that by introducing substituents at the position adjacent to the donor nitrogen on Tp^R ligands, it was possible to sterically confine the reactive face of the metal ion.[1,2] The comparison between Tp and Tp*, which differ only by the introduction of a methyl group, are quite striking. For example, the complexes of Tp with vanadium and ruthenium are observed to form sandwich species. However, the corresponding Tp* complexes are half sandwich species completing their coordination sphere with small ligands such as hydroxides or chlorides.[3] As the importance of steric effects became accepted, it became important to systematically grade the effects of the various substituents. Consequently, it is now quite common to define Tp^R ligands by their cone and wedge angles (figure 6.1 Table 6.1).[1,2]

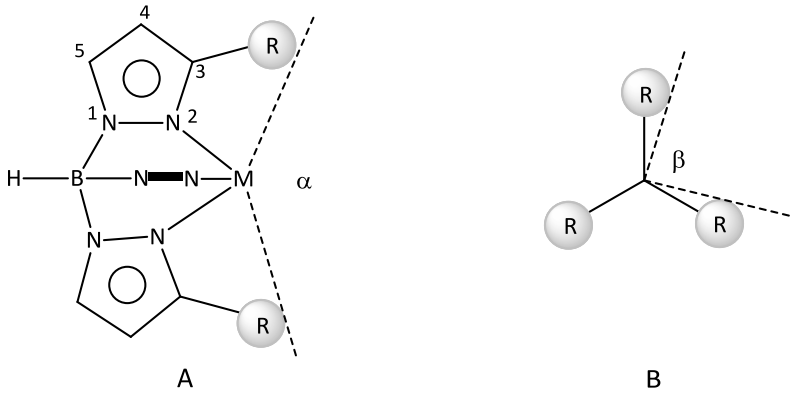

Figure 6.1: Pictorial representation of cone angle and wedge angle. Left: the cone angle = (360-α). Right: the wedge angle (β).[1]

Cone angles in scorpionates are calculated by measuring the angle (α) formed from the outermost hydrogen in the substituent with the metal (figure 6.1). Wedge angles (β) are calculated by measuring the angle formed by the heterocyclic rings (in this case pyrazole) with the metal (figure 6.1).[1] By measuring both cone angle and wedge angle it is possible to assess the steric influence of the ligand around that particular metal

atom. From the above diagram (figure 6.1) it is clear that the substitution at 3rd position on the pyrazole ring has the most effect as it lies in close proximity to the metal ion and coordinated ligand.[1] Large cone angles and small wedge angles imply that the steric influence of the substituent is high.[1] Table 6.1 gives the calculated values of cone angles and wedge angles for a range of complexes of Tp^R ligands with thallium.

Complex	Cone angle	Wedge angle
Tp	183	70
Tp^{Cpr}	223	68
Tp^{Cbu}	234	51
Tp^{Br3}	234	60
$Tp^{(CF3)2}$	237	49
Tp*	239	67
$Tp^{iPr,4Br}$	243	28
$Tp^{tBu,Me}$	243	31
Tp^{tBu}	251	29
Tp^{Cpe}	253	46
$Tp^{Cy,4Br}$	273	46
Tp^{Cy}	281	53

Table 6.1: Cone angles and wedge angles (^{o}) of thallium complexes of Tp^R.[1,2]

Scorpionate ligands can be classified using cone angles and wedge angles into three groups.

(a) Ligands with a small steric effect (small cone angles). These ligands (e.g. R = Me) normally form $M(Tp^R)_2$ type complexes.

(b) Ligands with large steric effects (large cone angles). These generate complexes of the form $Tp^{R}MX$ (R = tBu, mesityl; X = halide).

(c) Ligands with a moderate steric influence (e.g. R = Ph). Here a mixture of $M(Tp^{R})_2$ and $Tp^{R}MX$ type complexes form depending on which metal is being studied.

When Tm^{Me} was introduced as a member of the scorpionate family, researchers immediately applied the information obtained on Tp to the chemistry of Tm^{R}.[2,4] However, there are some fundamental differences between the two systems (figure 6.2). Tp^{R} forms complexes with six membered chelate rings whereas Tm^{R} forms 8 membered chelate rings. The pyrazol rings do not articulate around the B-N bond. In contrast the presence of eight member rings allows the methimazoles to rotate around the B-N bond in such a way that the heterocycle is never found parallel to the nominal H-B-M axis. The formation of eight membered rings also ensures that the substituents on Tm^{R} are directed away from the metal pocket and thus the space available to reactants is much larger.[4,5]

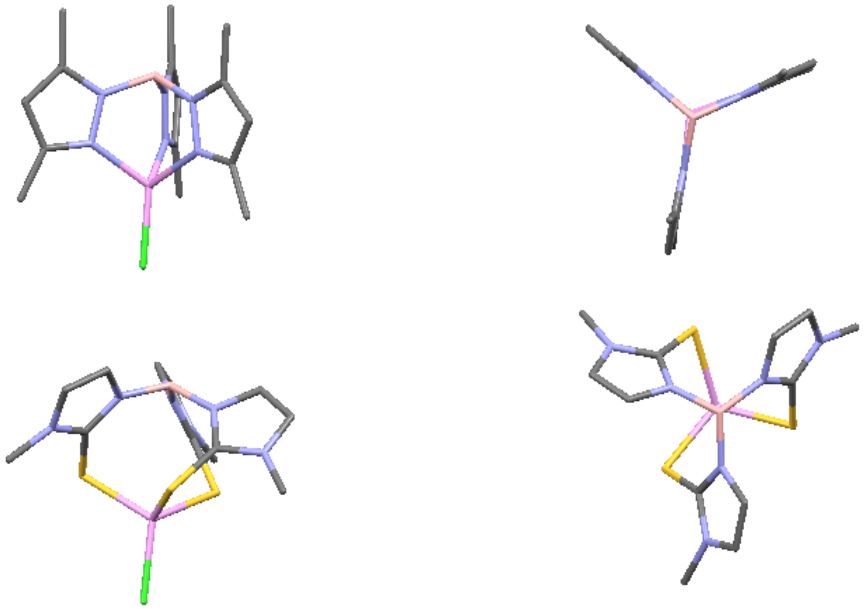

Figure 6.2: Molecular diagram of ZnTp*Cl (top) and $ZnTm^{Me}Cl$ (bottom). The hydrogen atoms are omitted for clarity. The impact of the formation of eight membered rings is evident.[6-7]

It is notable that with Tm^R ligands and so-called bulky substituents (i.e. R= tBu) metals such as gallium and indium still form sandwich complexes.[8-10] The direct application of data collected using Tp^R ligands to the chemistry of Tm^R chemistry is thus thought to lack rigour. The ability to control and predict the steric effects of the various ligands is, however, extremely important. Consequently, the aim of the study is to explore and grade the steric effects of Tm^R complexes and make due comparison with their Tp^R analogues. This study will be achieved by studying the coordination chemistry of zinc and manganese. Zinc has been chosen as it is representative of Tm^R in a tetrahedral environment. Furthermore, as a result of the extensive studies on biomimetic zinc a number of the complexes required to complete this study are already available.[1,2] Manganese (I) tricarbonyl adducts have been adopted as representative of an octahedral environment. Again a number of the key compounds have been reported previously.

A short series of substituents (Tm^R; R = Me, Ph, iPr, tBu) were selected for analysis; the methyl being the least sterically demanding and the tBu the most sterically demanding. Many of the complexes required have been reported previously and their relevant structural data can be accessed using the Cambridge crystallographic database (table 6.2).[3] For zinc, the chloro species have been adopted as this family of complexes is the most complete. However, not all the complexes have been structurally characterised and to complete the analysis it is first important to prepare, crystallise and structurally characterise the missing species. Thus the first aim of this study is to prepare missing complexes, $[Zn(Tm^{Ph})Cl]$, $[Zn(Tm^{iPr})Cl]$, $[Mn(Tm^{Ph})(CO)_3]$, $[Mn(Tm^{iPr})(CO)_3]$ and $[Mn(Tm^{t\text{-}Bu})(CO)_3]$ and obtain good quality crystals for X-ray structural analysis.

Crystallographic Reference Code	Compound	R factor
HOQBUK	$[Zn(Tp^{(Me)2})Cl]$	3.85
LEVVAK	$[Zn(Tp^{(iPr)2})Cl]$	6.2
YAZXEC	$[Zn(Tp^{Ph})Cl]$	3.0
VOJWEW	$[Zn(Tp^{tBu})Cl]$	3.75
AGEZAN	$[Zn(Tm^{Me})Cl]$	2.67
NEBNOX	$[Zn(Tm^{tBu})Cl]$	3.68
VARZEU	$[Mn(Tm^{Me})(CO)_3]$	2.87

Table 6.2: Data for the selected complexes to be used in the analysis of the steric influence of scorpionate ligands.[11-15]

The majority of the calculations on the steric influence of scorpionates are based on measurement of the cone angles and wedge angles.[16] This analysis is acceptable for unsymmetrical phosphines and for rigid ligand systems such as Tp. However, as discussed above (figure 6.2) soft scorpionate ligands are flexible and the use of cone and wedge angles might not give a good assessment of the steric demand of the ligand. As such this study adopted the method of Poater *et al.* which seeks to assess the influence of a ligand using the concept of percentage buried volume ($\%V_{Bur}$).[16] This method of analysis was developed to calculate the steric influence of N-heterocyclic carbene ligands, which similar to soft scorpionate ligands have unusual shape and symmetry (C_2, C_3v symmetry respectively) and are flexible. The $\%V_{Bur}$ tool helps to calculate the three dimensional volume around the central metal atom which is occupied by the ligand (figure 6.3).

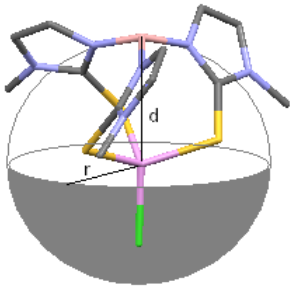

Figure 6.3: Pictorial representation of the sphere which is used to calculate the total volume occupied by the scorpionate ligand around the central metal atom. 'd' is the distance between boron and metal and 'r' is the sphere radius used in the calculation.

Thus the second aim of the study is to identify the steric influence of the substituents on the soft scorpionates (Tm^R where R = Me, iPr, Ph, tBu) using $\%V_{Bur}$. To make a comparison with Tp^R the study will re-analyse the crystallographic data previously reported for the relevant Tp^R species. The Tp^R complexes absent from the data base will be synthesised to complete the data series.

6.2 Experimental section

All chemicals used were commercially available and used without any purification. $NaTm^{Me}$,[17] $NaTm^{tBu}$,[18] $NaTm^{iPr}$ and $NaTm^{Ph}$ [19] were prepared as previously reported. NMR spectra were recorded using a Bruker AV500 or Bruker DPX400. All the spectra obtained were referenced to the residual solvent peaks. IR spectra were recorded as KBr discs using a Nicolet Avatar 360 FT-IR spectrometer. Mass spectra were recorded using a Thermo Finnigan LCQDuo by electrospray ion trap. Crystals obtained were coated in mineral oil and mounted on glass fibres or a glass loop. Data were collected at 123K on Oxford diffraction diffractometer using graphite monochromated Mo-Kα radiation. The heavy atom positions were determined by Patterson methods and the remaining atoms located in the difference electron density maps. Data were solved using Shelx 97[20] and Sir 92[21] and the Wingx graphical interface.[22] All non-hydrogen atoms are made anisotropic with the hydrogen atoms placed as a mixture of independent and constrained refinement in the calculated positions around the parent atoms.

The structural data (cif format) for [Zn(Tp*)Cl] (HOQBUK),[6] $[Zn(Tp^{(iPr)2})Cl]$ (LEVVAK),[7] $[Zn(Tp^{Ph})Cl]$ (YAZXEC),[11] $[Zn(Tp^{tButyl})Cl]$ (VOJWEW),[12] $[Zn(Tm^{Me})Cl]$ (AGEZAN),[13] $[Zn(Tm^{tButyl})Cl]$ (NEBNOX)[14] and $[Mn(Tm^{Me})(CO)_3]$ (VARZEU)[15] were downloaded from the Cambridge crystallographic database.[3]

6.2.1 Buried volume analysis

Buried volume analysis around the central metal atoms (Zn, Mn) were calculated by using the online tool SambVca.[16]

Metal atoms and other simple ligands (chlorides in the case of zinc and carbonyls in the case of manganese) and any solvent molecules were deleted from the 'cif' file and the file saved in an '*xyz*' format for the calculation. For the programme to function the

boron atom was replaced in the structure by an sp^3 carbon atom which was regarded as the central atom for calculations. The three donor atoms (nitrogen in the case of Tp^R and sulphur in the case of Tm^R) were used to calculate the centre of gravity of the molecule (figure 6.4), and this, in conjunction with the pre-measured B-M distance, is used to re-introduce the metal into the model for calculation and the total volume around the central metal atom occupied by the ligand was calculated ($\%V_{Bur}$ = 100 x V_{Bur}/V_{Sphere}).

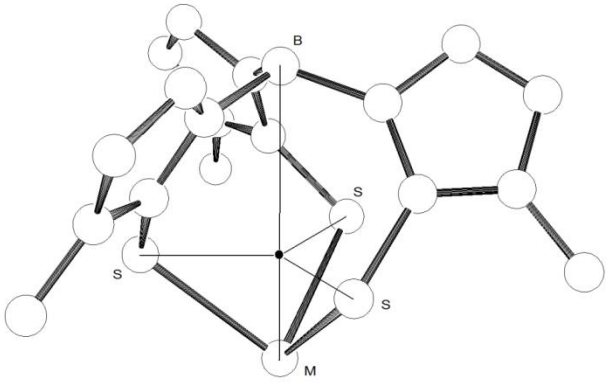

Figure 6.4: Pictorial representation of the model used for the $\%V_{Bur}$ calculation of soft scorpionate complexes of zinc and manganese.

The geometry of the system requires a negative sign in order to place the metal atom in the correct position. Calculations were performed by generating a sphere (as defined below) with the metal at its centre.

Four different sphere radii were used for the calculations. These were the distance (a) between the metal from the coordinated atom

(b) between the metal and nitrogen connected to the bridgehead atom.

(c) between the metal and the atom to which the substituent is attached: nitrogen for Tm^R, carbon for Tp^R and the

(d) between the metal and the carbon in the substituent which is connected to the heterocycle.

All the calculations were performed using a mesh size of radius 0.05 Å. The sphere is broken down into a specific number of voxels with a volume of 1.25 x 10^{-4} Å. The analysis performed for NHC's (N-heterocyclic carbenes) by Poater *et al.* obtained 99.97% accuracy using the same mesh size.[16] For greater accuracy Bondi radii scaled by 1.17 were used in the calculation. Bondii radii are radii which were obtained by fitting the DFT binding energy of 33 N-heterocyclic carbene (NHC) ligands to the atom in Cp*Ru(NHC) complexes.[16] Studies in NHCs reveal that the 'Old set' radii were not quantitatively validated for computational data.[9] Moreover in the 'Old set' the radii of an atom depends on the hybridization states of the atoms. This is difficult to assign accurately within these complexes.[16] Using larger radii, it is possible to include all the hybridization states, thus giving the whole procedure more flexibility.[16] Hydrogen atoms were excluded for the calculations as they are absent from a number of the data sets. This was seen as an acceptable compromise as the steric influence of hydrogen is low (table 6.3).

Sphere radius	with Hydrogen atoms	without hydrogen atoms
2.01	62.7	62.6
2.05	62.6	62.5
2.10	62.4	62.3

Table 6.3: The calculation of percentage buried volume for [Zn(Tp^{iPr})Cl] with hydrogen atoms present and absent. The values confirm that the absence of the hydrogen atoms does not have any significant effect on the calculations. For this analysis only one sphere radius was employed i.e. the M-N distance.

6.2.2 Preparation of hydro*tris*(phenylthioimidazolyl)boratochlorozinc(II); [Zn(Tm^{Ph})Cl].

A solution of $NaTm^{Ph}$ (0.28 g, 5 mmol) in DCM (20 ml) was stirred with (0.68 g, 5 mmol) anhydrous zinc chloride. The solution was initially cloudy, becoming clear after 5 minutes. The mixture was stirred overnight during which time a precipitate formed. The solution was taken to dryness and the product recrystallised by the vapour diffusion of diethyl ether into a solution of the product in DMF. Anal. Calcd for $C_{27}H_{22}N_6BS_3ClZn$: C, 50.79; H, 3.48; N, 13.18%. Found C, 51.02; H, 3.41; N, 13.46%. ESI-MS $[ZnTm^{Ph}]^+$: 601 (100%). FT-IR (KBr, cm^{-1}): 2422 (B-H), 748 (C=S).

6.2.3 Preparation of hydro*tris*(isopropylthioimidazolyl)boratochlorozinc(II); [Zn(Tm^{iPr})Cl].

A solution of $NaTm^{iPr}$ (0.46 g, 1 mmol) in chloroform was stirred overnight with 1 equivalent zinc chloride (0.14 g, 1 mmol). The white precipitate which formed was filtered off and the solution taken into dryness. The resulting product was recrystallised by the vapour diffusion of diethyl ether into a solution of the product in DMF. Anal. Calcd for $C_{18}H_{28}N_6BS_3ClZn.DMF$: C, 41.37; H, 5.79; N, 16.09%. Found C, 41.76; H, 5.61; N, 15.71%. ESI-MS $[ZnTm^{iPr}]^+$: 499 (100%). ^{1}H-NMR (400 MHz, DMSO): δ =7.47 (br, 3H, -CH), 7.14 (br, 3H, =CH), 4.87 (m, 3H, -CH), 1.28 ppm (br, 18H, $-CH_3$). FT-IR (KBr, cm^{-1}): 2427 (B-H), 758 (C=S).

6.2.4 Preparation of hydro*tris*(phenylthioimidazolyl)borato tricarbonyl manganese(I); [Mn(Tm^{Ph})$(CO)_3$].

A solution of $Mn(CO)_5Br$ (0.07 g, 0.25 mmol) in chloroform was stirred overnight with $NaTm^{Ph}$ (0.15 g, 0.26 mmol). The yellow solution formed was filtered, taken to dryness and recrystallised by the vapour diffusion of diethyl ether into a solution of the product in DMF. Anal. Calcd for $C_{30}H_{22}N_6BS_3MnO_3.DMF$: C, 52.86; H, 3.90; N, 13.09%. Found C,

52.11; H, 3.68; N, 13.75%. ESI-MS $[Tm^{Ph}\text{-}S]^+$: 505 (100%), $[Mn(Tm^{Ph})_2]^+$: 1128 (30%). FT-IR (KBr, cm^{-1}): 2443 (B-H), 2003, 1906 (C=O), 738 (C=S).

6.2.5 Preparation of *bis*(hydro*tris*(isopropylthioimidazolyl)borato)manganese(II); $[Mn(Tm^{iPr})_2]$.

A solution of $Mn(CO)_5Br$ (0.07 g, 0.25 mmol) in chloroform was stirred overnight with $NaTm^{iPr}$ (0.11 g, 0.24 mmol). The solution was filtered, taken to dryness and the re-crystallised by the vapour diffusion of diethyl ether into a solution of the product in DMF. Anal. Calcd for $C_{36}H_{56}N_{12}B_2S_6Mn$: C, 46.00; H, 5.92; N, 17.16%. Found C, 46.69; H, 6.10; N, 18.16%. ESI-MS $[Mn(Tm^{iPr})_2]^+$: 926 (100%), $[Mn(Tm^{iPr})]^+$: 491 (45%). FT-IR (KBr, cm^{-1}): 2361 (B-H), 723 (C=S).

6.2.6 Preparation of hydro*tris*(isopropylthioimidazolyl)borate tricarbonyl manganese(I); $[Mn(Tm^{iPr})(CO)_3]$.

To avoid the photochemical side reaction all the reactions and further procedures were carried out in the dark. A solution of $Mn(CO)_5Br$ (0.07 g, 0.25 mmol) in chloroform was stirred overnight with $NaTm^{iPr}$ (0.11 g, 0.24 mmol). The solution was filtered in the dark, taken to dryness and the re-crystallised by the vapour diffusion of diethyl ether into a solution of the product in DMF under dark. Anal. Calcd for $C_{21}H_{28}N_6BS_3MnO_3$: C, 43.90; H, 4.92; N, 14.64%. Found C, 44.40; H, 4.70; N, 14.73%. ESI-MS $[Mn(Tm^{iPr})(Mt^{iPr})]^+$: 632 (100%), $[Mn(Tm^{iPr})]^+$: 491 (60%), $[Mn(Tm^{iPr})_2]^+$: 926 (40%). ^{1}H-NMR (400 MHz, DMSO): δ =7.47 (d, 3H, CH), 7.05 (d, 3H, =CH), 5.17 (m, 3H, -CH), 1.32 ppm (t, 18H, $-CH_3$). FT-IR (KBr, cm^{-1}): 2433 (B-H), 1998, 1890 (C=O), 738 (C=S).

	[Zn(Tm^{Ph})Cl]	[Zn(Tm^{iPr})Cl]	[Mn(Tm^{Ph})(CO)$_3$]	[Mn(Tm^{iPr})(CO)$_3$]
Empirical formula	$C_{27}H_{22}B_1Cl_1N_6S_3Zn_1$	$C_{18}H_{28}B_1Cl_1N_6S_3Zn_1$	$C_{30}H_{22}B_1Mn_1N_6O_3S_3$	$C_{21}H_{28}B_1Mn_1N_6O_3S_3$
FW	637.97	536.02	676.03	574.08
Crystal system	Trigonal	Orthorhombic	Monoclinic	Monoclinic
Space group	R 3 c	P b c a	P -1	P 2_1/c
a/Å	12.4044(7)	17.8259(2)	9.4923(1)	14.8184(4)
b/ Å	12.4044(7)	18.0782(3)	13.4511(2)	11.8323(4)
c/ Å	34.387(2)	35.1979(5)	23.4424(3)	15.0415(5)
α/^{o}	90.0	90.0	90.0	90.0
β/^{o}	90.0	90.0	92.449(1)	90.532(2)
γ/^{o}	120.0	90.0	90.0	90.0
Z	6	8	4	4
V/A^3	4581.93(155)	11342.85(47)	2990.44(1)	2637.20(2)
μ_{calc}/mm-^{1}	1.124	1.197	0.695	0.773
No. Reflns Measd	4226	12723	10720	14697
No. Unique reflns	1866	4493	7403	5683
No Observed reflns	1735	4324	6917	4108
No. Parameters	120	561	801	326
R^a (1>2σ(I))	0.063	0.075	0.034	0.047
R$_w$^{b} (all reflns)	0.179	0.252	0.089	0.088
GOF	1.093	1.086	1.211	1.004

Table 6.4: Crystal parameters of [Zn(Tm^{Ph})Cl], [Zn(Tm^{iPr})Cl], [Mn(Tm^{Ph})(CO)$_3$] and [Mn(Tm^{iPr})(CO)$_3$].

6.3 Results and Discussion:

Understanding the steric influence of a ligand is very important. The studies on steric influence conducted previously on the pyrazolyborates pre-date the introduction of soft scorpionate and specifically Tm^R. As the reports of the synthesis of new scorpionates, which include alternative heterocycles, increase it is appropriate that we re-visit the concept of ligands and their steric influence. Previous studies have assessed steric influence by measuring the cone angles and wedge angles (figure 6.1). This was an acceptable method of assessment for the pyrazolylborates as they formed very regular (C_3) complexes. However, the methimazolylborates are more flexible and it is appropriate that methods which are applicable to ligands which are of lower symmetry are applied. Poater *et al.* have had great success in estimating the steric influence of N-heterocyclic carbenes using the % buried volumes (%V_{Bur}).[16] This method calculates the total three dimensional space occupied by the ligand around the metal atom. Clavier *et al.* successfully used this method to investigate the steric hindrance in both phosphine and NHC ligands.[23] This is the method adopted here.

The study here focussed on the two common geometries adopted by Tp and Tm complexes namely tetrahedral and octahedral geometry. Zinc, as $[Zn(Tm^R)Cl]$ and $[Zn(Tp^R)Cl]$ are representative of a tetrahedral geometry and manganese, as $[Mn(Tm^R)(CO)_3]$ and $[Mn(Tp^R)(CO)_3]$ are representative of octahedral geometry. This formative study has adopted ligands with R = Me, Ph, iPr and tBu substituents such that it could cover an increase in the steric influence of the ligand. Many of these complexes have been reported previously. However, in the initial phase of this study, it was essential to synthesis, crystallise and characterise missing complexes, $[Zn(Tm^{Ph})Cl]$, $[Zn(Tm^{iPr})Cl]$, $[Mn(Tm^{Ph})(CO)_3]$, $[Mn(Tm^{iPr})(CO)_3$, $Mn(Tm^{tBu})(CO)_3$.

6.3.1 Structural analysis

The compounds required were prepared using standard methods as outlined by the equations shown below.

$$ZnCl_2 + NaTm^R \xrightarrow{CHCl_3} [Zn(Tm^R)Cl] + NaCl \qquad (1)$$

$$MnBr(CO)_5 + NaTm^R \xrightarrow{CHCl_3} [Mn(Tm^R)(CO)_3] + NaBr + 2CO \qquad (2)$$

To control the solvent effect during the crystallisation all the complexes were re-crystallised by the vapour diffusion of diethyl ether into a solution of the complex in DMF. The crystals obtained were subjected to X-ray crystallographic analysis (figure 6.5). In these instances it was important that the data refined to a good standard as defined by the 'R' factor (table 6.4) before proceeding with the calculations.

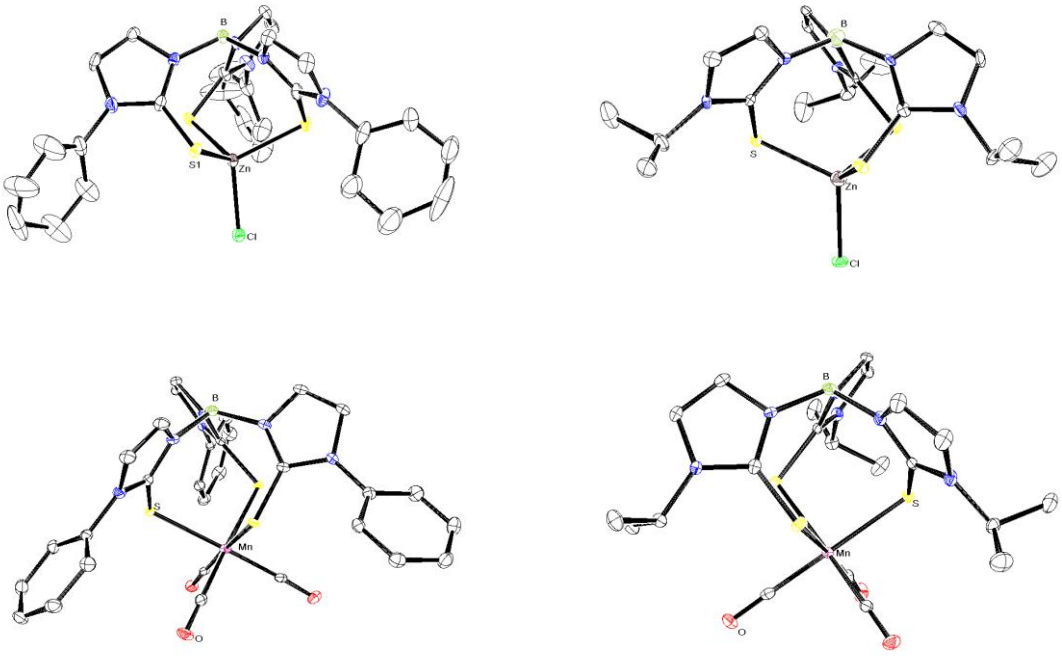

Figure 6.5: Molecular structures of $[Zn(Tm^{Ph})Cl]$ (top left), $[Zn(Tm^{iPr})Cl]$ (top right), $[Mn(Tm^{Ph})(CO)_3]$ (bottom left) and $[Mn(Tm^{iPr})(CO)_3]$ (bottom right). Hydrogen atoms are omitted for clarity. Thermal ellipsoids are shown at a probability of 30%. The metrical parameters for these complexes are given above (table 6.4).

Preparation of the zinc complexes was straightforward. However the preparation of the manganese tricarbonyl complexes required special care. In presence of light certain species apparently photo-oxidise to produce [Mn(Tm^{R})$_2$] complex (figure 6.6). Similar behaviour has been observed previously for [Mn($MeTm^{Me}$)(CO)$_3$] , where the hydride on the boron had been replaced by a methyl group.[24] In this instance the synthesis was conduced in the dark. Thus repeating the reaction above (equation 2) in the dark including the crystallisation allowed the synthesis of [Mn(Tm^{iPr})(CO)$_3$].

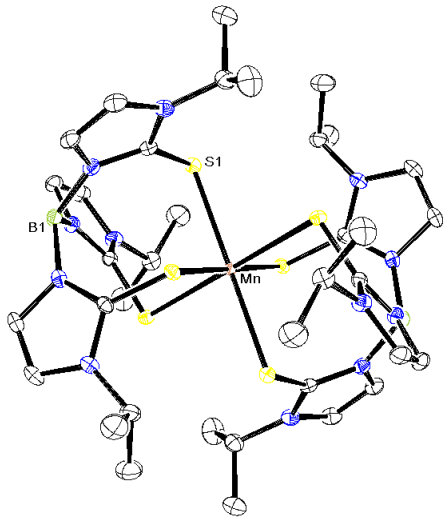

Figure 6.6: The molecular structure of *bis*(hydro*tris*(isopropylthioimidazolyl)borate) manganese (II), [Mn(Tm^{iPr})$_2$]. Hydrogen atoms are omitted for clarity. Thermal ellipsoids are shown at a probability of 30%.

Despite protracted efforts [Mn(Tm^{tBu})(CO)$_3$] was found to be unstable in the dark also and it remains absent from the data set. The infra red data clearly supports the formation of the desired complex. However during crystallisation the complex re-arranges to form an unusual *bis*-manganese complex, where the manganese carbonyl unit is bound through both nitrogen and sulphur of one thio-imidazole while bridging to the second manganese using the sulfur on the adjacent thio-imidazole. The Mn-S bond

distances are 2.42- 2.45 Å, and Mn-N distance is 2.03 Å. The S-Mn-S, S-Mn-N and O-C-Mn bond angles are 84.93, 68.97 and 177.78^{o} respectively. Efforts to isolate X-ray quality crystals of [Mn(Tm^{tBu})(CO)$_3$] were abandoned and the %V_{Bur} calculations on octahedral systems were performed using the data for only three complexes (Figure 6.7).

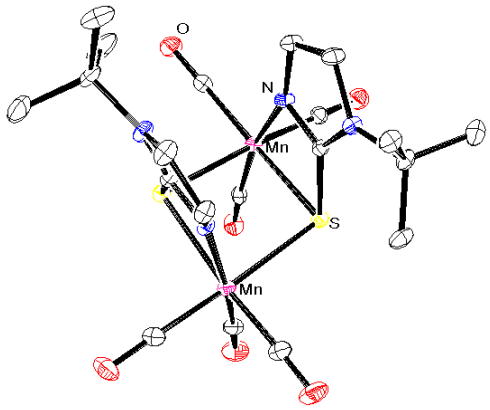

Figure 6.7: X-ray molecular structure of *bis*-(μ-S-thioimidazolemanganesetricarbonyl) which forms from the decomposition of [Mn(Tm^{tBu})(CO)$_3$] during re-crystallisation. Hydrogen atoms are omitted for clarity. Thermal ellipsoids are shown at a probability of 30%.

	B-N	M-N/S	M-B	$M\text{-}N_{(B)}$	$M\text{-}N/C^{(3)}$	$M\text{-}C_{(R)}$
[Zn(Tp*)Cl]	1.57(1)	2.034(8)	2.9882	2.8482	3.1228	3.6039
	1.57(1)	2.016(6)		2.8482	3.1228	3.6039
	1.56(1)	2.016(6)		2.8531	3.1590	3.6518
$[Zn(Tp^{(iPr)2})Cl]$	1.543(5)	2.019(4)	2.9856	2.8648	3.1594	3.6097
	1.55(1)	2.019(4)		2.8672	3.1431	3.6297
	1.543(5)	2.018(4)		2.8672	3.1431	3.6297
$[Zn(Tp^{Ph})Cl]$	1.539(3)	2.047(2)	2.9787	2.8459	3.2079	3.7656
	1.540(3)	2.048(2)		2.8465	3.2090	3.7667
	1.539(2)	2.047(2)		2.8463	3.2085	3.7662
$[Zn(Tp^{tBu})Cl]$	1.532(8)	2.046(5)	2.9418	2.8237	3.2349	3.7931
	1.531(5)	2.054(3)		2.8319	3.2343	3.8254
	1.531(5)	2.054(3)		2.8319	3.2343	3.8254
$[Zn(Tm^{Me})Cl]$	1.550(3)	2.356(1)	3.6272	3.4840	4.0579	4.6663
	1.555(3)	2.3644(7)		3.4878	3.9677	4.5358
	1.547(3)	2.3502(9)		3.5671	4.3191	5.0211
$[Zn(Tm^{iPr})Cl]$	1.5492(4)	2.3376(5)	3.6452	3.5825	4.0638	4.6517
	1.5513(3)	2.3693(3)		3.5430	4.0845	4.8336
	1.5257(2)	2.3461(5)		3.5296	4.2292	4.6632
$[Zn(Tm^{Ph})Cl]$	1.553(7)	2.350(2)	3.6161	3.4767	4.0305	4.6390
	1.553(8)	2.350(2)		3.4767	4.0305	4.6390
	1.553(6)	2.350(2)		3.4767	4.0305	4.6390
$[Zn(Tm^{tBu})Cl]$	1.556(8)	2.335(2)	3.5555	3.4563	4.0725	4.7047
	1.548(7)	2.343(2)		3.4760	4.1755	4.8939
	1.566(7)	2.340(2)		3.4821	4.1467	4.8173
$[Mn(Tm^{Me})(CO)_3]$	1.553(2)	2.4017(4)	4.1256	3.9544	4.2322	4.6274
	1.553(1)	2.4008(5)		3.9541	4.2317	4.6261
	1.554(2)	2.4018(5)		3.9546	4.2311	4.6269
$[Mn(Tm^{iPr})(CO)_3]$	1.551(4)	2.4311(9)	4.1433	3.9968	4.2202	4.5881
	1.546(4)	2.4232(7)		3.9441	4.1988	4.6728
	1.544(4)	2.4202(8)		3.9615	4.2881	4.5311
$[Mn(Tm^{Ph})(CO)_3]$	1.548(5)	2.4240(9)	4.0709	3.9126	4.4925	4.9704
	1.547(5)	2.4130(9)		3.9506	4.4519	4.7836
	1.552(5)	2.4138(9)		3.9645	4.2925	5.0534

Table 6.5: Selected bond lengths (Å) of complexes which used in the buried volume (%V_{bur}) calculation. M indicates metal, $N/C^{(3)}$ indicates the carbon (in Tm it is nitrogen) to which the R group is attached. $M\text{-}C_{(R)}$ is the distance between the metal and the carbon in the substituent which is connected to the heterocycle.

6.3.2 Buried volume calculation

As discussed above it has been decided to assess the steric influence of the soft scorpionates using the concept of percentage buried volume (%V_{Bur}) which was developed by Poater *et al.* To date there has been no rigorous assessment of the steric influence of Tm ligands and due to their flexibility, it remains unclear how the effect of %V_{Bur} will manifest itself in these complexes. The steric influence of Tp^R has been assessed previously using cone and wedge angles and it seemed prudent to perform the %V_{Bur} calculations on Tp^R complexes first, to identify the appropriate parameters such as the sphere radius. For this reason we have deliberately employed four different sphere radii for the calculations. They are (1) distance between the metal and donor atom which is represented in light blue colour (2) distance between the metal and Nitrogen (which is connected to the boron bridgehead) represented in dark blue (3) distance between the metal and nitrogen (to which the substituent is attached) represented in maroon and (4) distance between the metal and the substituent atom which is represented in yellow green colour (figure 6.8).

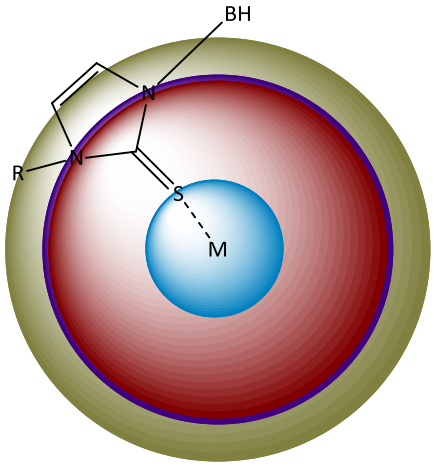

Figure 6.8: Pictorial representation of different sphere radii used in the buried volume calculations.

6.3.2.1 Metal-Donor atom (M-Donor atom)

Poater *et.al.* used the distance between the donor atom and metal to calculate the buried volume.[16] For Tp^R, using the metal-donor distance (M-N distance) did not result in any variation of the $\%V_{Bur}$ with the substituent. The data did not suggest any significant contribution to the $\%V_{Bur}$ (figure 6.9). The analysis of this data suggests that using the primary donors the sphere generated is too small and consequently it excludes the majority of the ligand. Hence it does not give a meaningful measure of the steric influence of the ligands and further data sets based (although routinely measured and calculated) on the metal-donor distance will not be considered further.

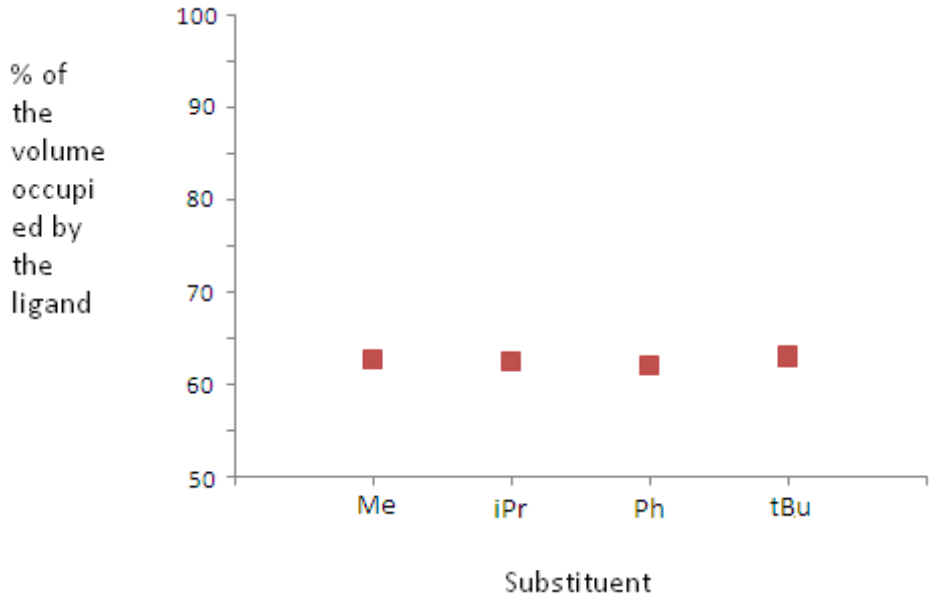

Figure 6.9: Graphical representation of the data obtained for the calculation of [Zn(Tp^R)Cl] (where R= Me, iPr, Ph and tBu) by using the metal to donor atom (nitrogen) distance as sphere radius (2.05 Å)

6.3.2.2 Other sphere radii

Basing the $\%V_{Bur}$ calculation on alternative atoms in the ligand system increases the sphere radii as discussed above (figure 6.8) this can be done by measuring

(i) The distance between the nitrogen bonded to boron and the metal atom

(ii) The distance from the atom in the ring to which the substituent responsible for the steric effects is attached. For methimazole this is a nitrogen and for pyrazole this is a carbon atom, and

(iii) The distance between the substituent and the metal atom.

The three different input values are tabulated and plotted for Tp^R and Tm^R respectively .

6.3.3 Buried volume calculation of tetrahedral zinc system

The $\%V_{Bur}$ data for Tp^R is shown (table 6.6, figure 6.10). Among the four selected substituents, methyl is seen to be the least sterically demanding. While the t-butyl group generates the ligand with the most steric influence. The progression obtained is in line with that published previously for cone angles and wedge angles (Table 6.1).[1,2] This observation validates the $\%V_{Bur}$ analysis. The three sphere radii employed give broadly the same progression indicating that we have identified key points on the ligand for analysis. Since no particular measurement identifies itself as being more appropriate, we have carried all three measurements through this formative study.

	Sphere radius	Me	iPr	Ph	tBu
Zn-N(B)	2.85	59.8	59.6	62	66.6
Zn-C	3.182	58.5	58.4	61.7	67.4
Zn-C(R)	3.71	55.5	56.5	60	67

Table 6.6: The volume occupied by the ligand in [Zn(Tp^R)Cl] complex. Where R = Me, iPr, Ph or tBu for four coordinate zinc metal. Zn-N(B) is the distance between the zinc and the nitrogen to which boron is attached. Zn-C is the distance between the zinc and the carbon atom to which the substituent is attached. Zn-C(R) is the distance between the zinc and the carbon in the substituent which is attached to the heterocycle

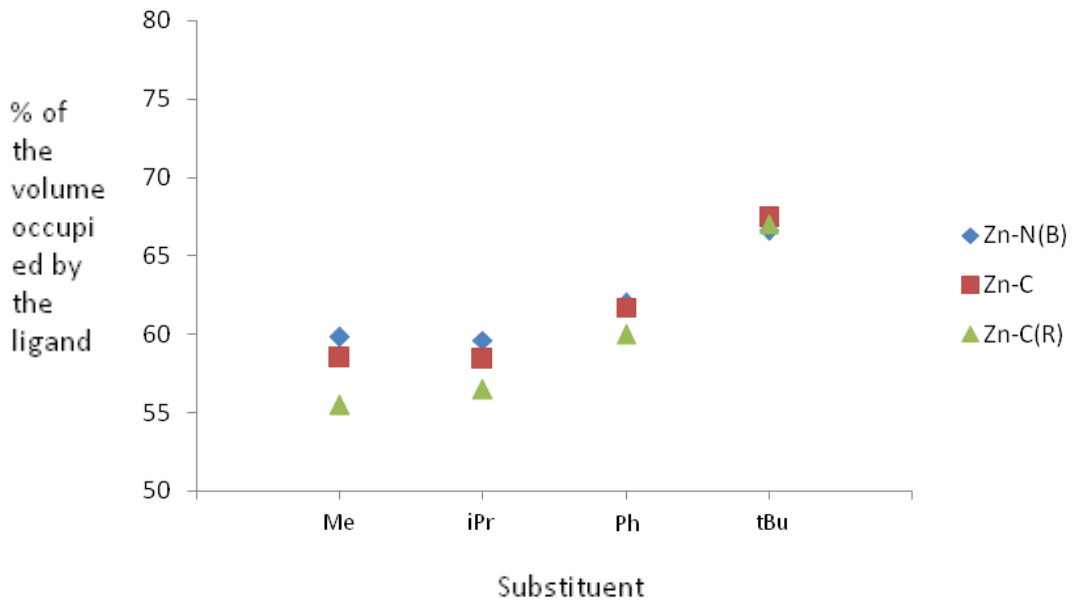

Figure 6.10: Graphical representation of %V_{Bur} for [Zn(Tp^{R})Cl], where R =Me, iPr, Ph and tBu. Zn-N(B) is the distance between the zinc and the nitrogen to which boron is attached. Zn-C is the distance between the zinc and the carbon atom to which the substituent is attached. Zn-C(R) is the distance between the zinc and the carbon in the substituent which is attached to the heterocycle.

Applying the same calculation to the zinc complexes of the soft scorpionates ([Zn(Tm^{R})Cl], where R = Me, iPr, Ph and tBu) we observe a similar trend for the %V_{Bur} analysis. Unlike Tp^{R} however, the data obtained from the three sphere radii are not in good agreement. This is most likely due to the manner in which the methimazoles lie in relation to the H-B-metal axis. As expected greater care must be exercised when calculating the %V_{Bur} of a flexible ligand. Parkin *et al*. have recently reported the zinc chloride complexes of Tm with an adamantyl substituent.[25] This they claim is the most sterically demanding S3 donor tripodal ligand. Consequently we have included this species in our analysis here. Although it can be seen that as we progress from methyl to t-butyl and adamantyl (table 6.7, figure 6.11) the %V_{Bur} increases, the form of the plot suggests that a maximum value is reached e.g. ~65% i.e. we have reached a point where it is not possible to confine the reactive face of the metal further. This contrasts

markedly with Tp where the plot suggests that there is still scope for compressing the reactive face of the metal.

	Sphere radius	Me	iPr	Ph	tBu	Ad
Zn-N(B)	3.512	59.9	62.2	65.1	64.4	66.1
Zn-N(R)	4.132	54.7	58.5	61.7	61	63.4
Zn-C(R)	4.775	48.1	52.6	55.7	55.7	59.4

Table 6.7: Buried volume of Tm^R ligands (where R= Me, iPr, Ph, tBu, or Ad) around a four coordinate zinc metal. Zn-N(B) is the distance between the zinc and the nitrogen to which boron is attached. Zn-N(R) is the distance between the zinc and the nitrogen atom to which the substituent is attached. Zn-C(R) is the distance between the zinc and the carbon in the substituent which is attached to the heterocycle. Average sphere radiuses are used in the calculation.

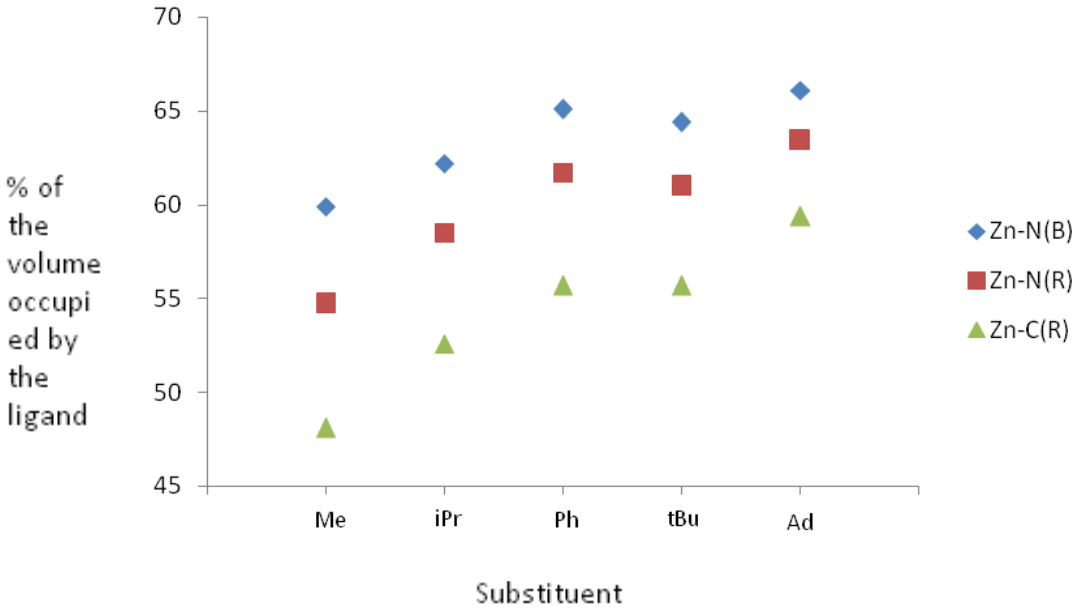

Figure 6.11: Graphical representation of the $\%V_{Bur}$ for a series of zinc complex of Tm^R ligand (where R= Me, iPr, Ph, tBu, or Ad). Zn-N(B) is the distance between the zinc and the nitrogen to which boron is attached. Zn-N(R) is the distance between the zinc and the nitrogen atom to which the substituent is attached. Zn-C(R) is the distance between the zinc and the carbon in the substituent which is attached to the heterocycle. Average sphere radiuses are used in the calculation. Graph is drawn based on the values shown in table 6.7.

The calculations show that the these two classes of scorpionates (Tp and Tm) have markedly different abilities to influence the steric properties of metal complexes due to the positioning of the substituent on the rings. Unsurprisingly, the proximity of the substituent to the metal in Tp has a significant effect. However, for Tm^R, the donor atom lies *exo* to the heterocyclic ring and the influence of the substituent groups are heavily diminished.

6.3.4 Buried volume calculation of an octahedral manganese system

Turning our attention to an octahedral system we analysed the $\%V_{Bur}$ of the three ligand systems in $[Mn(Tm^{Me})(CO)_3]$, $[Mn(Tm^{Ph})(CO)_3]$ and $[Mn(Tm^{iPr})(CO)_3]$. The sphere radii based on the distance between the metal and the donor atom was again assessed and it again showed no effect. Consistent with the study on zinc the analysis of $\%V_{Bur}$ was assess using sphere radii based on metal to nitrogen which is connected to boron, metal to nitrogen to which the substituent is attached and metal to the carbon atom of the substituent by which it is connected to the heterocycle. The data obtained is summarised below.

	Sphere radius	Me	Ph	iPr
Mn-N(B)	3.9598	48.1	49.4	52.3
Mn-N(R)	4.3522	44.7	47	50.1
Mn-C(R)	4.8078	40.5	44	46.8

Table 6.8: The buried volume occupied by the Tm^R ligand (where R is Me, Ph and iPr) around the six coordinate manganese tricarbonyl complex. Mn-N(B) is the distance between the manganese and the nitrogen to which boron is attached.Mn-N(R) is the distance between the manganese and the nitrogen atom to which the substituent is attached. Mn-C(R) is the distance between the manganese and the carbon in the substituent which is attached to the heterocycle. Average sphere radiuses are used in the calculation.

From the data it is clear that the buried volume occupied by the ligand around a four coordinated metal and six coordinated metal are different. The data confirms that the ligand has a greater effect when complexed to a tetrahedral cation. In general the steric influence of these ligands in an octahedral space is low. This supports the observation that sandwich complexes $[M(Tm^{R})_2]$ still form despite the size of the R group.

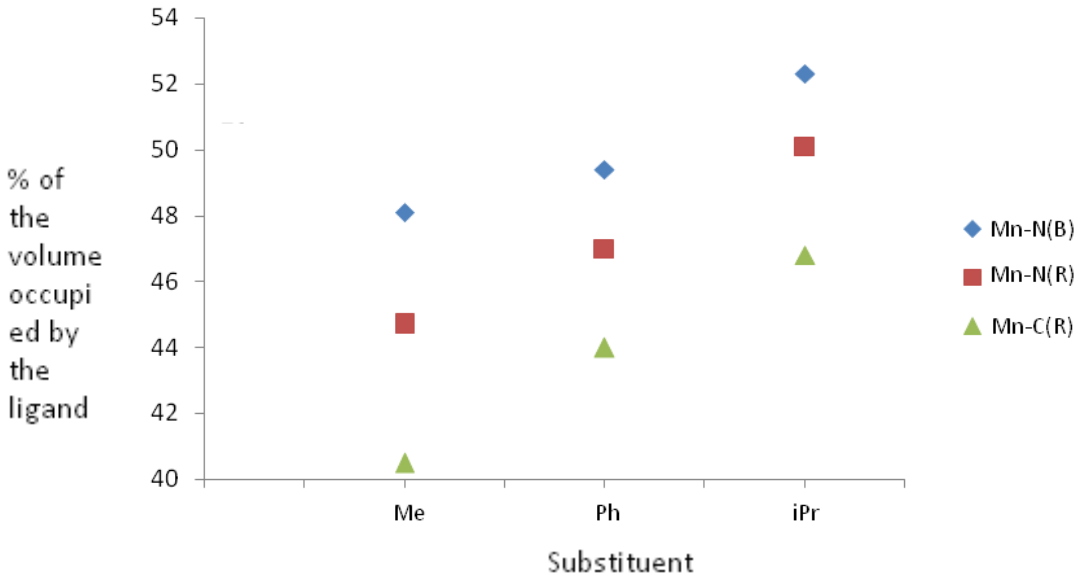

Figure 6.11: Graphical representation of the buried volume calculation of Tm^{R} (where R is Me, Ph and iPr) manganese tricarbonyl complexes. Mn-N(B) is the distance between the manganese and the nitrogen to which boron is attached.Mn-N(R) is the distance between the manganese and the nitrogen atom to which the substituent is attached. Mn-C(R) is the distance between the manganese and the carbon in the substituent which is attached to the heterocycle. Average sphere radii are used in the calculation. The tert-butyl substituted complexes are not reported. The hypothesis would be that it will occupy a slightly higher volume than the isopropyl substituent.

The data obtained for manganese tricarbonyl complexes of Tm^{R} indicates that among the selected three substituents, methyl is the least sterically demanding. The most sterically demanding substitute is isopropyl. In contrast to the data obtained for tetrahedral complexes (figure 6.10) the phenyl substituent is now found to be less sterically demanding than the isopropyl substituent. This observation probably reflect the greater ease with which the phenyl can rotate about the C-N bond in an octahedral geometry.

6.4 Conclusion:

The concept of steric hindrance using the buried volume calculation developed by Poater *et al.* as applied to Tm^R ligands in a tetrahedral and octahedral geometry has been assessed. The ligands have an enhanced effect when placed in a tetrahedral geometry. However, of some interest is the effect of a phenyl and the isopropyl substituents. These do not appear in a uniform position indicating that the free rotation about the C-N bond is important. The methimazole based scorpionates were designed to expand the electronic properties of scorpionates. Moving the donor atom to a position *exo* to the heterocyclic ring displaced the substituent (e.g. methyl) away from the metal. Thus the alteration in the electronic nature of the ligand by this route means that it is more difficult to control the steric influence of the substituent. This has not been universally accepted by other workers. However the reaction of the Tm^{Ph} ligand with Fe^{2+} and Fe^{3+} supports our view. The former forms the octahedral complex in κ^3-H,S,S mode whereas the latter forms common κ^3-S,S,S bound complex even though it is smaller in size.[26] The analysis here on % buried volume clearly shows that even remarkably bulky substituents (e.g adamantyl) have only a limited impact on the steric confinement of the metal.

6.5 Future work:

The study on manganese chemistry was only a partial success and it would be prudent to re-visit a metal which presents in an octahedral geometry for Tm^R ligands such that the relative position of the t-Bu substituent can be assessed. It would also be of interest to expand this analysis to a series of heteroscorpionates around the metals to compare the effect of the heterocyclic rings themselves.

6.6 References:

1. Trofimenko, S. *Scorpionates The coordination chemistry of polypyrazolylborate ligands, Imperial College Press.* **1999.**

2. Pettinari, C. *Scorpionates II: Chelating borate ligands, Imperial College Press*. **2008**.

3. Allen, F. H. *Acta Crystallogr., Sect. B* **2002**, *58*, 380–388.

4. Spicer, M. D.; Reglinski, J. *Eur. J. Inorg. Chem*. **2009**, 1553-1574.

5. Reglinski, J.; Garner, M.; Cassidy, I. A.; Slavin, P. A.; Spicer, M. D.; Armstrong, D. R. *J. Chem. Soc. Dalton Trans*. **1999**, 2119-2126.

6. Bonitatebus Junior, P. J.; Armstrong, W. H. *Chem. Commun*. **1999**, 55-56.

7. Cassidy, I.; Garner, M.; Kennedy, A. R.; Potts, G. B. S.; Reglinski, J.; Slavin, P. A.; Spicer, M. *Eur. J. Inorg. Chem*. **2002**, 1235-1239.

8. Yurkerwich, K.; Buccella, D.; Melnick, J. G.; Parkin, G. *Chem. Commun*. **2008**, 3305-3307.

9. Tesmer, M.; Shu, M.; Vahrenkamp, H. Inorg. Chem. 2001, 40, 4022- 4029.

10. Yurkerwich, K.; Buccella, D.; Melnick, J. G.; Parkin, G. *Chem. Sci*. **2010**, *1*, 210-214.

11. Fujisawa, K.; Matsunaga, Y.; Ibi, N.; Amir, N.; Miyashita, Y.; Okamoto, K. *Bull. Chem. Soc. Jpn*. **2006**, 79, 1894-1896.

12. Hartmann, F.; Klaui, W.; Kremer-Aach, A.; Mootz, D.; Strerath, A.; Wunderlich, H. *Z. Anorg. Allg. Chem*. **1993**, 619, 2071-2076.

13. Yoon, K.; Parkin, G. *J. Am. Chem. Soc*. **1991**, 113, 8414-8418.

14. Tesmer, M.; Shu, M.; Vahrenkamp, H. *Inorg. Chem*. **2001**, 40, 4022-4029.

15. Bailey, P. J.; Lorono-Gonzales, D. J.; McCormack, C.; Parsons, S.; Price, M. *Inorg. Chim. Act*a **2003**, 354, 61-67.

16. Poater, A.; Cosenza, B.; Correa, A.; Giudice, S.; Ragone, F.; Scarano, V.; Cavallo, L. *Eur. J. Inorg. Chem*. **2009**, 1759-1766.

https://www.molnac.unisa.it/OMtools.php.

17. Garner, M.; Reglinski, J.; Cassidy, I.; Spicer, M. D.; Kennedy, A. R. *Chem Commun*. **1996**, 1975-1976.

18. Singh, A. K.; Mehtab, S.; Singh, U. P.; Aggarwal, V. *Anal. Bioanal. Chem*. **2007**, *388*, 1867-1876.

19. Bakbak, S.; Bhatia, V. K.; Incarvito, C. D.; Rheingold, A. L.; Rabinovich, D. *Polyhedron* **2001**, *20*, 3343-3348.

20. Sheldrick, G. M. *Acta Crystallogr*. **2008**, *A64*, 112-122.

21. Altomare, A.; Cascarano,G.; Giacovazzo, C.; Gualardi, A. *J. Appl. Crystallogr*. **1993,** *26*, 343-350.

22. Farrugia, L. J. *J. Appl. Crystallogr.* **1999**, *32*, 837.

23. Clavier, H.; Nolan, S. P. *Chem. Commun*. **2010**, *46*, 841-861.

24. Wallace, D. PhD Thesis **2008**, University of Strathclyde, An insight into the chemistry and applications of soft scorpionates.

25. Yurkerwich, K.; Yurkerwich, M.; Parkin, G. *Inorg. Chem*. **2011**, *14*, A-L.

26. Kimblin, C.; Churchill, D. G.; Bridgewater, B. M.; Girard, J. N.; Quarless, D. A.; Parkin, G. *Polyhedron* **2001**, *20*, 1891-1896.

Chapter 7

Final Conclusion

7.1 Final Conclusion

The chemistry of soft scorpionates continues to expand. This work has shown that these interesting anions can act as acceptors for alkyl groups. Through this work we have shown that a small positive charge develops within the heterocycle and this causes a small elongation of the B-N bond. In the case of the Tm^{Me} anion this change does not compromise product stability. In contrast the alkylated Tbz and tzTtz anions quickly degrade. This observation has implications for the chemistry of the soft scorpionates in general.

The ability of soft scorpionates to act as alkyl group acceptors led us to synthesise a series of cationic rings. These results suggested that it would be interesting to study other oxidising electrophiles (NO^+, I_2). The treatment of soft scorpionate anions with these species generated new and unique polycyclic compounds. The Tm^{Me} anion generates a tricyclic species (figure 7.1) which contains three sulfur atoms, whereas Tm^{Ph} produces a tricyclic ring via the elimination of a sulfur from one of the thioimidazole units. This study reveals the effects of the substituent on the nitrogen in the thio-imidazole ring. Not only do we see changes due to the steric influence of the substituent, we also observe a change in reactivity due to the electronic structure of the heterocycles.

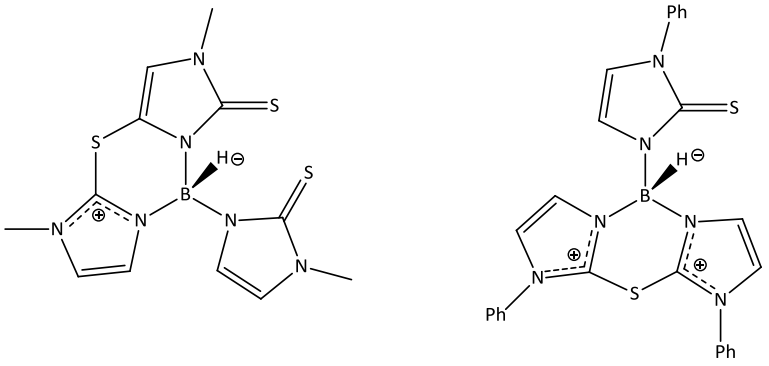

Figure 7.1: Two different tricyclic rings formed by the reaction of soft scorpionate with NO^+. Left is the crossbow product obtained by the reaction between Tm^{Me} and NO^+ and the one in right is the polycyclic cation obtained by the reaction between Tm^{Ph} and NO^+.

DFT calculations identified a chemical weakens in the Tbz ligand system and this was thought important enough to test. The hypothesis was that the ligand might not be able to produce complexes with hard metals, but could generate the metal complexes with soft metals. Modest success was had with this study. The key complexes were isolated and a reaction pattern leading to complex degradation established using NMR spectrum. This study suggests that it is possible to generate metal complexes of the Tbz ligand but their utility will be poor. The major outcome from this study was not in the field of inorganic chemistry but in the sphere of advanced heterocyclic chemistry. In this case we were able to synthesis new polycyclic heterocycles (figure 7.2). These have a unique chemical footprint and may have some utility in the design of new bio-active organic compounds.

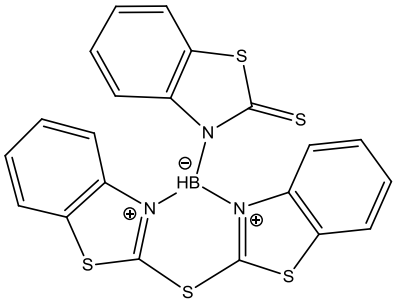

Figure 7.2: Pictorial representation of polycyclic cationic hetrocycle (Tbz-S) obtained by the decomposition of antimony and mercuric Tbz complex.

The established interest in nitric oxide chemistry initiated above was transferred to the chemistry of Bm^{Me} compounds. Santos *et al.* had shown that π acceptors can displace the M-hydride interaction in soft scorpionates. We were interested in using Bm^{Me}-ruthenium complexes as nitric oxide scavengers. We introduced $Ru(Bm^{Me})_2$ (ruthenium κ3-H,S,S- hydro bis(methimazolyl)borate) to nitric oxide in its various forms. Unfortunately this universally leads to the oxidation of the ruthenium with the metal hydride interaction remaining unchanged.

In the final chapter the estimation of the degree of steric influence that the soft scorpionates was attempted using buried volume analysis. A comparison of four-coordinated zinc complexes and six-coordinated manganese tricarbonyls provided enough information to show that unlike Tp^R, Tm^R ligands do not impart as great a steric influence of the metal centre. The study on the manganese complexes did however suggest that there is an interesting photochemical dismutation reaction in progress. Time did not permit an in-depth investigation of this but the small amount of data suggests that this would be worth further study.

Appendix

8.1 Appendix

Many attempts were made to identify a suitable method for the preparation of NaTbz. Hill *et al*. introduced a method where the thione and alkali borohydride were refluxed in xylene.[1] This method proved unsuccessful for NaTbz. However, from the reaction we obtained bis(1,3-benzothiazole)-2,2'-disulfide. This species was crystallographically characterised. (figure 8.1).

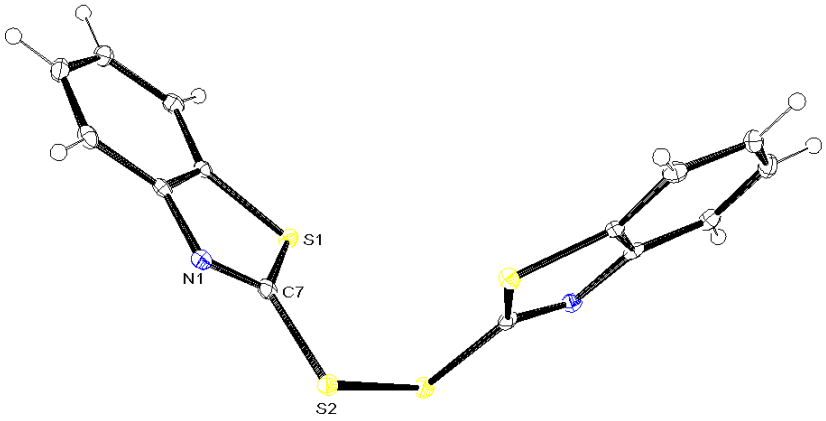

Figure 8.1: The molecular structure of bis (1,3- benzothiazole)-2,2'-disulfide, obtained by refluxing 2-mercaptobenzothiazole with $NaBH_4$ in xylene. The bond length between N1 and C7 is 1.279(3) Å which is consistent with double bond character (c.f. C-N single bond ~1.47 Å). The torsion angle of $C_7S_2S_2C_7$ is 88.2(1). Thermal ellipsoids are shown at a probability of 30%.

Reference

1. Hill, A. F.; Owen, G. R.; White, A. J. P.; Williams, D. J. *Ang. Chem. Int. Ed.* **1999**, *38*, 2759-2761.